University College London

Hedgehog Signalling in Haematopoiesis

Ching-In LAU

A Thesis submitted to the University College London

for the Degree of Doctor of Philosophy

February 2014

Immunobiology Unit

Institute of Child Health

Project supervisor: Prof. Tessa Crompton
Dr Anna Furmanski

This is a declaration that all the work presented in this thesis is my own.
Where information has been derived from other sources,
that has been indicated in the thesis.

Ching In Lau

February 2014

Abstract

The Hedgehog (Hh) family proteins and their signalling pathway are key mediators of, and important in, many mammalian developmental processes. Malfunction of the Hh signalling pathway contributes to developmental disorders and birth defects. This project aims to investigate the role of the Hh signalling pathway in murine haematopoiesis. In our study, we found that Dhh plays a negative regulatory role in normal erythropoiesis and under stress conditions. However, it is not required for regulating erythropoiesis in the fetal liver during embryo development. In contrast, analysis of conditional deletion of Smo in haematopoietic cells revealed that Smo controls early haematopoietic differentiation in the fetal liver but is dispensable for regulating haematopoiesis in adult bone marrow and spleen. Furthermore, pervious studies have demonstrated that Hh signalling is involved in T-cell development throughout maturation. We tested the hypothesis that Foxa2, a downstream target gene of Hh during pre-TCR signalling, is also required for late T-cell development and activation. Analysis of mice conditionally Foxa2-deficient in mature T-cells revealed that Foxa2 is important in the process of maturation in late thymocyte development. In addition, Foxa2 is also involved in regulation of T-cell activation, and the differentiation of T helper cells. Gene expression experiments confirmed that Foxa2 is also a Hh target gene in the thymus. Taken together, our findings revealed that the Hh signalling pathway and its target genes play critical roles in haematopoiesis during embryogenesis and in adult mice.

Acknowledgements

It's a pleasure to thank those all who have made this thesis possible. First, I'd like to express my deepest gratitude to my supervisor Prof. Tessa Crompton. I sincerely appreciate the opportunity she gave me to work with her four years ago. She has been so patient and supportive throughout these four years, and I am grateful for her trust and freedom. She has also inspired me a lot in the aspect of basic science. She is simply the best mentor I've ever had and I couldn't thank her enough.

I would also like to thank all other members in the group. Anna, José, Alessandro, baby Sue and Sue O. I thank them sincerely for their kindness, and endless technical supports, valuable scientific and life advices. Hemant, Anisha, Amal, Kostas, Sonia, Diana and also Nancy, they all are brilliant PhD students. Thanks for their friendly support and for cheering me up during the tougher days. We had so many laughs, and we also learnt and grew together to become better scientists.

Thanks to my mum, dad, sister and also my in-laws for their support throughout my PhD, and forgiveness for being absent from all the family gatherings all these years while being in the UK.

Last but not least, thanks to my husband, Fui Fui for his constant moral support and his kindness and tolerance to my silliness, and for putting up with me on the moody days!

Table of Contents

Table of Figures

Table of Tables

Abbreviations

µg	Microgram
µl	Microlitre
-/-	Knockout
+/-	Heterozygous
Actβ	Beta-actin
Afp	Alpha-fetoprotein
AGM	Aorta-gonad-mesonephros
APC	Antigen presenting cells
au	Arbitrary unit
BFU-E	Erythroid burst-forming units
BM	Bone marrow
BMP	Bone Morphogenetic protein
bp	Base pair
BSA	Bovine Serum Albumin
CD	Clusters of Differentiation
cDNA	Complementary DNA
CFU-E	Erythroid colony-forming units
CLP	Common lymphoid progenitor
CMP	Common myeloid progenitor
CFSE	Carboxyfluorescein diacetate succinimidyl ester
dNTPs	Deoxynucleotide triphosphates
Dhh	Desert Hedgehog
DN	Double negative
DNA	Deoxyribonucleic acid
DP	Double Positive
E	Embryonic day
Epo	Erythropoietin
EpoR	Erythropoietin receptor
EryP	Primitive erythroid progenitor
EryD	Definitive erythroid progenitor
FACS	Fluorescence activated cell sorter
FITC	Fluorscein Isothiocyanate
Fl	Floxed
FOX	Forkhead box
FSC	Forward scatter
FTOC	Fetal thymus organ cultures
Gli	Glioma-associated oncogene
GMP	granulocyte-monocyte progenitors
HDM	House dust mite
Hh	Hedgehog
HNF	Hepatocyte nuclear factor
HPRT	hypoxanthine guanine phosphoribosyltransferase
HSA	Heat-stable antigen

HSCs	Hematopoietic stem cells
IFN	Interferon
Ihh	Indian Hedgehog
IL	Interleukin
KO	Knockout
Lmo2	LIM domain-only protein 2
LN	Lymph node
LSK	$Lin^{-}Sca\text{-}1^{+}C\text{-}kit^{+}$
mAB	Monoclonal antibodies
MacP	Primitive macrophage progenitor
MegaP	Primitive megakaryocyte progenitor
MEP	Megakaryocyte-erythroid progenitors
MHC	Major histocompatibility complex
ml	Milliliter
mm	Millimeter
mRNA	Messenger ribonucleic acid
NK	Natural killer
p	p-value
PBS	Phosphate buffered saline
PCR	Polymerase chain reaction
PHZ	Penylhydrazine
PI	Propidium iodide
PMA	Phorbol myristate acetate
Prog	Myeloid progenitor
Ptch	Patched
r-	Recombinant
RNA	Ribonucleic acid
RP	Red pulp
RT-PCT	Real-Time Polymerase Chain Reaction
SCF	Stem cell factor
SEM	Standard error of mean
SP	Single positive
Shh	Sonic Hedgehog
Smo	Smoothened
SSC	Side scatter
TCR	T-cell receptor
Th	T helper cells
TNF	Tumor necrosis factor
Treg	Regulatory T-cells
WP	White pulp
WT	Wild type

Chapter One : Introduction

1.1 Murine Haematopoiesis

Haematopoiesis is the process by which haematopoietic stem cells (HSCs) develop into different lineages of mature functional blood cells. HSCs are the common multipotent progenitors, which are capable of self-renewal, and are responsible for the continuous production of all the blood cells.

Haematopoiesis takes place in different tissues during embryogenesis and in adult life. During embryonic development, two sequential phases of haematopoiesis are defined, which are known as primitive and definitive haematopoiesis. Murine primitive haematopoiesis can be detected at E7 in the yolk sac, and produces progenitors that give rise to macrophages, megakaryocytes and erythrocytes (Palis et al. 1999, Tober et al. 2007). Subsequently, definitive haematopoiesis is initiated by the aorta-gonad-mesonephros (AGM) region at E10-11 and starts to produce HSCs (Medvinsky and Dzierzak 1996). Shortly after this, haematopoiesis migrates to the fetal liver up until birth, and the blood lineage progenitors, such as myeloid and lymphoid progenitors that are derived from HSCs start to appear (Orkin and Zon 1997). After birth and throughout life, HSCs are produced continuously in the bone marrow and generate all of the haematopoietic progenitors that proliferate and differentiate into committed haematopoietic lineages. (Figure 1.1)

Different models of haematopoietic lineage commitment have been proposed, including the classical model in which, HSCs first give rise to either one of the two

distinct haematopoietic lineage progenitors: common lymphoid progenitor (CLP) and common myeloid progenitor (CMP). The CLP produce T and B lymphocytes and natural killer (NK) cells, whereas CMP generate all the myeloid cells, including erythrocyte, megakaryocyte, granulocyte and monocyte lineages. (Figure 1.2) However, commitment and lineage separation between CMP and CLP is not absolute, and even in the thymus, some early thymic progenitors (ETP) are capable of giving rise to myeloid cells (Bell and Bhandoola 2008).

1.1.1 Erythroid development

In the erythroid lineage, the earliest committed erythroid progenitors are the erythroid burst-forming units (BFU-E). These BFU-E cells further differentiate into erythroid colony-forming units (CFU-E) (Gregory and Eaves 1978). After that, the CFU-E cells give rise to proerythroblasts, which are the first morphologically recognizable erythroid cells. These cells mature through successive basophilic erythroblast stages to late basophilic and chromatophilic erythroblasts, and finally differentiate into the late stage erythroblasts, ortho-chromatophilic erythroblasts (Zhang et al. 2003). (Figure 1.3)

In mice, these erythroblast populations can be recognized by the expression of the cell surface markers, CD71 and Ter119. As differentiation proceeds, the erythroblasts gain the expression of Ter119 and lose expression of CD71. The pathway of erythroblast differentiation is summarized as follows: $CD71^{high}Ter119^{med}$ (population I), $CD71^{high}Ter119^{high}$ (population II), $CD71^{med}Ter119^{high}$ (population III), $CD71^{low}Ter119^{high}$ (population IV) (Socolovsky et al. 2001). During erythroid

maturation, the erythroblasts decrease in cell size and increase in haemoglobin concentration. Gradually, the nucleus shrinks and will be finally excluded, then the cells become erythrocytes. (Figure 1.3) The regulation of erythropoiesis will be discussed in more detail in later chapters.

1.1.2 Thymocyte development and activation

Thymocyte development begins with the lymphoid progenitors, which are found and released from the fetal liver and bone marrow after birth, and migrate to the thymus, where they undergo differentiation and become mature T-cells (Crompton et al. 2007, Shortman and Wu 1996). The process of T-cell development is complex, and thymocytes pass through a series of distinct stages before they leave the thymus. The various stages of differentiation can be marked by changes in their cell surface protein expression and the expression of the T-cell receptor (TCR) (Shortman et al. 1990).

In mouse, the first thymocyte progenitor population are double-negative (DN) cells, that lack both CD4 and CD8 cell surface proteins. The DN population of thymocytes is further subdivided into four developmental stages, based on the expression of CD44 and CD25 cell surface markers (Godfrey et al. 1993, Killeen et al. 1998). DN1 is the earliest thymic subset, which initially expresses CD44 but not CD25. The thymocyte then acquires the expression of CD25 and is called the DN2 stage. CD44 expression is then lost and the cell differentiates into DN3. At the last DN stage, CD25 expression is down-regulated which leads to negative expression of CD44 and CD25 at the cell surface, known as DN4. This pathway is summarized as follows: CD44+CD25-

(DN1), CD44+CD25+(DN2), CD44-CD25+(DN3), CD44-CD25-(DN4). DN thymocytes then develop into double-positive (DP) thymocytes, expressing both CD4 and CD8. At the final step, DP thymocytes progress to give rise to mature functional T-cells, either CD4+CD8-(CD4SP) or CD4-CD8+(CD8SP) (Godfrey et al. 1993). (Figure 1.4)

The development of thymocytes is tightly regulated, and only about 3% of mature thymocytes are selected and leave the thymus to migrate to the peripheral lymphoid organs, such as the lymph nodes and the spleen (Egerton et al. 1990, Shortman et al. 1990). The maturation of T-cells requires developing thymocytes to undergo TCR gene rearrangements, which are critical to T-cell development and maturation. The earliest rearrangement process takes place in the DN3 population by the gene rearrangement of TCR β chain locus (Godfrey et al. 1994, Mallick et al. 1993). This rearrangement will lead to expression of TCR β chain at the cell surface which interacts with the pre-TCR α chain to form the pre-TCR complex (Fehling et al. 1995). Cells that fail to rearrange the gene coding the TCR β-chain will not differentiate further and will undergo apoptosis (Shortman et al. 1990). This process is named β-selection and requires pre-TCR signalling. The DN3 thymocytes pass through β-selection then lose expression of CD25 and differentiate into the DN4 population, which subsequently differentiate into DP thymocytes with expression of CD4 and CD8 molecules (Fehling and von Boehmer 1997, Guidos 2006). Once β-selection has completed, TCR α chain rearrangement occurs in DP thymocytes, and TCR α chains pair with the TCR β chain to form the αβ TCR (Robey and Fowlkes 1994).

Following TCR αβ chain rearrangement, DP cells undergo positive and negative selection to ensure that CD4 and CD8 SP cells that exit the thymus have appropriate

major histocompatibility complex (MHC) restriction, and will not be self-reactive. At this stage, survival of thymocytes depends on the specificity and affinity of the TCR they express. Positive selection selects T-cells on the capability of their TCR to recognize MHC class I or MHC class II molecules with appropriate (moderate) affinity (Jameson et al. 1995). T-cells commit to either the CD4SP or CD8SP lineage at this stage. The DP cells with TCR that interacts appropriately with MHC class II become CD4SP T-cells, whereas those recognizing MHC class I develop into CD8SP T-cells (Robey et al. 1991). The process of negative selection follows positive selection during which T-cells expressing a high affinity TCR for self-MHC binding to self-peptide are eliminated and undergo apoptosis to thus clear out potentially self-reactive T-cells. (Goldrath and Bevan 1999, Jameson et al. 1995).

Additionally, it is thought that CD4/8 lineage commitment and positive selection may be affected by TCR signal strength, with a stronger TCR signal leading to commitment to the CD4+ lineage, and a weaker TCR signal leading to commitment to the CD8+ lineage (Bommhardt et al. 1999, Kappes and He 2005). Following positive and negative selection, mature CD4 or CD8 T-cells then leave thymus and migrate to the lymphoid organs in the periphery (Robey et al. 1991). (Figure 1.4)

To trigger mature naïve CD4 and CD8 T-cell activation, it is necessary for the TCR/CD3 complex on the T-cell to recognize the MHC-peptide complex on antigen presenting cells (APC), and the co-stimulatory molecule, CD28 on the T-cells to interact with B7 family members (June et al. 1994). After activation by these two signals, the activated T-cell undergoes proliferation, CD4 T-cells then differentiate into T-helper (Th) effector cells, while CD8 T-cells become cytotoxic T-cells.

Activated CD4+ T-cells can be subdivided into several types of Th cell subsets based on distinct cytokines production and their functions. Th1 cells secrete mainly Interferon(IFN)γ, interleukin (IL)2 and tumour necrosis factor(TNF)α, which enhance pro-inflammatory cell-mediated immunity in response to eliminate intracellular pathogens. Th2 cells produce IL4, IL5, IL9 and IL13, which are involved in allergic inflammatory disease and protect against extracellular parasites (Constant and Bottomly 1997). IL17 is produced by Th17 cells, that play important roles in protection against extracellular bacteria and fungi and are responsible for some inflammation, as well as autoimmune disease (Korn et al. 2009). Lastly, regulatory T-cells (Treg) are also a subpopulation of CD4+ T-cells, which play a critical role in maintaining immune self-tolerance and lymphoid homeostasis. Treg are subclassified into natural Treg (nTeg) and induced (iTreg). Both are recognized by their expression of CD25 and Foxp3. The differentiation of nTreg takes place in the thymus, whereas iTreg are developed in the periphery. (Curotto de Lafaille and Lafaille 2009)

1.2 Hh signalling pathway

The family of Hedgehog (Hh) proteins was first identified in a large scale screen for mutations in Drosophila in 1980. The screen revealed that Hh protein is involved in controlling the development of the larval body plan in Drosophila (Nusslein-Volhard and Wieschaus 1980). Since then the Hh signalling pathway has been widely studied due to its vital role in embryonic patterning and development. There are three highly related Hh proteins that have been identified in mammals, namely, Sonic Hedgehog

(Shh), Indian Hedgehog (Ihh) and Desert Hedgehog (Dhh) (Ingham and McMahon 2001). The three Hh proteins are important in regulating a wide variety of functions, including cell differentiation, survival and cell fate (Jiang and Hui 2008, Varjosalo and Taipale 2008).

The Hh signalling pathway is still not fully understood, but several components involved in Hh signalling are highly conserved in vertebrates (Varjosalo and Taipale, 2008). There are two receptors crucial to the mammalian Hh signalling pathway. Patched (Ptch), which is a 12-span transmembrane protein, acts as a suppressor of another transmembrane protein, Smoothened (Smo), which is a 7-span transmembrane protein and acts as a signal transducing molecule in the Hh signalling pathway (Alcedo et al., 1996, van den Heuvel and Ingham, 1996). In the absence of Hh, Ptch inhibits Smo activity and results in repression of down-stream transcriptional activation. The Hh signalling pathway is initiated by binding of Hh to Ptch, which relieves the inhibition of Smo activity thus leading to the transcription of specific Hh target genes by the activation of the glioma-associated oncogene (GLI) family transcription factors Gli1, Gli2 and Gli3 (Crompton et al. 2007, Matise and Joyner 1999, Taipale et al. 2002)(Figure 1.5). The Gli family proteins have distinct and specialized functions, which promote target gene transcription when Hh signalling is present. Gli1 acts as an activator of Hh target gene transcription. It is also a target gene of the Hh signalling pathway, thus detection of its transcription level can indicate the degree of Hh signalling in a population of cells. Gli2 and Gli3 can function as both transcriptional activators and transcriptional repressors (Marigo et al. 1996, Ruiz i Altaba 1998).

1.2.1 Regulation of Hh activity

The Hh signalling pathway plays multiple roles in a large number of developmental processes in vertebrates, ranging from cellular growth to patterning of different tissues.

The Hh proteins act as morphogens to regulate different developmental processes. Studies of vertebrate nervous system development showed that Shh acts in a gradient dependent manner to control the pattern of cellular differentiation. Various subsequent studies have confirmed that this concentration dependent effect regulates the generation of a number of different cell types and allows the responding cell to be exposed to different concentrations of Hh (Harfe et al. 2004, Varjosalo and Taipale 2008). Duration of signal received is another important factor that influences outcome (Briscoe and Ericson 1999, 2001). Thus, Hh controls cellular development dependent on the responding cell type, the concentration and the duration of exposure to Hh by the target cells (Harfe et al. 2004, Varjosalo and Taipale 2008).

It has been shown that the amount of Hh signal received by a cell correlates with the concentration of the Gli proteins. Also, the ratio of the Gli activator to Gli repressor forms of the protein is affected by the Hh signal gradient received by the target cell. Cells closer to the Hh secreting source will increase the amount of activator forms of Gli protein whereas the repressor forms of Gli protein will be inhibited and vice versa. (Stamataki et al. 2005)

1.2.2 Developmental defects caused by mutation of Hh proteins

Present studies indicate that all three Hh proteins share a common signalling pathway, and have similar physiological effects, however, the three Hh proteins are implicated in a wide variety of different biological functions. The differences in their roles in development are thought to be due to the different expression patterns of the Hh proteins and loss of each of them causes different developmental defects. (Varjosalo and Taipale 2008)

Shh expression can be found in a wide variety of tissues and it is the most broadly expressed Hh protein in mammals. Thus, it has been suggested that Shh plays essential roles in many development processes and in controlling cellular differentiation and proliferation (Varjosalo and Taipale 2008). During embryogenesis, Shh is expressed in midline tissues and regulates the patterning of embryonic tissues, including the spinal cord, the axial skeleton and limb development (Chiang et al. 1996). Shh is also involved in organogenesis, including development of eye, ear and kidney (Varjosalo and Taipale 2008). Thus, aberrations in Shh signalling cause serious developmental defects in many tissues and lead to embryonic lethality (Heussler and Suri 2003).

On the other hand, expression of Ihh is more restricted. Approximately half of Ihh-/- embryos die during early embryogenesis due to poorly developed yolk sac (Dyer et al. 2001). In later development, Ihh is important for bone growth. Defects in Ihh signalling cause reduced proliferation of chondrocytes and osteoblast leading to truncation of long bones. (Razzaque et al. 2005, St-Jacques et al. 1999).

Finally, Dhh has been shown to be essential for proliferation of the male germ-line. Dhh mutant mice are viable and do not show notable phenotypes in most tissues but have severe defects in spermatogenesis and defects in Schwann cell function (Clark et al. 2000, Parmantier et al. 1999).

1.3 The role of Hh signalling in haematopoiesis

In the last decade, a growing body of evidence has supported the hypothesis that Hh signalling plays an important role in various stages of haematopoiesis. The first two studies that showed Hh signalling is involved in the control of hematopoietic differentiation were conducted by Detmer et al. (2000) and our lab (Outram et al. 2000). In the Detmer study, when haematopoietic progenitors were cultured in formulated semisolid medium in the presence of cyclopamine, an inhibitor of Hh signal transduction, the number of erythroid colonies generated by bone marrow cells was significantly reduced and the process of erythroid maturation was delayed. In contrast, when recombinant Shh peptide was added to cultures of hematopoietic progenitors, the number of granulocyte and monocyte colonies was increased and the erythroid colonies were noticeably larger.

In addition, Bhardwaj et al. (2001) found that cell proliferation and the numbers of human primitive haematopoietic progenitors were significantly increased when they were treated with soluble forms of either Shh or Dhh. It was also suggested that the activity of Shh was associated with control of bone morphogenetic protein (BMP)-4 signalling and this association was critical to the proliferation and differentiation of primitive hematopoietic cells.

Supporting these studies, analysis of HSC from Gli1-null mice has indicated that Gli1 is essential for the regulation of haematopoiesis. Loss of Gli1 results in reduced production of granulocytes and also defects in the differentiation of myeloid progenitors and stress haematopoiesis (Merchant et al. 2010). A study of Ptch-/- mice showed that the HSC pool is expanded when the Hh signal is enhanced (Trowbridge et al. 2006).

In addition to its role in HSC proliferation and differentiation, a growing body of evidence shows that Hh signalling plays essential roles in controlling survival, proliferation and differentiation of thymocytes. The first study demonstrated that Hh signalling influences thymocyte development was published in 2000 by our lab (Outram et al. 2000). In those studies, treatment of mouse fetal thymus organ cultures (FTOC) with recombinant (r)-Shh protein resulted in an arrest of thymocyte development, whereas adding Hh inhibitors to neutralize the endogenous Hh signals led to an increase in DP cell production (Outram et al. 2000, Shah et al. 2004). These studies suggested that Hh signalling was a negative regulator of T-cell development.

On the other hand, *ex vivo* analysis of Shh -/- mice thymus suggested that Hh proteins play a positive role in differentiation from the DN to DP stage, as thymus isolated from Shh knock out (KO) embryos contain a smaller number and proportion of DP cells when compared to wildtype (WT) littermates (Shah et al. 2004). It was believed that the dual functions of Shh in regulating the transition of DN to DP stage might be due to concentration and the duration of the signals received by thymocytes (Crompton, Outram, & Hager-Theodorides 2007).

In fact, the role of Hh signalling in thymocyte development has been widely studied in the last decade, the more detail will be discussed in chapter 6.

Although there is a growing body of evidence showing that Hh signalling plays essential roles in controlling proliferation and differentiation of haematopoiesis, two studies were conducted recently implied that Hh signalling is not required for haematopoietic homeostasis. Both of these studies used conditional deletion of Smo and suggested that loss of Smo had no effect on the regulation of adult HSC and progenitor homeostasis differentiation, and maintenance, neither under normal nor under stress conditions (Gao et al. 2009, Hofmann et al. 2009).

Objectives

The role of the Hh signalling pathway and its mediators in haematopoiesis is still not fully understood and controversial. In this project, I will mainly investigate the role of Hh signalling and its components in two areas: (1) erythroid development and (2) regulation of the T-cell lineage. The functions of Hh proteins in these two areas will be discussed in the rest of the thesis. In **chapter 3** and **chapter 4**, I will investigate if Dhh plays a role in erythropoiesis in normal conditions and under haematopoietic stress. In **chapter 5**, I will test the function of different Hh components in definitive erythropoiesis during embryogenesis. Finally, in **chapter 6**, the role of Hh target genes, Foxa1 and Foxa2 in T-cell development and their functions in peripheral T-cell homeostasis will be studied.

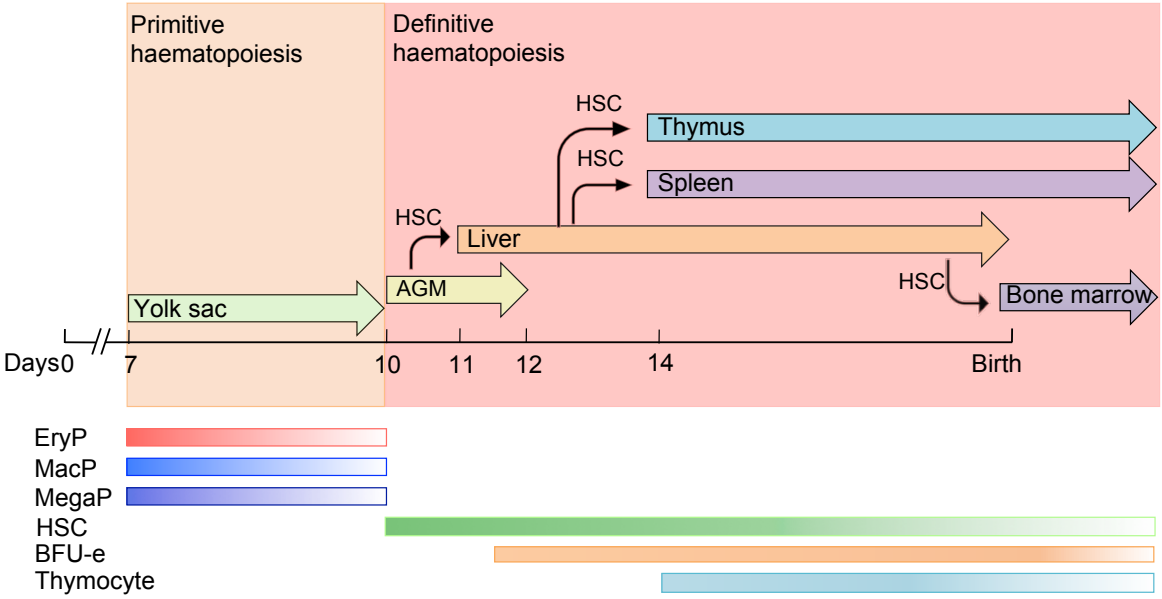

Figure 1.1 Primitive and definitive haematopoiesis in mouse

Primitive erythroid development starts at E7. At this stage, the EryP are produced at the yolk sac and up until E10, few MacP and MegaP are detected. Haematopoiesis then shifts to AGM to produce definitive HSC, and so the definitive haematopoiesis wave begins. Shortly after, HSC are seeded to the fetal liver and initiate the differentiation of haematopoietic cell development at E11. Thereafter, BFU-E are detected at E11.5 in the fetal liver. In the mid-gestation, HSC seed the spleen and thymus from fetal liver to continue haematopoiesis and T-cell development before birth.
HSC = Haematopoietic stem cell, AGM = Aorta-gonads-mesonephros, EryP = Primitive erythroid progenitor, MacP = Primitive macrophage progenitor, MegaP = Primitive megakaryocyte progenitor

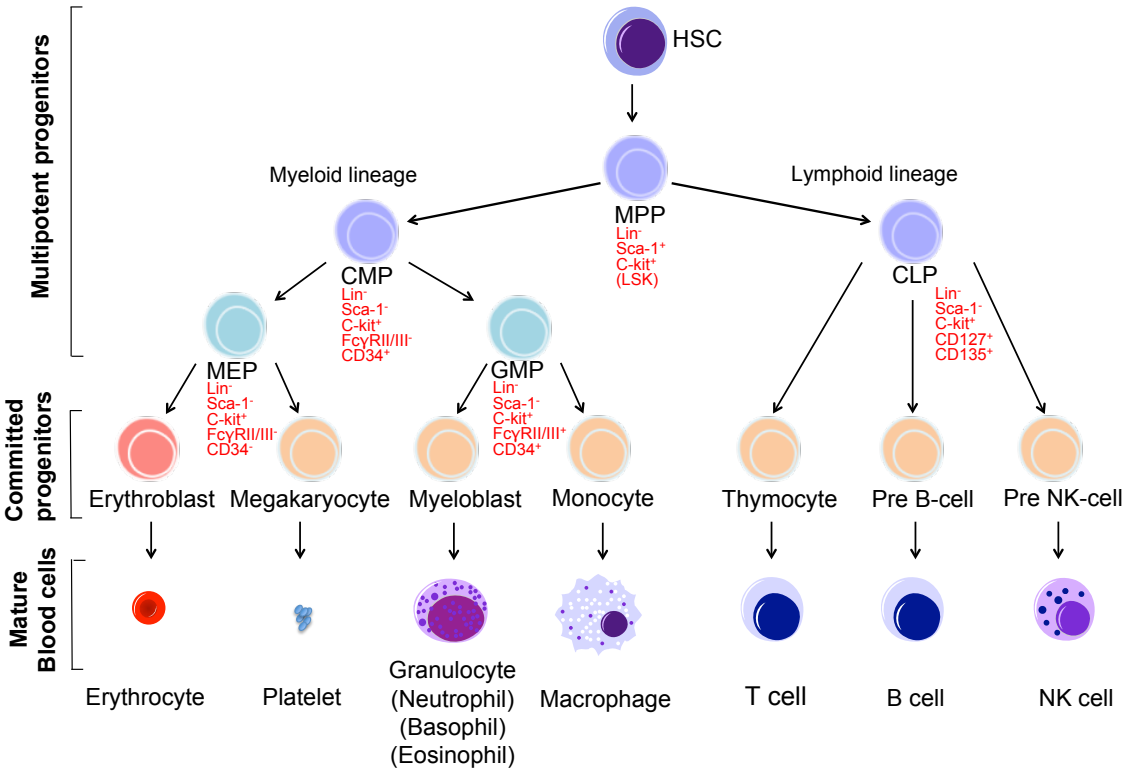

Figure 1.2 Haematopoietic cell development

Figure showed haematopoietic cell development from HSC to mature blood cell. HSC first give rise to MPP (LSK), which then differentiate into either CMP or CLP to commit to either myeloid or lymphoid lineage. The CMP then differentiate into either MEP or GMP and finally give rise to mature erythrocyte, platelet, neutrophil, basophil, eosinophil and macrophage, while CLP give rise to T and B lymphocyte and NK cell. The multipotent progenitors can be identified by their expression of cell surface makers (written in red).
HSC = Haematopoietic stem cell, MPP = Multipotent progenitor CMP = Common myeloid progenitor, CLP = Common lymphoid progenitor, MEP = Megakaryocyte-erythroid progenitor, GMP = Granulocyte-monocyte progenitors.

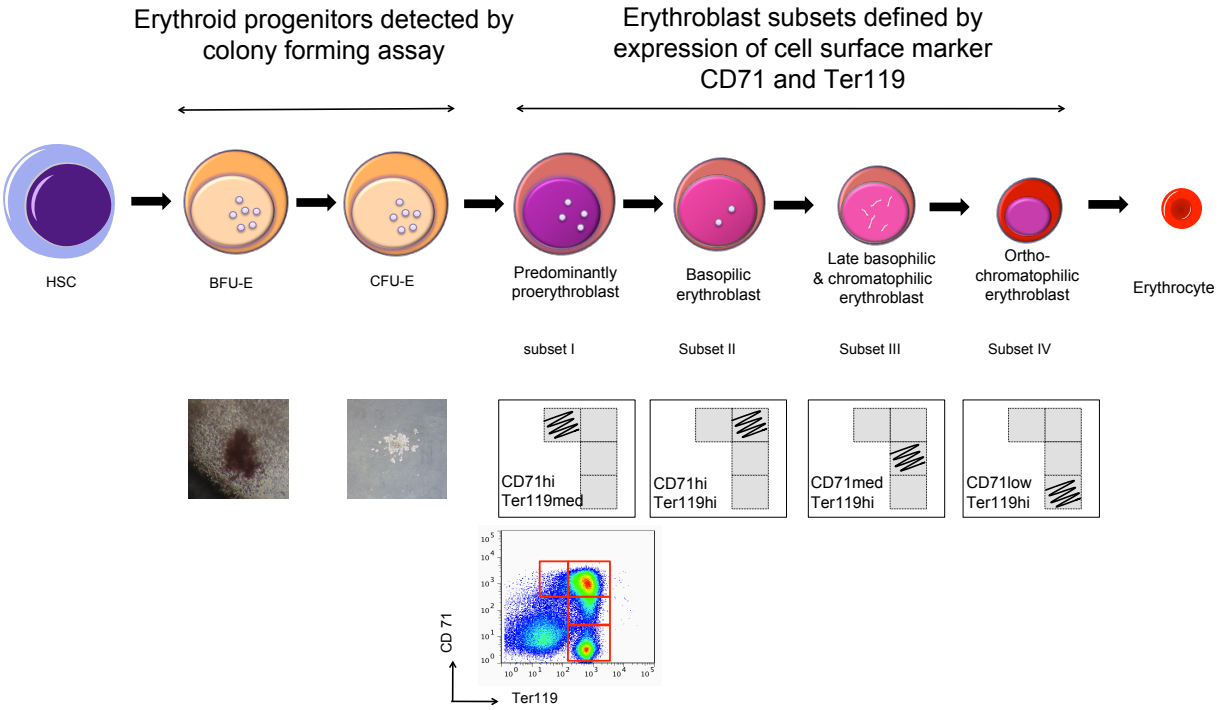

Figure 1.3 Erythroid development in mouse

Figure showed erythroid development from HSC to fully developed erythrocyte. BFU-E is the first erythroid committed progenitor, that give rise to the more mature CFU-E progenitor. These two populations can be identified and enumerated by colony forming cell assays. Photos represent BFU-E and CFU-E forming in methylcellulose medium. CFU-E then differentiate into erythroblast populations. There are four subsets of erythroblast that have been identified and can be recognized by the expression of the cell surface markers, CD71 and Ter119. Finally, erythroblasts expel their nuclei and become fully mature erythrocytes.

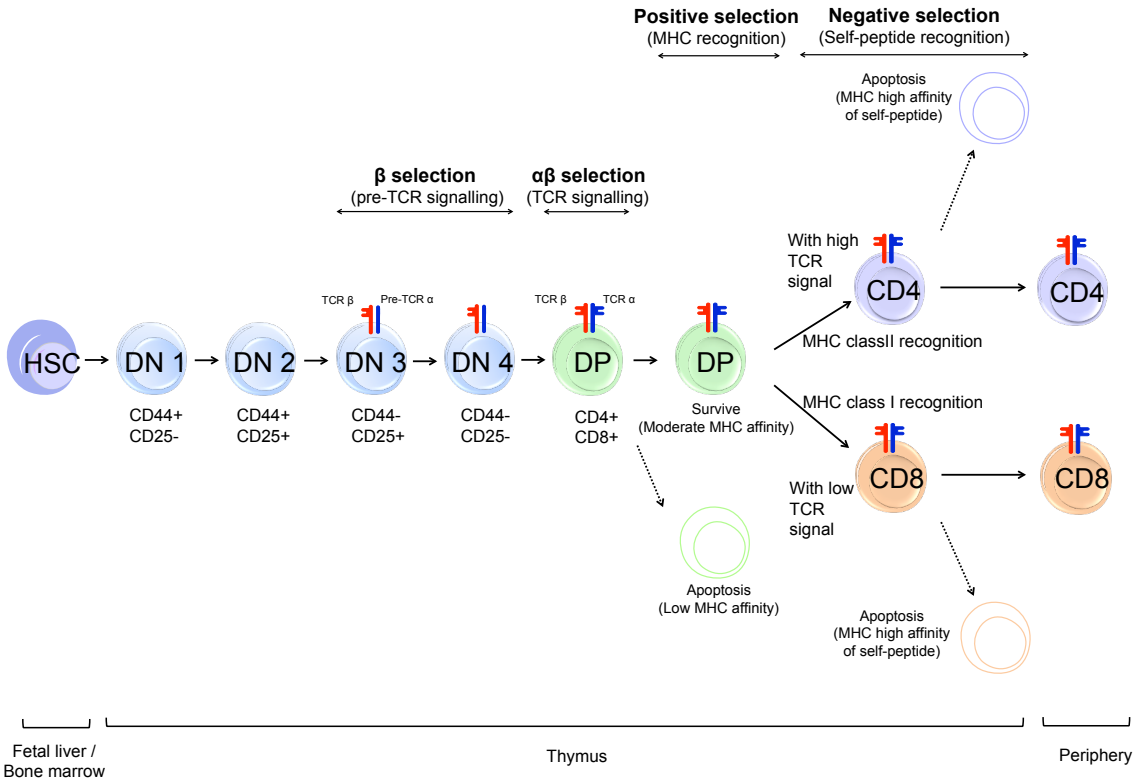

Figure 1.4 T-cell development in mouse

Thymocyte development undergoes a series of stages and selection processes. β selection occurs at the DN3 stage, in which TCR β chain genes are rearranged and form a pre-TCR complex with pre-TCR α chain. TCR α chain rearrangement occurs in DP to complete the αβ TCR signalling and complete αβ selection. Positive selection selects DP thymocytes with moderate affinity of MHC, in which their TCR with a strong signal and which recognizes MHC class II molecules are committed to CD4SP T-cells, while their TCR with a weak signal which recognizes MHC class I molecules are committed to CD8SP T-cells. DP cells with TCR that cannot recognize MHC or with low MHC affinity undergo apoptosis. Before exiting the thymus and migrating to the lymphoid organs in the periphery, thymocytes go through negative selection to eliminate T-cells with high affinity TCR for self-peptide.
DN = Double negative cells, DP = Double positive cells, TCR = T-cell receptor

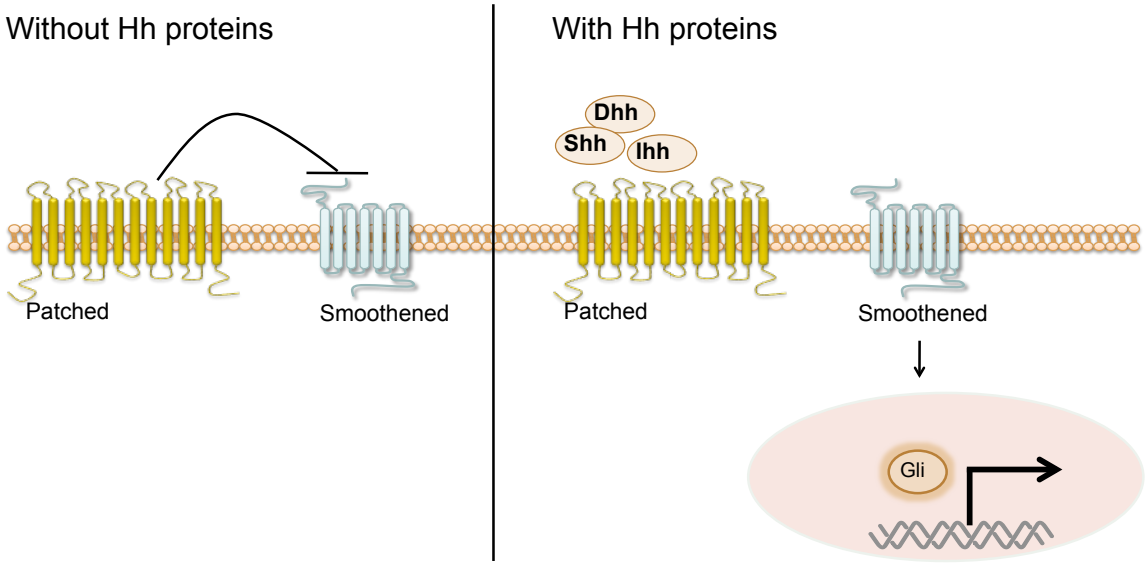

Figure 1.5 Hedgehog signalling

In the absence of Hh proteins, Ptch inhibits Smo activity and results in repression of down-stream transcription activation. On activation by binding a member of the Hh proteins to Ptch, inhibition of Smo activity is relieved thus leading to the transcription of specific Hh target genes by the Gli family of transcription factors.

Chapter Two : Methods and Materials

2.1 Mice

$Smo^{flox/flox}$, Gli3+/- and CD4-cre transgenic mice were purchased from The Jackson Laboratory (Bar Harbour, Maine). C57BL/6 mice were purchased from Charles River (UK). Dhh+/- and Ihh+/- mice were kind gifts from Dr. Andrew McMahon (Bitgood et al. 1996, St-Jacques et al. 1999). Vav-cre transgenic mice were a gift from Dr. Dimitris Kioussis (de Boer et al. 2003). $Foxa1^{flox/flox}$ $Foxa2^{flox/flox}$ mice were a gift from Dr. Siew-Lan Ang (Ferri et al. 2007). All mice were bred and maintained at University College London (U.K.). Genotypes of adult mice were determined by polymerase chain reaction (PCR) of genomic DNA as described in below (**2.13**).

2.2 Irradiation

Mice aged 4-6 weeks were given a single total-body dose of 4 Gy from a ^{60}Co gamma-ray source at a dose rate of 0.28 Gy/min. The mice were placed in ventilated containers during irradiation.

2.3 Cell Isolation

Bone marrow cells were isolated from the femur. The ends of the femur were trimmed to expose the interior marrow shaft, and then the bevel of a needle attached to a 1ml syringe, containing 1 ml of cold AIM-V medium, (Life Technologies, Gaitersburg, MD) was inserted into the marrow shaft and used to

flush out the bone marrow cells. Cells isolated from fetal liver, adult thymus, spleen and lymph nodes were harvested and crushed between two frosted glass slides.

2.4 Antibodies and Flow Cytometry

2.4.1 Cell surface staining

Cells were stained using combinations of the following directly conjugated antibodies supplied by BD Pharmingen (San Diego, CA): anti-CD3^{FITC}, anti-CD4^{FITC}, anti-CD4^{APC}, anti-CD5^{PE}anti, anti-CD8^{APC}, anti-CD8^{cychrome}, anti-CD25^{FITC}, anti-CD69^{PE}, anti-CD71^{FITC}, anti-Gr-1 ^{FITC}, anti-HSA$^{PerCP\text{-}cy5.5}$anti-Ly6G^{PE}, anti-Mac-1$^{PerCP\text{-}cy5.5}$, anti-Qa2^{Fitc} and anti-TER119^{PE} . Progenitor cell population analysis was done by staining with lineage specific antibodies (anti-CD3 ^{PE}, anti-CD4^{PE}, anti-CD8 ^{PE}, anti-B220 ^{PE} anti-Mac-1^{PE}, anti-Gr-1^{PE}, anti-CD19 ^{PE}), anti-CD34^{Fitc}, anti-FcϒII/III$^{PerCP\text{-}cy5.5}$, anti-Sca-1^{APC} and anti-C-kit$^{Pe\text{-}cy5}$. Cell suspensions were stained for 30 minutes on ice in phosphate buffered saline (PBS) (Sigma-Aldrich) supplemented with 2% FCS and 0.01% sodium azide.

2.4.2 Annexin-V apoptosis staining assay

Annexin-V staining was carried out using an Annexin-V-FITC apoptosis detection kit (BD Pharmingen) according to manufacturer's instructions. Prior to Annexin-V staining, cells were stained as described above.

2.4.3 Smoothened(Smo) and Patched(Ptch) surface staining

For cell surface Smo or Ptch staining, cells were first incubated for 30 minutes in PBS with 1.5% donkey serum (Santa Cruz Biotechnology). After washing with PBS, cells were incubated with 0.5µg anti-CD16/CD32 (Pharmingen) in 50µl of PBS for 5 minutes. Cells were then incubated with 2µg of anti-Smo, N-19 or anti-Ptch (Santa Cruz Biotechnology) or goat IgG (Santa Cruz Biotechnology) as isotype control in 50µl of PBS for 60 minutes and washed with PBS and 0.5%BSA. Cells were then incubated with 2µg of Biotin-conjugated $F(ab')_2$ fragment of donkey anti-goat IgG (Santa Cruz Biotechnology) in 50µl of PBS and 1.5% donkey serum for 30 minutes and washed with PBS and 0.5%BSA. Cells were finally incubated with directly conjugated antibodies: anti-streptavidin^{cychrome}, anti-CD71^{FITC}, anti-Ter119^{PE} as above.

2.4.4 Propidium iodide staining

For propidium iodide (PI) staining, cells were permeabilized in 0.1% Triton X-100 (Sigma) and incubated with 50µg/ml PI (Sigma) in 100µg/mL of RNase (Sigma) in PBS for 10 minutes in the dark at room tempature. Samples were analysed on a FACSCalibur (Becton Dickinson) or Accuri C6.

2.4.5 Intracellular staining for cyclin B1

Purified Ter119+ve cells were incubated with permeabilization buffer for 30 minutes in the dark. Following this, cells were washed twice with permeabilization buffer then stained with anti-cyclinB1 antibody in

permeabilization buffer for 30 minutes. After incubation, cells were washed twice with permeabilization buffer followed by washing with FACS buffer. Samples were analysed on FACSscan (Becton Dickinson, Franklin Lakes, NJ)

2.4.6 Intracellular staining for Foxp3

Intracellular staining of Foxp3 was performed using the PE anti-mouse Foxp3 Staining Set (eBiosciences, San Diego, CA). Splenocytes were isolated and stained with anti-$CD4^{Percp\text{-}cy5.5}$ and anti-$CD25^{FITC}$. After washing with PBS, cells were incubated with Fixation/Permeabilization working solution for 30 minutes in the dark. Following this, cells were washed twice with permeabilization buffer then stained with anti-Foxp3 antibody in permeabilization buffer for 30 minutes. After incubation, cells were washed twice with permeabilization buffer followed by washing with FACS buffer. Samples were analysed on an Accuri C6.

2.4.7 Intracellular staining for Cytokines

Splenocytes were isolated and cultured in AIM-V medium (Life Technologies) supplemented with 50ng/ml PMA (Sigma), 500ng/ml Ionomycin (Sigma) and 3μg/ml Brefeldin A (eBiosciences) (Sigma-Aldrich) at a concentration of 5×10^6 cells/ml in 12 well plates (Nunc) at 37°C and 5% CO_2. Activation of the cells was carried out using 0.01μg/ml of anti-CD3 and anti-CD28 (BD Pharmingen). Cells were harvested at 4 hours and stained with anti-$CD4^{Percp\text{-}cy5.5}$ and anti-$CD8^{APC}$. Cells were then fixed and permeabilized (Fix and Perm cell permeabilization

kit, Caltag Laboratories) and stained for intracellular anti-IL-2, anti-IFN-γ, anti-IL-4, anti-IL13 and anti-IL17 expression.

2.5 Cell sorting and purification

Thymocytes, granulocytes and macrophage were removed using a cocktail of PE- conjugated antibodies: anti-CD3, anti-CD4, anti-CD8, anti-Gr-1 and anti-Mac-1. The remaining cells were stained with $CD71^{FITC}$ and $Ter119^{Percp\text{-}cy5.5}$ and sorted using Molecular Flow Cytometer (Cytomation, Fort Collins, CO). To obtain populations of developing thymocytes, cell suspension from thymus were stained anti-$CD4^{PE}$, anti-$CD8^{PerCP\text{-}cy5.5}$, anti-$CD25^{FITC}$, anti-$CD44^{APC}$ and sorted using Molecular Flow Cytometer. To obtain erythroblast subsets, erythroid lineage cells (Ter119+ve) in bone marrow and spleen cell suspensions were purified by magnetic bead separation using the EasySep Biotin positive selection kit (StemCell Technologies, UK), according to the manufacturer's instructions.

Progenitor cell populations were acquired on LSRII (BD Pharmingen). All other samples were acquired on a FACScan (Becton Dickinson, New Jersey, USA) or Accuri C6 (Becton Dickinson, New Jersey, USA). Data were analyzed using FlowJo 7.6.5 software. Live cells were gated according to their forward scatter (FSC) and side scatter (SSC) profiles.

2.6 Foetal Thymic Organ Cultures

C57BL/6 mice E17.5 foetal thymi were cultured on 0.8μm membrane filters (Millipore, Massachusetts, US) on 1 ml AIM-V medium (Life Technologies, US) in 24-well plates (Nunc) with treatment of 0.5μg/ml of recombinant mouse Shh (Cat: 464-SH, R&D, US).

2.7 Reticulocyte counts

Blood smears were prepared by tail bleeding from mice. Assessment of reticulocytes in blood was carried out by counting of reticulocytes under microscope after staining with Giemsa-stain. The staining and counting was performed by Dr Johannes Dessens (London School of Hygiene and Tropical Medicine, London, UK).

2.8 Spleen Histology

Spleens were isolated and fixed in phosphate-buffered formalin (10% volume/volume), paraffin-embedded, and sectioned for H&E staining, performed by Histopathology, Great Ormond Street Hospital. Pictures were photographed by Leica DFC320 digital camera (Leica Microsystems) with Leica DMIL Microscope (Leica Microsystems), and acquired by software Leica Qwin vLite3.2.1 (Leica Microsystems). Quantification of red pulp (RP) and white pulp (WP) surface area on H&E-stained sections was carried out using ImageJ (v1.45b software http://imagej.nih.gov/ij/).

2.9 Haematopoietic Colony Assay

Colony forming cell assays were performed using methocult methylcellulose based medium (StemCell Technologies, UK). 2 x 10^6 bone marrow cells and 2 x 10^7 spleen cells were plated in 1 ml of methylcellulose medium (M3434) in a 35mm culture dish (StemCell Technologies, UK). The cultures were incubated at 37^{o}C in 5% CO_2. BFU-E on methylcellulose medium were enumerated after 7 days in culture.

2.10 Erythroblast cell culture and purification

Bone marrow cells were isolated and cultured at a concentration of 5x10^6 cells/ml in AIM-V medium at 37^{o}C and 5% CO_2. Cells were harvested at 18 hours and Ter119+ erythroblast populations were purified by magnetic bead separation using the EasySep Biotin positive selection kit (StemCell Technologies, UK) according to the manufacturer's instructions.

2.11 T-cell activation assay

Splenocytes were isolated and cultured in AIM-V serum-free medium (Life Technologies) at a concentration of 5 x 10^6 cells/ml in 12-well plates (Nunc) at 37°C and 5% CO_2. Activation of the cells was carried out by treatment with 0.01μg/ml of anti-CD3 and anti-CD28 (BD Pharmingen). Cells were harvested at 4, 18 and 40 hours and analyzed by flow cytometry, on the Accuri C6.

2.12 Carboxyfluorescein diacetate succinimidyl ester (CFSE) proliferation assay

CFSE (Sigma-Aldrich) intracellular labelling was carried out by incubating spleen cells at $1x10^6$ with 10μM CFSE and resuspended in PBS for 10 minutes at 25°C in the dark. Labelled cells were then washed twice in PBS in order to ensure cultures did not contain any non-incorporated CFSE that would interfere with results. Cells were cultured in AIM-V medium with 0.01μg/ml of anti-CD3 and anti-CD28 at 37°C and 5% CO_2 for up to three days. Cultured cells were stained with anti-CD4 and anti-CD8 as described above and analyzed by flow cytometry, on the Accuri C6.

2.13 Genotyping

2.13.1 DNA Extraction

DNA from mice was extracted from 2mm ear biopsies by placing in 100μl lysis buffer (50mM KCL, 10mM Tris HCL (pH 8.5), 1.5mM $MgCL_2$, 0.01% gelatin, 0.45% Noident P-40, 0.45% Tween20) and 1μl of 0.5μg/ml Proteinase K (Sigma-Aldrich) in ultra pure water (Life Technologies) and incubating on a shaker at 500rpm at 56°C overnight. Samples were then spun at 13000rpm in a micro-centrifuge for 5 minutes before use.

2.13.2 Polymerase chain reaction (PCR)

DNA(1μl) prepared as above was used as a template in each PCR reaction. The primers used for amplifying the specific PCR products are listed in table 2.1.

Each PCR reaction was carried out in 20μl mix consisting of 1 μl of DNA, 10 μl of 50% 2x GreenTaq DNA Polymerase (Sigma-Aldrich, US) and 1μM of each relevant primer made up with ultra pure water (Life Technologies, US). PCR was carried out on a Stratagene Robocycler (Stratagene, US) as follows:

For Dhh: 5 minutes at 94°C, 38 cycles for 1 min 30 sec at 94°C, 1 minute at 58°C, 1 min 20 sec at 72°C and 10 minutes at 72°C.

For Foxa1 and Foxa2 floxed gene: 5 minutes at 94°C, 35 cycles for 1 min 20 sec at 94°C, 1 minute at 57°C, 1 min 20 sec at 72°C and 10 minutes at 72°C.

For CD4-cre: 5 minutes at 94°C, 32 cycles for 1 min 20 sec at 94°C, 1 minute at 61°C, 1 min 30 sec at 72°C and 10 minutes at 72°C.

For Vav-cre: 5 minutes at 94°C, 29 cycles for 30 seconds at 94°C, 1 minute at 65°C, 30 seconds at 72°C and 8 minutes at 72°C.

PCR products were resolved on a 2 % agarose (Sigma-Aldrich, US) 1x TBE (Life Technologies, US) gel, stained with GelRed (Biotium, US). A marker, HyperladderII ranging from 50 to 2000bp (Bioline, UK) was also electrophorised to estimate band size of samples. The gel was visualized under ultraviolet light (Herolab, Germany) and a photograph taken (Sony).

2.14 RNA extraction and cDNA synthesis

Cell suspensions were pelleted and resuspended in appropriate amounts of lysis buffer and β-mercaptoethanol (Stratagene). RNA was extracted according

to the protocol of the Stratagene Strataprep® Total RNA Miniprep Kit, including a DNase digestion step. cDNA was synthesised from this RNA using Superscript III (Invitrogen, Carlsbad, CA). The reaction mix was made up as follows: 50-100ng RNA, 800µ dNTPs (Promega), 500ng Random Primers (Promega), 13µl HPLC grade water (Sigma-Aldrich) and incubated at 65°C for 5 minutes to denature the RNA. RNA were placed on ice for one minute before being spun briefly, and the following solution added: 20% first stranded buffer (Invitrogen), 10mM DTT (Invitrogen), 200 units Superscript III Reverse Transcriptase (Invitrogen). Total volume of 20µl of the mix was taken and incubated at 25°C for 10 minutes to allow primer binding. The mix was then placed at 42°C for 50 minutes to allow elongation and it was heated to 70°C for 15 minutes to terminate the reaction. RNA was stored at -80°C and cDNA at -20°C.

2.15 Quantitative Real-Time Reverse Transcribed Polymerase Chain Reaction (qRT-PCR)

RT-PCR was carried out by analysis of each cDNA sample in triplicate on an iCycler (Bio-Rad Laboratories, Hercules, CA) using the iQ™SYBR® Green Supermix (Bio-Rad) according to manufacturer's instructions. The housekeeping gene Glyceraldehyde 3-phosphate dehydrogenase (GAPDH) was used to allow quantification of template and normalisation of each gene. Amplification of GAPDH was quantitated using a dilution series of cDNA prepared from embryo head RNA. The primers used for qPCR are listed in Table2.2. Primers were selected that span exon-exon boundaries to prevent the

amplification of genomic DNA. Each reaction mixture contained the following: approximate 10ng cDNA, 0.3M forward primer, 0.3M reverse primer, 10µl SYBR Green 2X supermix (containing 100mM KCL, 40mM Tris-HCL, pH8.4, 0.4mM of each dNTP (dATP, dCTP, dGTP, dTTP) iTaq™ DNA polymerase (50 units/ml), 6mM $MgCl_2$, SYBR Green 1, 20nM fluorescein and stabilizers) made up to 20µl with HPLC grade water.

RT-PCR was performed under the following conditions:

For *Gli1*: 3 minutes at 95°C, 30 seconds at 95°C then 45 cycles for 30 seconds at 60.4°C, 30 seconds at 95°C, 30 seconds at 48°C.

For *Smo*: 3 minutes at 95°C, 30 seconds at 95°C then 45 cycles for 30 seconds at 60°C, 30 seconds at 95°C, 30 seconds at 48°C.

For *Ptch*: 3 minutes at 95°C, 30 seconds at 95°C then 40 cycles for 30 seconds at 60.3°C, 30 seconds at 95°C, 30 seconds at 48°C.

For *Dhh*: 3 minutes at 95°C, 30 seconds at 95°C then 40 cycles for 30 seconds at 61.3°C, 30 seconds at 95°C, 30 seconds at 48°C.

For *Foxa1*: 3 minutes at 95°C, 30 seconds at 95°C then 40 cycles for 30 seconds at 57°C, 30 seconds at 95°C, 30 seconds at 48°C.

In each experiment a melt curve was also carried out, according to the manufacturer's programme, to check the melting temperature of the products

produced to insure the product was the size expected and not the result of primer-dimers.

Actβ, Hprt, Foxa2, Gata1 and *Lmo2* RT-PCR Primers were purchased from Qiagen (Quantitect primer assay).

2.16 Real time PCR arrays with sorted erythroblast subset II in WT and Dhh-/-

RNA was extracted from sorted erythroblast subset II and was used for cDNA synthesis using the RT^2 First strand kit (SABiosciences, QIAGEN, MD, USA) following the manufacturer's instructions. The mouse haematopoietic stem cells and haematopopiesis RT^2 profiler PCR arrays (PAMM-054) were carried out by analysis of cDNA sample on an iCycler (Bio-Rad Laboratories, Hercules, CA) according to the manufacturer's programme.

2.17 Statistical analyses

A paired t test using two-tailed p value was used to test the significance of differences between WT and KO/heterozygous littermates. Values of $p < 0.05$ were considered to be significance.

Transcript	Direction of Primer	Oligonucleotide Sequence	Product size (bp)
Dhh WT gene	Forward Reverse	ATCCACGTATCGGTCAAAGC GGTCCAGGAAGAGCAGCAC	442
Dhh mutated gene	Forward Reverse	GGCATGCTGGGGATGCGGTG GGTCCAGGAAGAGCAGCAC	110
CD4-cre	Forward Reverse	CGATGCAACGAGTGATGAGG GCATTGCTGTCACTTGGTCGT	300
Vav-cre	Forward Reverse	AGATGCCAGGACATCAGGAACCTG ATCAGCCACACCAGACACAGAGATC	300
Foxa1 WT and loxP gene	Forward Reverse	CTGTGGATTATGTTCCTGAT GTGTCAGGATGCCTATCTGGT	WT 290 loxP 450
Foxa2 WT and loxP gene	Forward Reverse	CCCCTGAGTTGGCGGTGGT TTGCTCACGGAAGAGTAGCC	WT 290 loxP 450

Table 2.1 Primers used for genotyping and PCR analysis

Transcript	Direction of Primer	Oligonucleotide Sequence
Dhh	Forward Reverse	CTGATGACAGAGCGTTGC TCGTAGTGGAGTGAATCCTG
Foxa1	Forward Reverse	AGGAGGCCTACTCCTCTGTC GCGTAGGACATGTTGAAGGA
Smo	Forward Reverse	TTCTTCAACCAGGCTGAGTG CGTATGGCTTCTCATTGGAGTG
Ptch	Forward Reverse	TGCTCTCCAGTTCTCAGACTC CCACAACCTTGGGTTTGG
Gli	Forward Reverse	AAACCTCAAGACGCACCTTCGG CGTATCCDTTCTCATTGGAGTG

Table 2.2 Primers used for RT-PCR

Chapter Three : Dhh in erythropoiesis

Abstract

The Hedgehog signalling pathway plays an important role in the regulation of cell differentiation in various tissues during development. Recent findings suggest that the Hh signalling pathway is involved in controlling haematopoiesis. However, the specific functions of Dhh in controlling erythroid development are yet to be determined. In this study, we showed that Dhh plays a negative regulatory role in erythropoiesis in normal conditions. Analysis of mice deficient in Dhh revealed that the production of erythroblast populations is increased which leads to a larger spleen in Dhh-/- mice. Further investigation of haematopoietic progenitors showed that Dhh is also involved in regulation of myeloid progenitor differentiation. Analysis of Lmo2 expression in Dhh-/- erythroblasts cultured with rDhh and anti-Hh neutralizing antibody, showed that Lmo2 is a direct functional target of Dhh signalling in the later stages of erythroblast differentiation.

Declaration of Publication

Some data in the following chapter is taken from a publication titled ”Regulation of murine normal and stress-induced erythropoiesis by Desert Hedgehog” in Blood. 2012 May 17;119(20):4741-51. The manuscript was written by. CI Lau and T Crompton. CI Lau and SV Outram are co-first authors in this paper.

3.1 Introduction

3.1.1 Regulation of erythropoiesis

The process of erythropoiesis occurs in several stages, and is tightly regulated, under the control of a series of growth factors and their regulated genes. The most well-known growth factor for development of erythrocytes is erythropoietin (Epo), which is a glycoprotein hormone. Epo is a key erythropoietic factor that acts through binding to its receptor (EpoR) to control cell survival, proliferation and differentiation of erythroid lineages (Lin et al., 1996). The proliferation of primitive erythroid lineages is dependent on the Epo signal, whereas Epo acts as a survival factor in the definitive erythroid lineage and also functions as a growth factor for the survival and proliferation of proerythroblasts (Koury and Bondurant 1990).

Furthermore, the differentiation of haematopoietic cells is highly regulated by the coordination of lineage specific transcription factors. The role of the transcription factor, Gata-1, in erythropoiesis has been well established. Gata-1 acts as a key regulator and plays a central role in erythroid development (Fujiwara et al. 1996). Expression of Gata-1 is essential throughout the process of erythropoiesis (Ghinassi et al. 2007). Loss of Gata-1 causes severe anaemia due to complete ablation of primitive and definitive erythropoiesis and results in embryonic death at day E10.5-E11.5 in mouse (Fujiwara et al. 1996). Gata-1 activity and the degree of its expression at each stage are also critical for the erythroid lineage commitment choice. It has been shown that loss of Gata1 impairs the maturation of the bipotent erythroid and megakaryocytic

progenitor, MEP (Ghinassi et al. 2007, Stachura et al. 2006). In contrast, enforced expression of Gata-1 is able to reprogram CLP and GMP to convert to MEP and differentiate into the erythroid lineage (Iwasaki et al. 2003).

In addition to Gata-1, other transcription factors are also important in the process of erythroid development. Gata-1 has been reported to interact with Lmo2, FOG-1, E2A, Scl and Ldb-1 to form a protein complex that regulates the transcription of Gata target genes that regulate erythropoiesis. All five of these proteins are required to assemble together and establish the DNA-binding complex (Wadman et al. 1997). Thus, each of these proteins is essential for the control of erythroid development. Interestingly, Lmo2 is a key element to this protein complex, which acts as a bridge to connect Scl, E2A to Ldb-1 and Gata-1 (Wadman et al. 1997).

3.1.2 Desert hedgehog (Dhh)

The three mammalian Hh proteins are highly conserved and share the same signalling pathway. However, their distinct patterns of expression may lead to different roles in development (Varjosalo and Taipale 2008).

In the murine embryo, Dhh is expressed in various tissues, including the fetal liver (Cridland et al. 2009), heart, blood vessels, epithelium (Bitgood and McMahon 1995), testis (Bitgood et al. 1996), ovaries (Ren et al. 2012) and peripheral nerve tissue (Parmantier et al. 1999). The distinct expression pattern of Dhh during embryogenesis indicates that it may play a role in a wide range of functions in development.

However, expression of Dhh is restricted to the spleen (Perry et al. 2009), thymus (Sacedon et al. 2003), testis (Szczepny et al. 2006), ovaries (Spicer et al. 2009) and peripheral nerves (Bajestan et al. 2006) in adult. Dhh is essential for the development of the gonads. Male Dhh-deficient mice are infertile due to a failure of spermatogenesis (Clark et al. 2000). In contrast, although Dhh is involved in follicle cell development, female Dhh KO mice are fertile and do not show disrupted ovarian phenotype (Wijgerde et al. 2005). Other specific roles for Dhh were identified in peripheral nervous tissue, where Dhh was shown to be necessary for survival and regeneration of Schwann cells, and for the peripheral nerve signals for ischemia-induced angiogenesis (Bajestan et al. 2006, Renault et al. 2013).

3.1.3 Hh signalling in erythroid development

Several studies have suggested that Hh signalling is involved in regulating the differentiation of the erythroid lineage. It was found that inhibition of Hh signalling pathway delays the morphological change of erythroid maturation and alters the formation of erythroid progenitor colonies (Detmer et al. 2005).

Although it has been suggested that Hh signalling is involved in regulating haematopoiesis and erythroid proliferation, these studies did not reveal which member of the Hh protein family mediates these functions *in vivo*. Recently, it was shown that Ihh is required for erythropoiesis and it was suggested that mid-gestational anaemia was responsible for the embryonic lethality of Ihh KO mice (Cridland et al. 2009).

In addition, Hh signalling has also been implicated in stress erythropoiesis, of which more detail will be discussed in chapter 4.

Objectives:

In previous studies, Hh signalling has been shown to be involved in proliferation and differentiation of erythroid cells. However, the functions of Dhh in controlling erythrocyte development in mice are yet to be determined. This chapter presents data from experiments using Dhh-/- adult mice to investigate the importance and functions of Dhh in erythroid development.

3.2 Results

3.2.1 Dhh and Hh signalling components are expressed in adult spleen and bone marrow

Erythropoiesis takes place in the spleen and bone marrow in adult mice. In order to investigate whether Dhh plays a role in erythropoiesis, the expression of *Dhh* mRNA in spleen and bone marrow was first examined by quantitative RT-PCR (qRT-PCR). We found that *Dhh* was highly expressed in the spleen, whereas low expression of *Dhh* was also detected in bone marrow, compared to Dhh-/- spleen and bone marrow, which acted as negative control (Figure 3.1A). Moreover, transcription of *Dhh* was also detected in WT spleen stroma but not in Dhh-/- spleen stroma (Figure 3.1B). These data are consistent with previous studies, which demonstrated that Dhh was expressed in stromal cells in bone marrow and non-hematopoietic cells of the spleen stroma (Hegde et al. 2008, Perry et al. 2009).

As we showed that Dhh is present in bone marrow and the spleen, the expression of Hh signalling pathway components in the erythroid lineage were also studied. There were four populations of erythroblasts identified, based on the cell surface expression of CD71 and Ter119, as follows: $CD71^{high}Ter119^{med}$ (I), $CD71^{high}Ter119^{high}$ (II), $CD71^{med}Ter119^{high}$ (III), $CD71^{low}Ter119^{high}$ (IV). These subsets were described as subsets I-IV respectively going from least to most mature cell (Figure 1.3).

Smo and Ptch1 expression is essential to Hh signal transduction. To study the pattern of cell-surface Smo and Ptch protein expression in the erythroblast subsets, flow cytometry was performed using anti-CD71, anti-Ter119, anti-Smo and anti-Ptch1 antibodies. Four populations of erythroblast subsets were identified by expression of CD71 and Ter119 (Figure 3.2A,B). In bone marrow, cell surface Smo expression was highest in erythroblast subset I and gradually down-regulated in subset II and subset III, while the expression was very low in subset IV (Figure 3.2C). Similarly, Smo expression peaked in subset I in the spleen, and then the expression was downregulated on subset II and subset III followed by a weak level of expression in erythroblast subset IV (Figure 3.2D).

A similar expression pattern was observed for Ptch in bone marrow, with highest expression in subset I and gradual down-regulation of expression in the rest of the subsets (Figure 3.2E). In the spleen, Ptch1 was also expressed most highly in subset I and down-regulated in subset II, however, the expression of Ptch1 in the third erythroblast population (subset III) was up-regulated followed by the lowest expression in subset IV (Figure 3.2F).

Furthermore, qRT-PCR was performed to study the mRNA transcription of *Smo*, *Ptch1* and *Gli1*, in erythroblast subsets I-III. In Figure 3.3, we showed that the two key receptors required for the Hh signalling pathway, *Ptch1* and *Smo*, and the downstream transcriptional regulators of the pathway as well as Hh specific target gene, *Gli1* were present in erythroblast subsets I-III. However, we could not measure expression of these three Hh signalling components in late

erythroblasts (subset IV), because the RNA isolated from these cells was of poor quality, as the nucleus is shrinking and will be shed.

Differential expression of *Ptch*, *Smo* and *Gli1* mRNA levels was observed in the different erythroblast subsets and the expression pattern in the bone marrow was similar to that seen in the spleen. Interestingly, the cell surface protein expression of Smo and Ptch were comparable to the mRNA expression levels. The pattern of *Smo* mRNA expression in erythroblast subsets I-IV in both bone marrow and spleen was similar to that of surface Smo expression: it showed highest expression in erythroblast subset I, and then was gradually down-regulated during erythroblast maturation to reach the relatively low expression level in subset III (Figure 3.3B,C). We also found that the *Ptch1* expression was highest in the early erythroblasts (subset I), as seen for expression of *Smo* in both bone marrow and spleen, but it was down-regulated about six-fold in subset II, and then further down-regulated in subset III in bone marrow and slightly increased in subset III in the spleen (Figure 3.3D,E). In contrast, the expression of *Gil1*, was highest in subset III, while it was comparatively low in subsets I and II (Figure 3.3F,G). Although the key Hh components are expressed in erythroblast subsets, Dhh mRNA transcripts were undetectable by qRT-PCR (data not shown).

In this experiment, we found that the main components of Hh signalling are present in the erythroblast populations.

3.2.2 Erythroblasts are Dhh-responsive *in vitro* and *ex vivo*

In order to verify that the Dhh signal can be transduced in erythrocyte lineage cells, we measured *Gil1* expression in the Ter119+ population of WT bone marrow, which was cultured with recombinant(r)Dhh or anti-Hh monoclonal antibody (5E1), or both treatments together for 18 hours. Before isolation of RNA, erythroblast subsets were analyzed by FACS to examine if stimulation or inhibition of Dhh signalling would affect the erythroblast subset distribution and cell cycle status of these cells after short periods of culture.

After 18 hours of treatment, no difference was observed in the erythroblast subsets between the control and treatment groups (Figure 3.4A). To examine the effects of treatments on cell cycle status of erythroblast subsets II-IV, Ter119+ve cells were purified by magnetic beads and cell cycle status was analysed by staining with propidium iodide (PI). No difference was observed in all groups (Figure 3.4B).

Thus, these data indicate that treatment of cultured bone marrow cells with rDhh or 5E1 did not change the erythroblast subset composition and cell cycle status at the end of the short culture period, and that it is therefore reasonable to compare gene expression between the culture conditions.

Therefore, in order to investigate whether erythroblasts respond to Dhh signalling, we studied the transcription level of the Hh target gene, *Gli1*. Ter119+ve cells were purified by magnetic beads and qRT-PCR was used to study the expression of *Gil1*. *Gli1* expression was up-regulated when rDhh was

added in the culture, whereas expression of *Gli1* was undetectable in these cells when Hh signalling was blocked by adding neutralizing anti-Hh antibody, 5E1. *Gli1* transcription was partially recovered when rDhh was added to the 5E1 treatment, demonstrating specificity of the rDhh and 5E1, whereas there was no significant reduction in *Gli1* expression when isotype control monoclonal antibody was added to the culture, compared with untreated control. (Figure 3.4C)

In Figure 3.5, qRT-PCR was used to analyze expression of *Gli1* in FACS sorted erythroblast subset II isolated from WT and Dhh-/- bone marrow and the spleen *ex vivo*. *Gli1* expression in bone marrow was about 2.5-fold higher than that in the spleen. Moreover, *Gli1* expression was down-regulated in Dhh-/- bone marrow and spleen compared to WT, which indicates that Dhh is required for normal *Gli1* expression in erythroblasts.

In conclusion, these experiments show that the Dhh signal is transducible in erythroblasts *in vitro*. Neutralisation of Hh ligands in erythroblast cultures reduced the expression of Hh target gene, *Gli1*. Moreover, loss of the Dhh signal from developing erythroblasts *in vivo* also reduced the expression of target gene *Gli1*, by more than a factor of two, but some *Gli1* expression remained. The remaining *Gli1* expression indicated that Hh signals from other family members (Ihh and/or Shh) also maintain expression of Gli1 in these cells.

3.2.3 Genotyping Dhh knockout mice by PCR

Since both heterozygous and Dhh KO mice cannot be reliably distinguished visually from WT mice, genomic DNA was extracted from ear biopsies and genotyped by PCR in order to distinguish between Dhh knockout and their littermates. In Figure 3.6, genomic DNA from three different mice was analyzed by PCR to distinguish between WT and mutant alleles. WT and mutant alleles were identified by PCR using gene-specific primers. According to this strategy, the WT allele should generate a 442bp PCR product, while mutant alleles should generate an 112bp PCR product. In Sample 1, only WT alleles were amplified, so therefore, it was genotyped as WT. Sample 2 shows PCR products from both WT and mutant alleles were generated, and indicates that it is Dhh heterozygous genotype. Sample 3 amplified only mutant allele PCR products, therefore, it was genotyped as Dhh -/- (Figure 3.6).

3.2.4 Increased spleen size and reticulocyte percentages in Dhh-/- mice

To determine if Dhh is involved in regulation of spleen development or homeostasis, the spleen size in WT and Dhh-/- mice was compared. Spleen cell numbers in Dhh-/- mice were 30% significantly greater than that of WT littermates ($p=0.003$) (Figure 3.7). The peripheral red blood cell concentration and reticulocyte percentage was also investigated. Although there were no significant differences found in red blood cell concentration when compared to WT, Dhh-/- mice had a significantly higher percentage of reticulocytes ($p=0.01$) (Figure 3.8). The larger spleen and higher reticulocyte percentage in Dhh-/-

indicates Dhh may play a negative regulatory role in erythroid development.

3.2.5 Abnormal erythropoiesis in Dhh-/- mice

In order to investigate further whether the increase in spleen size in Dhh-/- was due to an expansion of cells of the erythroid lineage, splenocytes were isolated and stained with anti-CD71 and anti-Ter119. The cell numbers of each of these four populations in the spleen in Dhh-/- mice were analyzed and shown relative to that of WT of erythroblast subset I-IV (Figure 3.9A). This revealed an increase in cell numbers of these erythroblast subsets in Dhh-/- mice compared to WT mice. The cell numbers of the erythroblast subsets II, III and IV in Dhh-/- were significantly higher than that in WT. Erythroblast subset II, III and IV were increased 84%, 35% and 75% respectively. (II, p=0.012; III, p=0.015; IV, p=0.006) (Figure 3.9B). These data suggest that Dhh acts as a negative regulator of erythroid development in the spleen.

Furthermore, to investigate whether Dhh regulates erythropoiesis in bone marrow in a similar fashion, we analyzed the percentage of the erythroblast subset I-IV in bone marrow (Figure. 3.10A). We found that the relative percentage of the subset III and IV were both increased 50% in Dhh-/- compared to WT (III, p=0.022 ; IV, p=0.020) (Figure 3.10B). These data are consistent with a negative regulatory role for Dhh during erythropoiesis in the bone marrow.

In addition, to study whether loss of Dhh increased the proliferation of these cells to cause the expansion of the more mature erythroblast populations, the

cell cycle status of Ter119+ve cells was analysed by PI and cyclinB1 staining.

However, no significant difference was detected between WT and Dhh-/- in bone marrow or spleen (Figure 3.11 and 3.12). Therefore, the increase in these cells was not due to increased proliferation.

3.2.6 Loss of Dhh alters growth of erythroid progenitors and hematopoietic progenitors

In the erythroid lineage, the earliest committed erythroid progenitors identified are BFU-E, which give rise to CFU-E. It is known that these two types of progenitors cannot be identified by their morphology or by cell surface expression of developmentally regulated markers using FACS. Instead of that, the numbers of BFU-E and CFU-E can be determined by culturing the cell suspension in methylcellulose with certain essential growth factors, such as Epo. The different colonies can be distinguished by their specific colony morphology (Figure 1.3).

To determine whether the formation of progenitors and differentiation of the erythropoietic lineage were altered by loss of Dhh, we analyzed numbers of the earliest erythroid progenitors using colony formation assays. We found that the numbers of BFU-E from bone marrow and spleen in Dhh-/- were both significantly higher than that in WT littermates (Figure 3.13).

In order to find out whether the increase in erythroid progenitors in Dhh-/- is influenced by the earlier cell progenitors, we carried out experiments to study the earlier haematopoietic populations. During erythroid development,

hematopoietic stem cells (HSC) give rise to multipotent progenitor (MPP), which then give rise to common myeloid progenitors (CMP), CMP can then give rise to granulocyte-monocyte progenitors (GMP) and megakaryocyte- erythroid progenitors (MEP) (Figure 1.2). After that, MEP will give rise BFU-E and be committed to the erythroid lineage. HSC are defined by their absence of lineage-specific markers and expression of Sca-1 and C-kit, as Lin- Sca-1+ ckit+ (LSK) (Figure 3.14A). Although there was no difference observed in haematopoietic stem cells (LSK) between WT and Dhh-/- bone marrow, the proportion of myeloid progenitors (Prog) was increased significantly in Dhh-/- compared to WT (P=0.019)(Figure 3.14B). We also observed both the MEP and CMP in the myeloid progenitor compartment were increased significantly (MEP, P=0.005; CMP, P=0.05) (Figure 3.14C). Interestingly, the percentage of the other lineage progenitor, GMP, was found to be reduced in the Dhh-/- ($p<0.001$)(Figure 3.14C). When we analysed the ratio of MEP to GMP, we found that it was increased 1.5 fold in Dhh-/- compared to WT (p=0.009)(Figure 3.14D). To investigate if Dhh influences the transition from CMP to MEP and GMP, the CMP:MEP and the CMP:GMP ratio were analysed. The CMP:GMP ratio in the Dhh-/- was 40% higher than that in WT (p=0.024), whereas the CMP:MEP ratio in the Dhh-/- did not show significant change when compared to WT (Figure 3.14D).

These data indicate that loss of Dhh effects the differentiation of myeloid progenitors. Differentiation from CMP to GMP was reduced, although the ratio of CMP to MEP remained unchanged in Dhh-/- compared to WT, and the

myeloid progenitor and CMP population were increased. The MEP population was also expanded which resulted in an overall increase in differentiation to the erythroid lineage.

Given that the proportion of GMP was decreased in Dhh-/-, the percentage of granulocytes and macrophages were analysed by staining with anti-Gr-1 and anti-Mac-1 (Figure 3.15A). The proportion of granulocytes was found to be significantly decreased in Dhh-/- when compared to WT ($p=0.04$), while the proportion of macrophages was not significantly different. (Figure 3.15B)

3.2.7 Dhh influences expression of Lmo2

To identify potential functional transcriptional targets of Dhh signalling in erythroblasts, we used quantitative RT2–PCR Profiler Array to examine the gene expression profiles exhibited by Dhh-/- erythroblasts relative to WT. RNA extracted from sorted erythroblast subset II from WT and Dhh-/- bone marrow were used to perform the haematopoiesis PCR array to analyse the expression of 84 genes that are related to the development of HSCs and haematopoietic progenitors. This analysis identified several genes that were highly expressed in population II. Highly expressed genes in population II included CD164, Eraf1, Gata-1, Lmo2, Runx1, Stat1, Tal1 and Trim10.

We then concentrated on genes which had at least two-fold change between WT and Dhh-/-, and thus may be related to the regulation of erythroblast differentiation by Dhh. Among these genes, Lmo2 was chosen for further investigation, as it was upregulated in Dhh-/- population II. We confirmed

expression by qRT-PCR and found that Lmo2 was significantly upregulated more that 2.5-fold in Dhh-/- bone marrow population II compared to WT (Figure 3.16A). We used the same strategy to analyse the expression of Gata-1, as Gata-1 is a central transcription factor for erythropoiesis. However, no difference was observed in the expression of Gata-1 between WT and Dhh-/- (Figure 3.16A). To test if loss of Dhh also affects the transcription of Lmo2 on later erythroblast populations, we purified Ter119+ve cells from WT and Dhh-/- to compare the expression of Lmo2. Lmo2 expression was 2-fold higher in Dhh-/- compared to WT, as seen in sorted population II. In contrast, the expression of Gata-1 was equivalent in both genotypes. (Figure 3.16B)

Furthermore, to investigate if Lmo2 is a direct functional target of negative transcriptional regulation by Dhh, we treated Dhh-/- bone marrow cells with rDhh for 18 hours and then purified Ter119+ve cells to extract RNA to perform qRT-PCR analysis. Treatment with the neutralizing anti-Hh monoclonal antibody 5E1 was also analysed to show the effect when Hh signalling is blocked. The expression of Lmo2 was down-regulated when rDhh was added to the Dhh-/- culture to expression levels equivalent to that found in control WT bone marrow. On the other hand, expression of Lmo2 was not significantly changed in Dhh-/- cultures when 5E1 was added. Addition of 5E1 to the rDhh-treatment neutralized the effect of rDhh-treatment on Lmo2 expression. (Figure 3.17)

These experiments revealed that Lmo2 is a functional target of Dhh in the later stage of erythroblast differentiation.

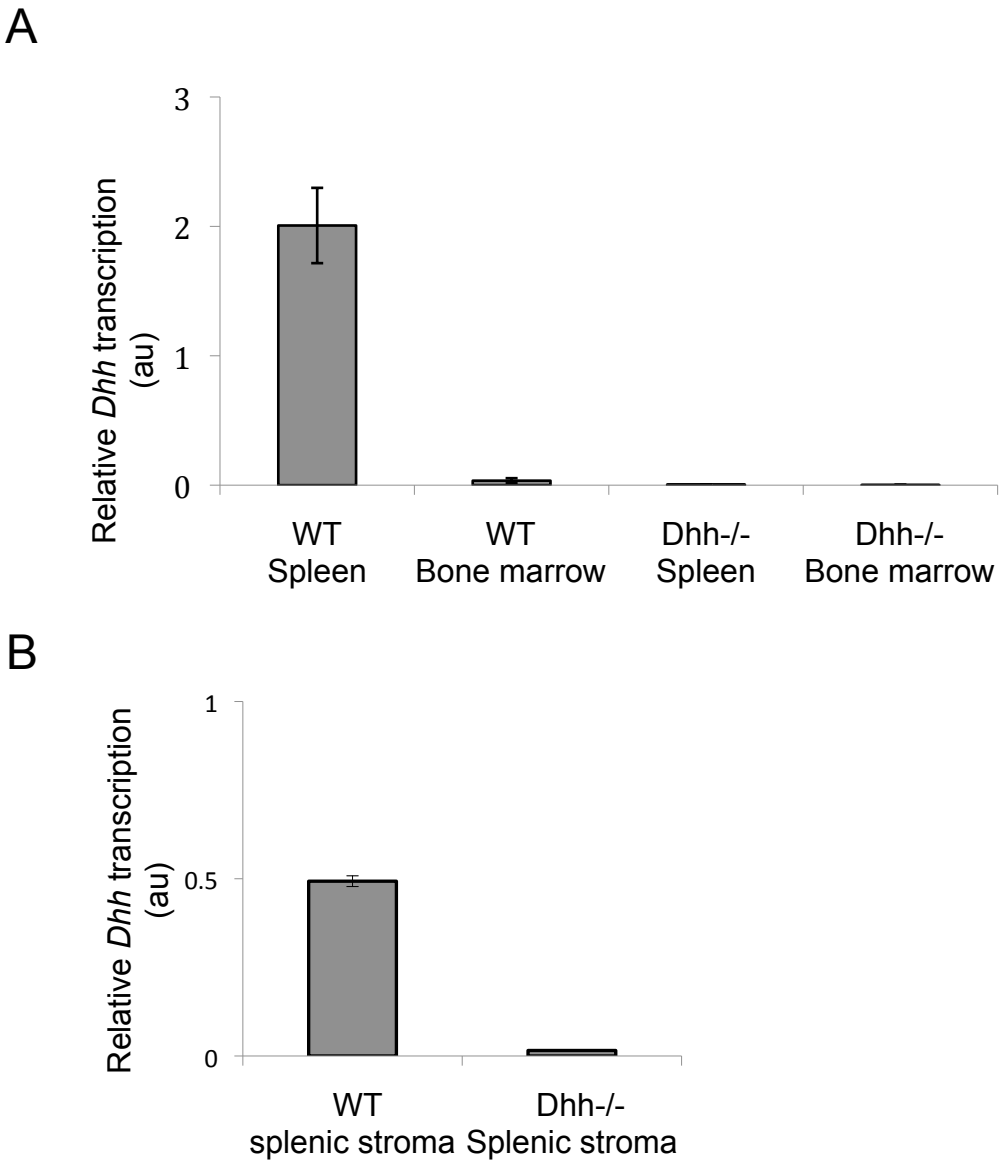

Figure 3.1 Dhh is expressed in spleen and bone marrow in WT mice

Bar chart to show relative *Dhh* expression in the spleen and bone marrow (**A**) and in the spleen stroma (**B**) in WT and Dhh-/- mice. The scales show expression normalised to the levels of the housekeeping gene *HPRT*. Error bars represent ± standard error of the mean (SEM). Data are representative of two independent experiments.

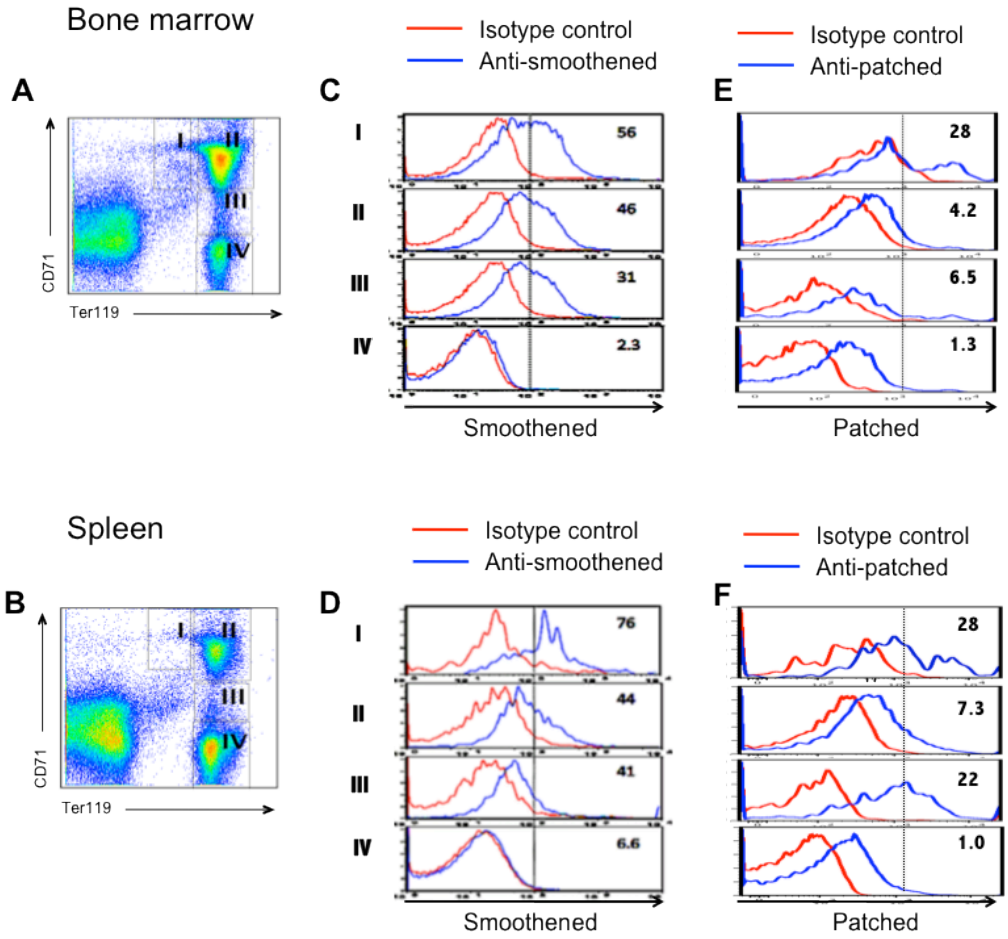

Figure 3.2 Expression of Smo and Ptch in erythroid subsets

Dot plots show CD71 versus Ter119 expression of erythroid subsets in bone marrow (**A**) and spleen (**B**). Histograms show the expression of Smo and Ptch (blue lines) in each of the gated erythroblast subsets populations (I, II, III, IV) shown in the dot plots. The red lines represent background fluorescence using isotype-matched control antibodies. The numbers in the right hand corner of the histograms indicated the percentages of cells positive for Smoothened and Patched. Data are representative of two independent experiments.

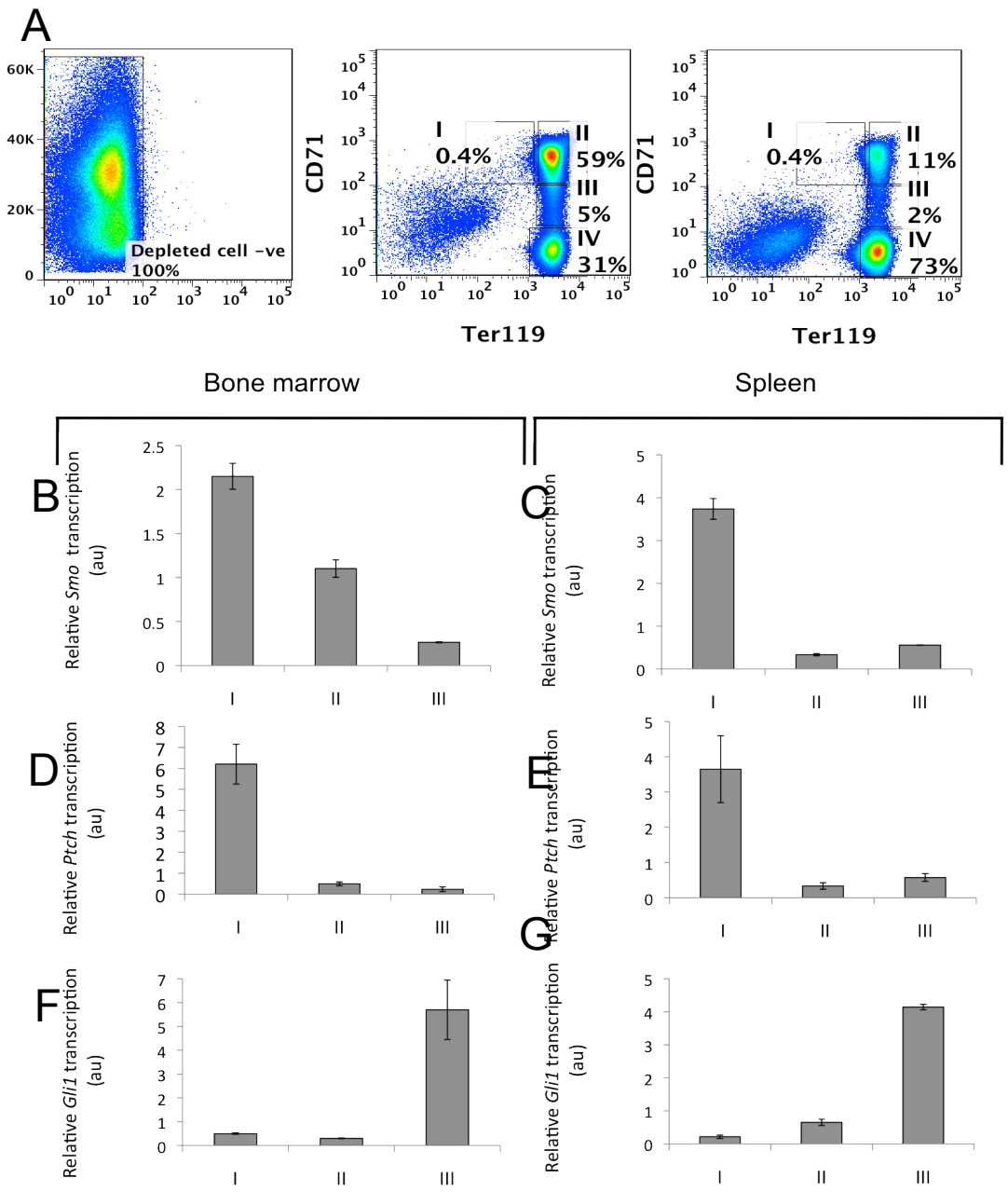

Figure 3.3 Expression of Hh components in sorted erythroblast subsets in bone marrow and spleen

(**A**) Dot plots show the sorting strategy of erythroblast subsets populations I-III from WT bone marrow and spleen. Cells were first magnetic bead depleted to remove lymphocyte, macrophage and granulocyte populations (left plot) and then stained with anti-CD71 and anti-Ter119 to distinguish four subsets of erythroblast populations in bone marrow (middle plot) and spleen (right plot). Bar chart to show relative transcription of *Ptch*(**B**,**C**), *Smo*(**D**,**E**) and *Gli1*(**F**,**G**) in FACS sorted populations of WT bone marrow and spleen erythroblast subsets. The scale shows expression normalised to the levels of the housekeeping gene *HPRT.* Error bars represent ± SEM. Data are representative of at least two independent experiments.

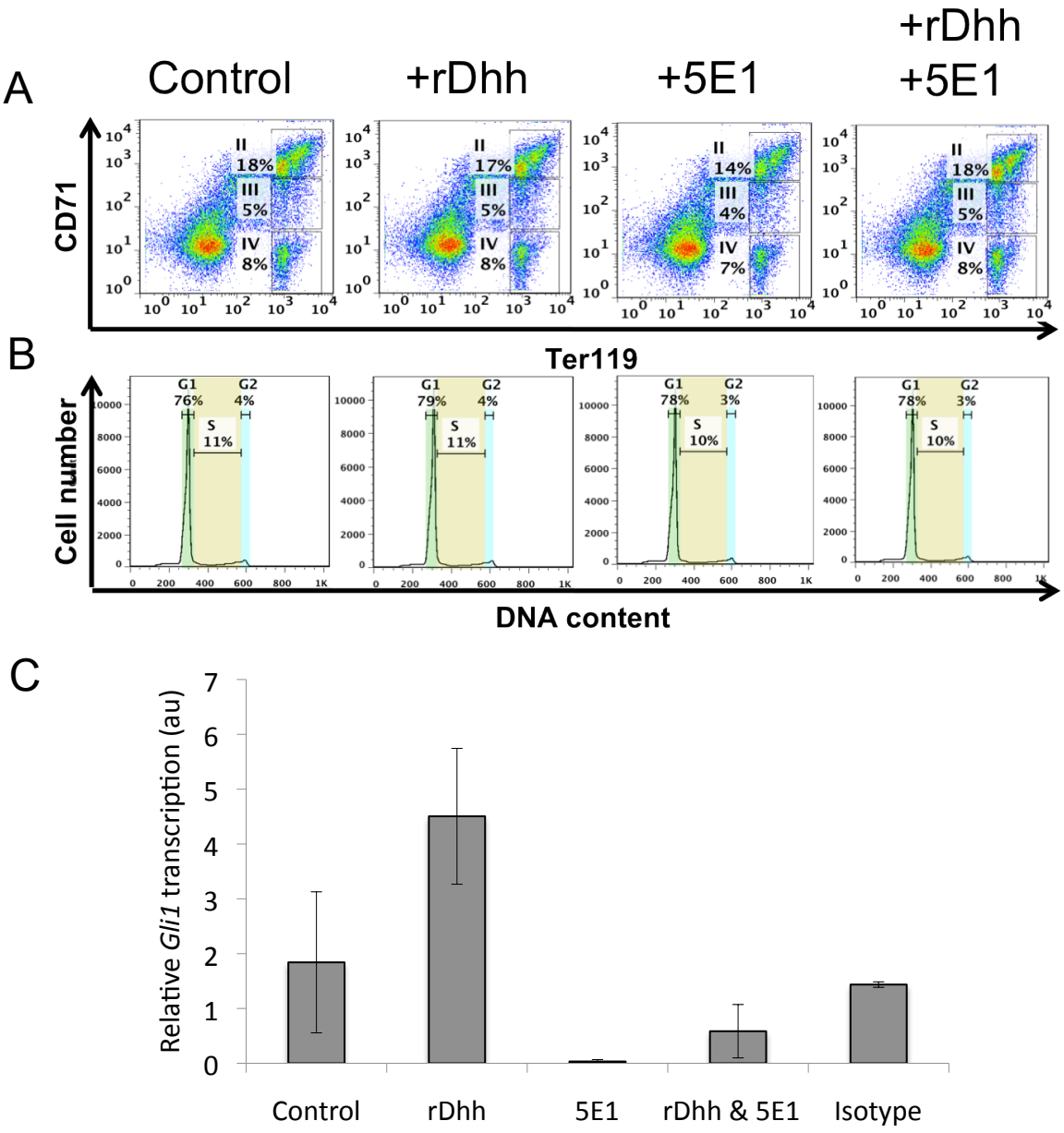

Figure 3.4 Response of bone marrow erythroblasts to rDhh and 5E1 after 18 hours culture

Bone marrow cells were isolated from WT mice and cultured with rDhh or 5E1 or both reagents for 18 hours.
(**A**) Dot plots show Ter119+ve (erythroblast subsets II-IV) populations in response to the treatments. (**B**) Histograms to show the cell cycle analysis of Ter119 +ve populations. Ter119+ve cells were purified with magnetic beads and the DNA content of these cells was analysed by propidium iodide nuclear staining. (**C**) Bar chart shows relative expression of *Gli1* in response to rDhh, anti-Hh 5E1 mAB and isotype control mAB. The scale shows expression normalised to the levels of the housekeeping gene *ActB*. Error bars represent ± SEM. Data are representative of at least two independent experiments.

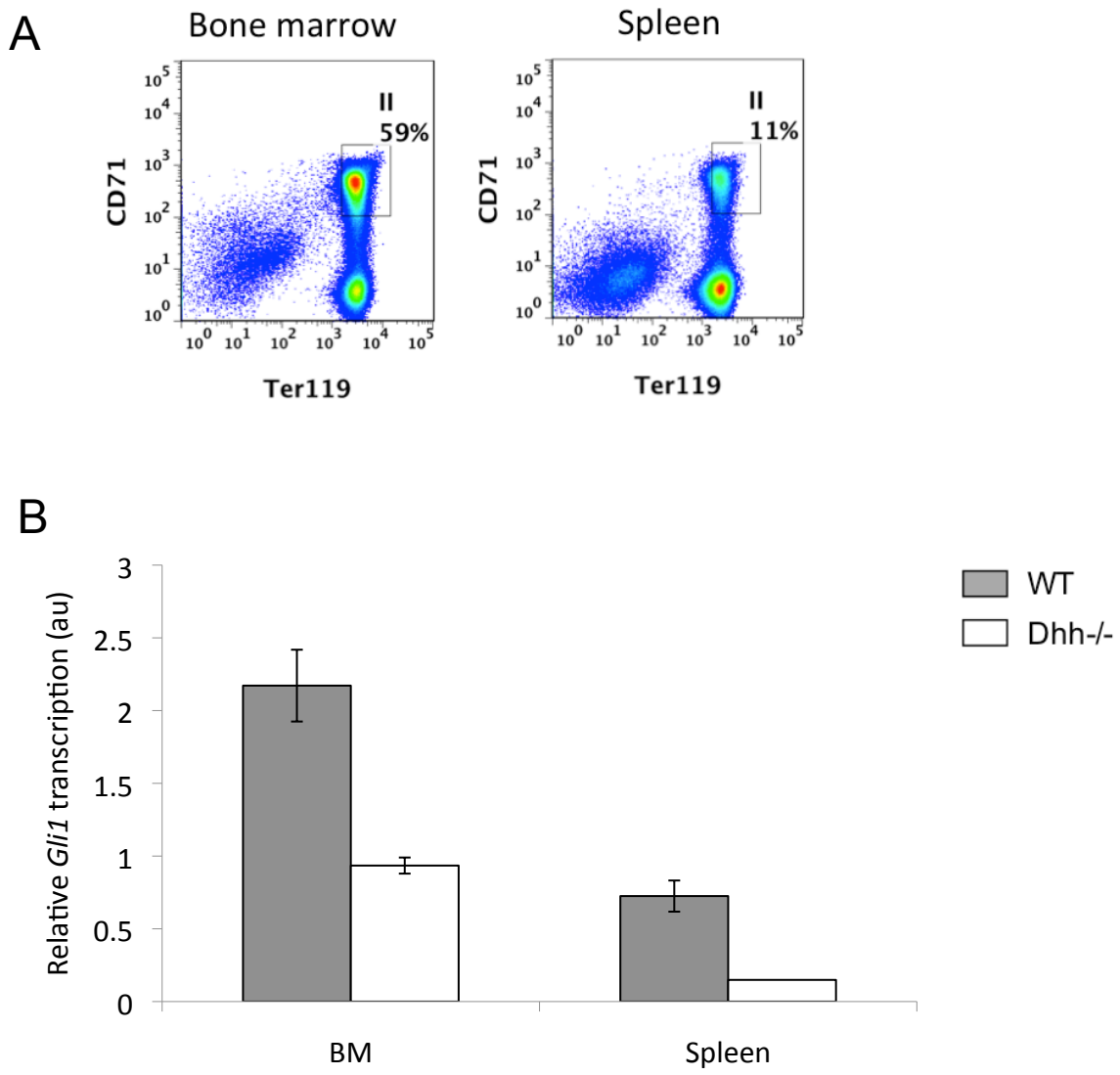

Figure 3.5 Expression of *Gli1* in erythroblast subset II

(**A**) Dot plot shows the sorted populations of erythroblast subset II, which were used to analyse (**B**) the *Gli1* expression of bone marrow and spleen in WT and Dhh-/- mice. The scale shows expression normalised to the levels of the housekeeping gene *ActB*. Error bars represent ± SEM. Data are representative of two independent experiments.

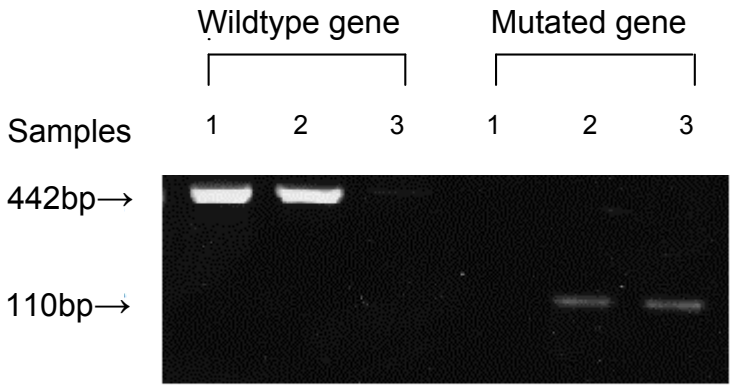

Figure 3.6 PCR genotyping for Dhh

PCR of genomic DNA for Dhh wildtype and Dhh mutated allele ran on a 2% agarose gel visualized using U.V.

A

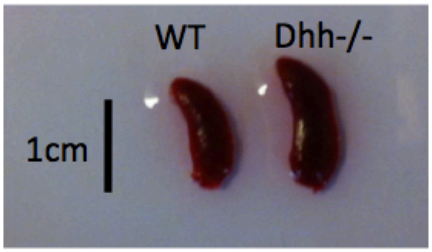

B

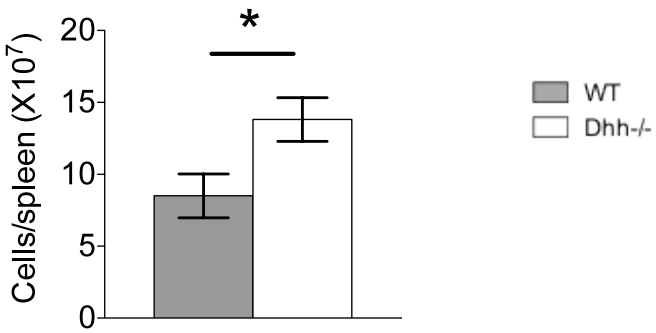

Figure 3.7 Spleen size of WT and Dhh-/- littermate

(**A**) The picture shows a representative experiment of spleen size from WT and Dhh-/- mice. (**B**) The total cell numbers of spleen isolated from WT and Dhh-/- mice. Error bars represent ± SEM. (n=17 of each genotype) *p<0.05, WT versus Dhh-/- littermates.

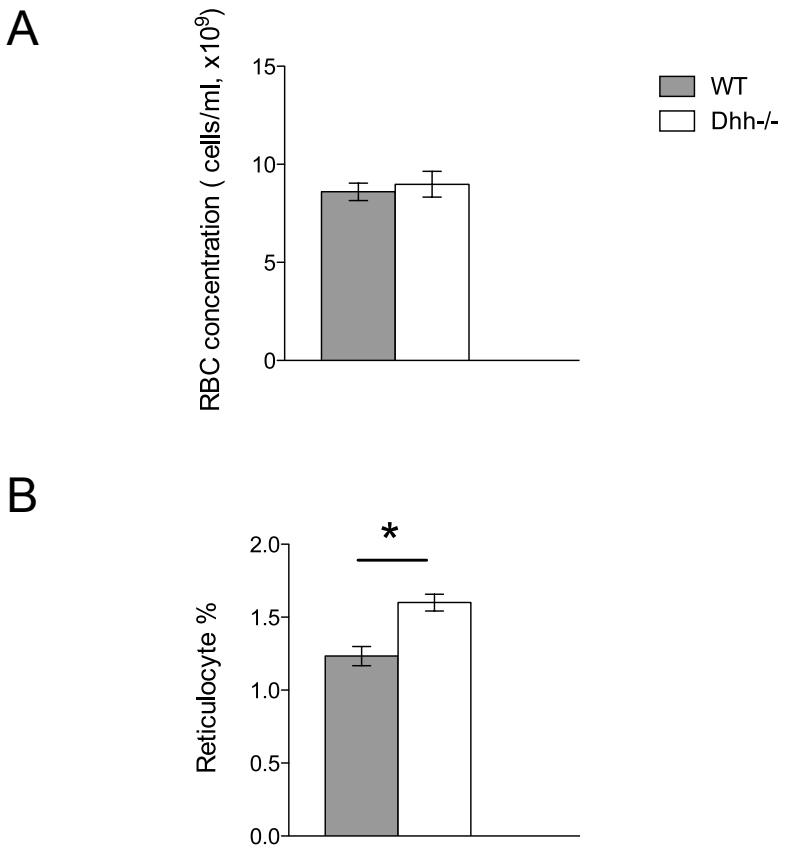

Figure 3.8 RBC concentration and percentage of reticulocytes in WT and Dhh-/- mice

Bar charts show the mean RBC count (**A**) and percentage of reticulocytes (**B**) obtained from blood of WT and Dhh-/- mice. Error bars represent ± SEM. (n=3 of each genotype) *p<0.05, WT versus Dhh-/-.

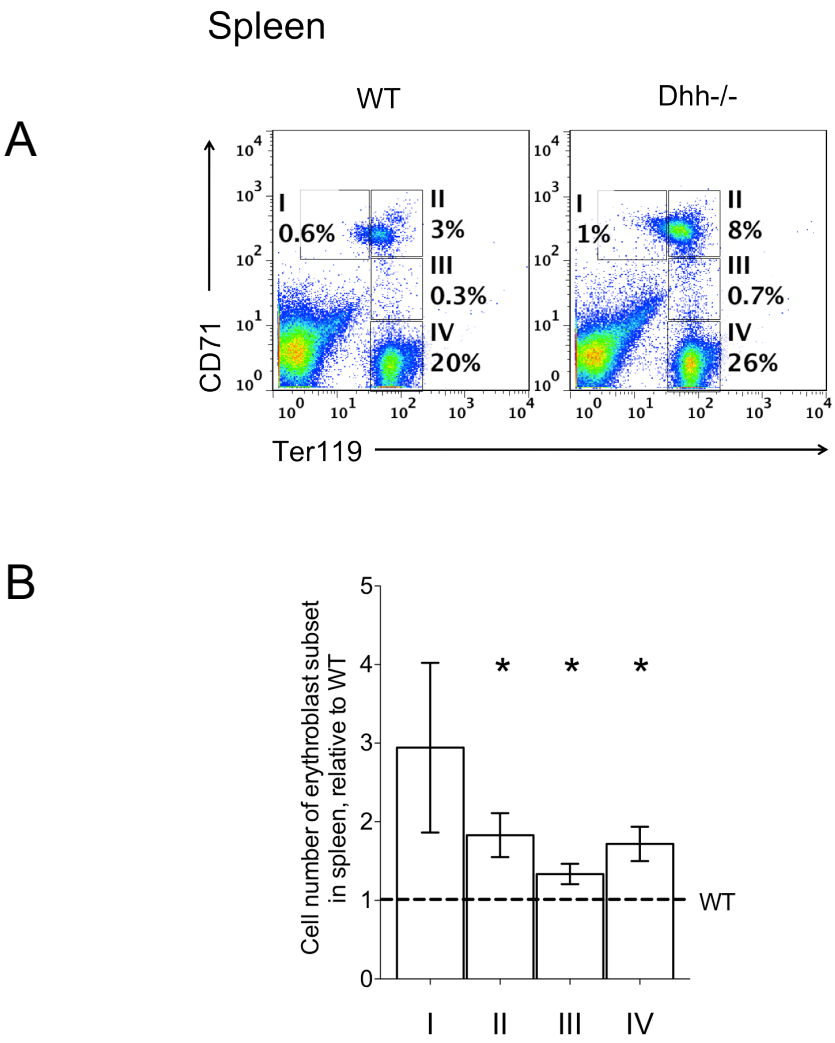

Figure 3.9 Erythropoiesis in Dhh-/- spleen

(**A**) The dot plots show Ter119 and CD71 staining of splenocytes isolated from WT and Dhh-/- mice. The four erythroblast populations (I-IV) were identified. (**B**) Bar chart shows cell number of erythroblasts population (I-IV) relative to WT in spleen. In each experiment the average value of the WT is set to 1, to allow comparison between experiments. Error bars represent ± SEM. (n=17 of each genotype) *p<0.05, WT versus Dhh-/-.

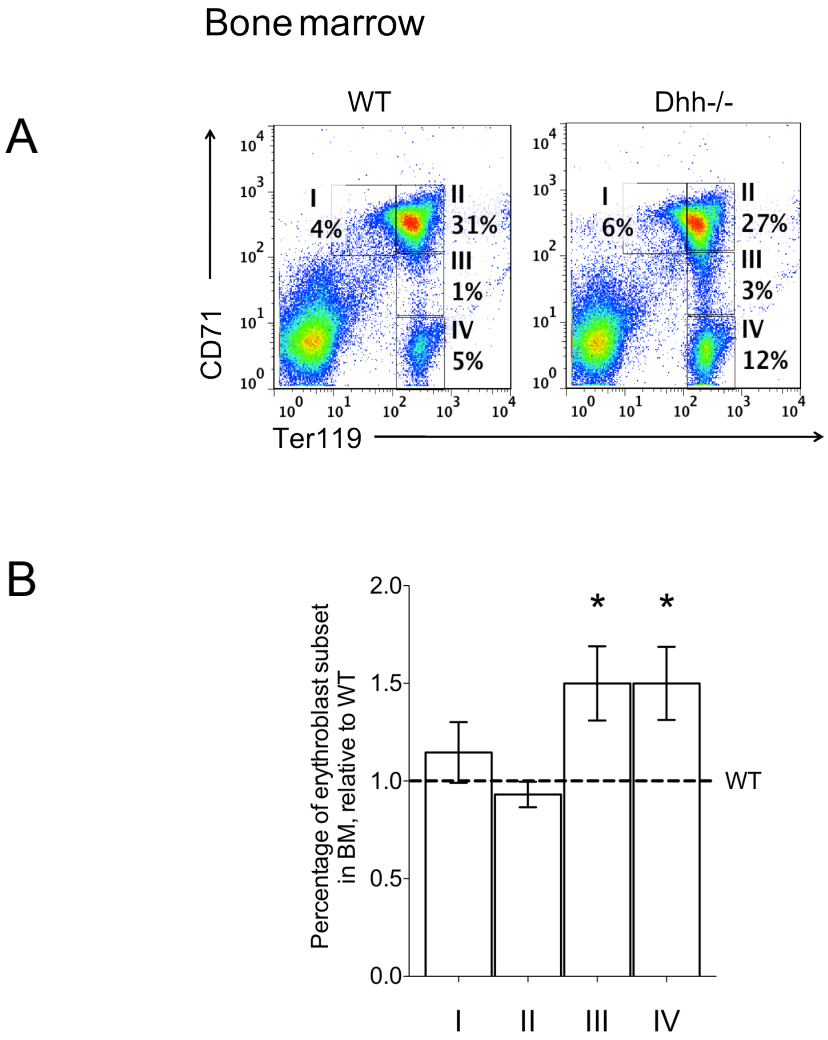

Figure 3.10 Erythropoiesis in Dhh-/- bone marrow.

(**A**) The dot plots show Ter119 and CD71 staining of bone marrow cells isolated from WT and Dhh-/- mice. The four erythroblasts populations (I-IV) were identified. (**B**) Bar chart shows relative percentage of erythroblast populations (I-IV) in bone marrow. In each experiment the average value of the WT is set to 1, to allow comparison between experiments. Error bars represent ± SEM. (n=17 of each genotype) *p<0.05 WT versus Dhh-/-.

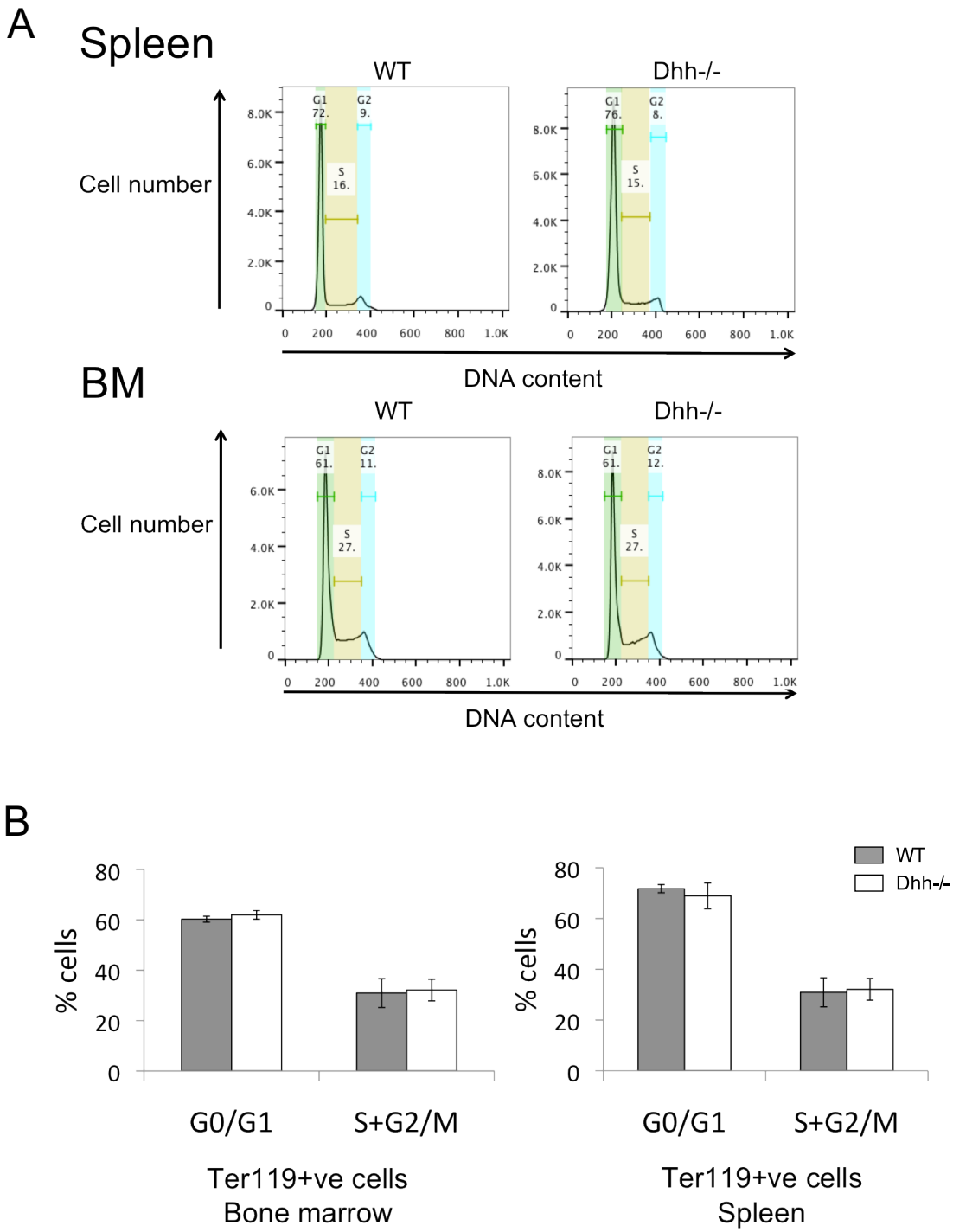

Figure 3.11 Cell cycle analysis of erythroblast subsets

(**A**) Histograms show representative PI staining for Ter119+ve populations in bone marrow and spleen from WT and Dhh-/-. Numbers inside histogram indicate percentages of each population (**B**) Bar charts show cell cycle analysis by PI staining. Error bars represent ± SEM. (n=3 of each genotype)

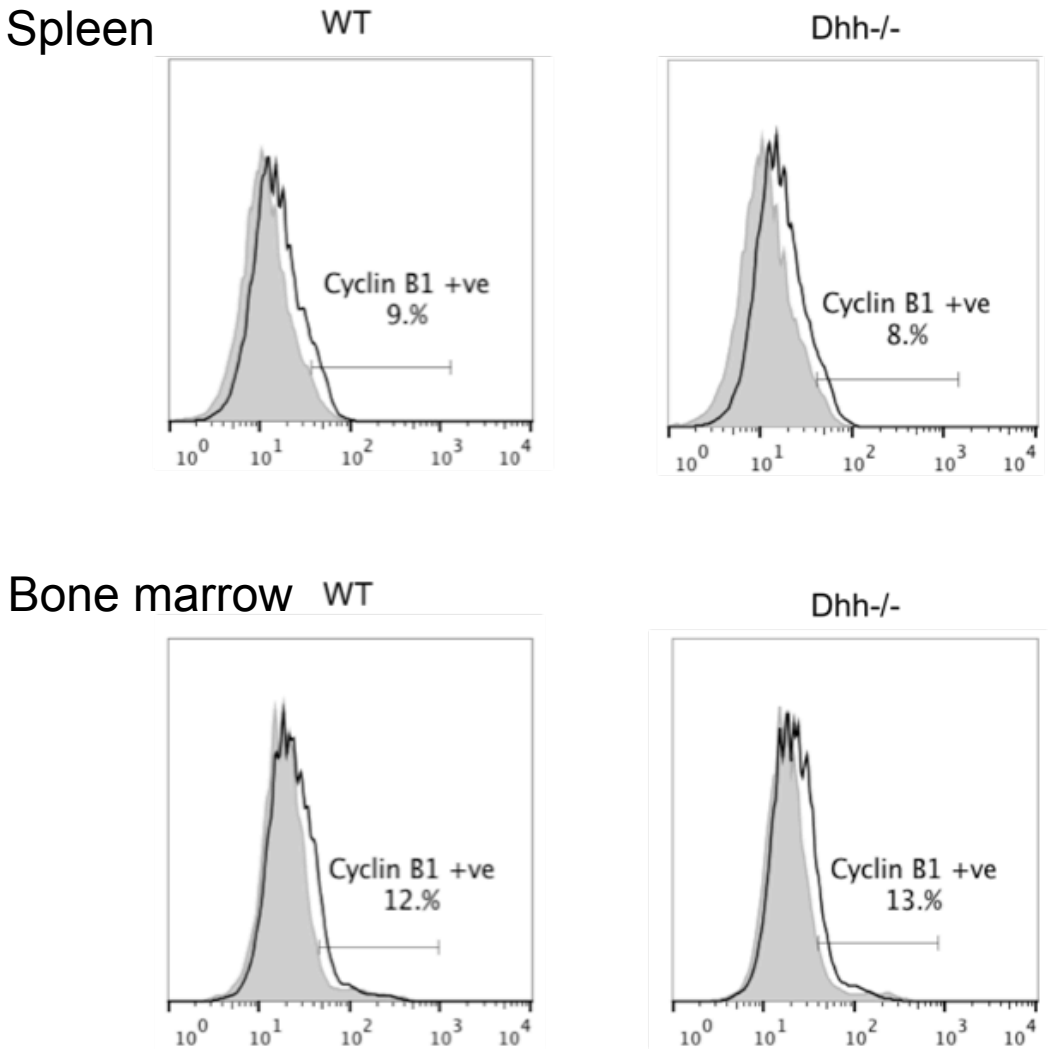

Figure 3.12 CyclinB1 analysis of erythroblast subsets

Histograms show cyclinB1 expression measured by flow cytometry in Ter119+ve cells in WT and Dhh-/- spleen and bone marrow. The grey shadows represent background fluorescence using isotype-matched control antibodies. Data are representative of two independent experiments.

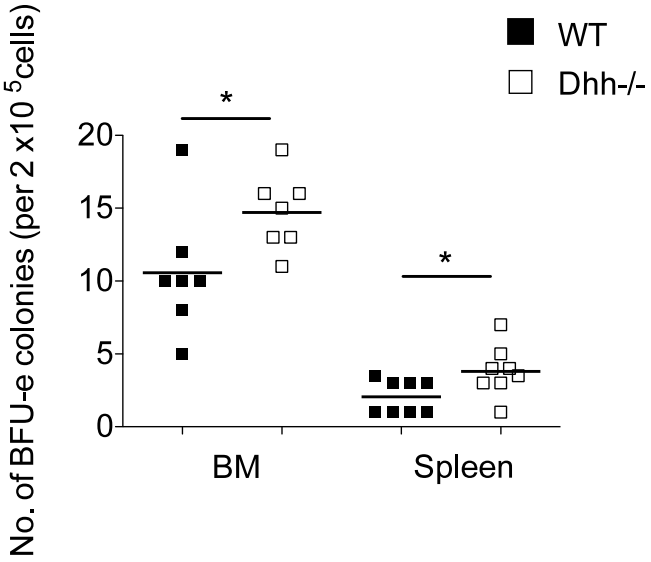

Figure 3.13 Numbers of erythroid progenitors in bone marrow and spleen

Scatter plot shows the numbers of BFU-E in bone marrow and spleen of individual WT or Dhh-/- mice. The mean of each group is indicated with a line. (n=7 for bone marrow, n=8 for spleen of each genotype) *$p<0.05$ WT versus Dhh-/- .

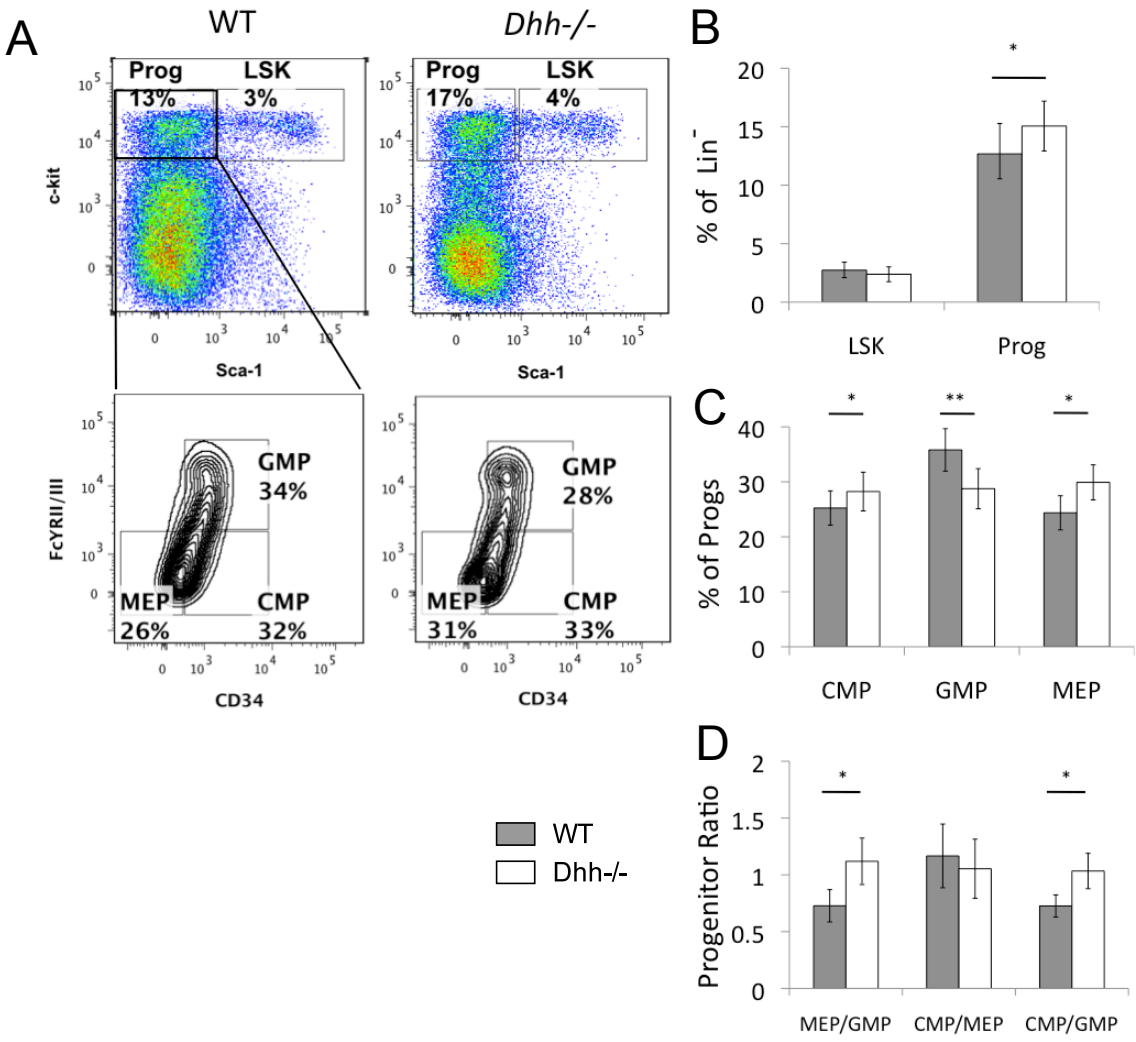

Figure 3.14 Numbers of haematopoietic progenitors in WT and Dhh-/- bone marrow

(**A**) Bone marrow cells were isolated and analyzed by mutliparameter flow cytometer to identify the haematopoietic stem cells Lin$^-$ Sca-1$^+$ C-kit$^+$ (LSK) and the myeloid progenitors, Lin$^-$ Sca-1$^-$ C-kit$^+$ (Prog). The Prog is further subdivided by expression of CD34 and FcϒRII/III which results FcϒRII/III$^+$ CD34$^+$(GMP), FcϒRII/III$^-$CD34$^+$(CMP), FcϒRII/III$^-$CD34$^-$(MEP). (**B**) Bar chart shows percentage of LSK and Prog within the Lineage negative compartment in WT and Dhh-/- bone marrow. (**C**) Bar chart shows percentage of CMP, GMP and MEP within the myeloid progenitor compartment in WT and Dhh-/- bone marrow. (**D**) Bar chart shows the ratio of progenitors of CMP, GMP, and MEP in WT and Dhh-/- bone marrow. Error bars represent ± SEM. (n=5 of each genotype) *p<0.05 WT versus Dhh-/-.

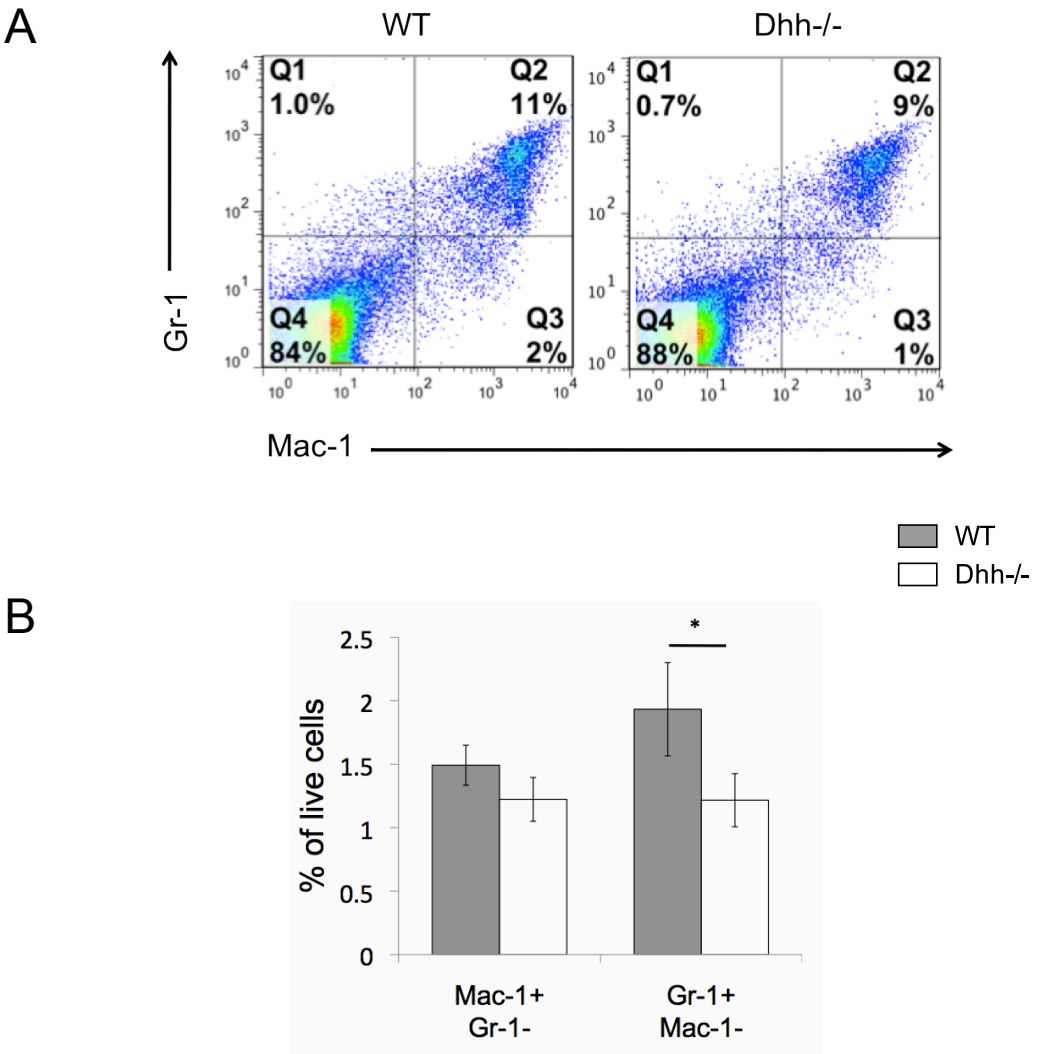

Figure 3.15 Macrophage and Granulocyte composition in WT and Dhh-/- bone marrow

(**A**) Dot plots show staining against Gr-1 and Mac-1 on bone marrow cells isolated from WT and Dhh-/- mice. The percentage of cells in each quadrant is shown. (**B**) Bar chart shows the mean percentage of macrophages (Mac-1+Gr-1-) and granulocytes (Gr-1+Mac-1-) in bone marrow. Error bars represent ± SEM. (n=17 of each genotype) *p<0.05 WT versus Dhh-/-.

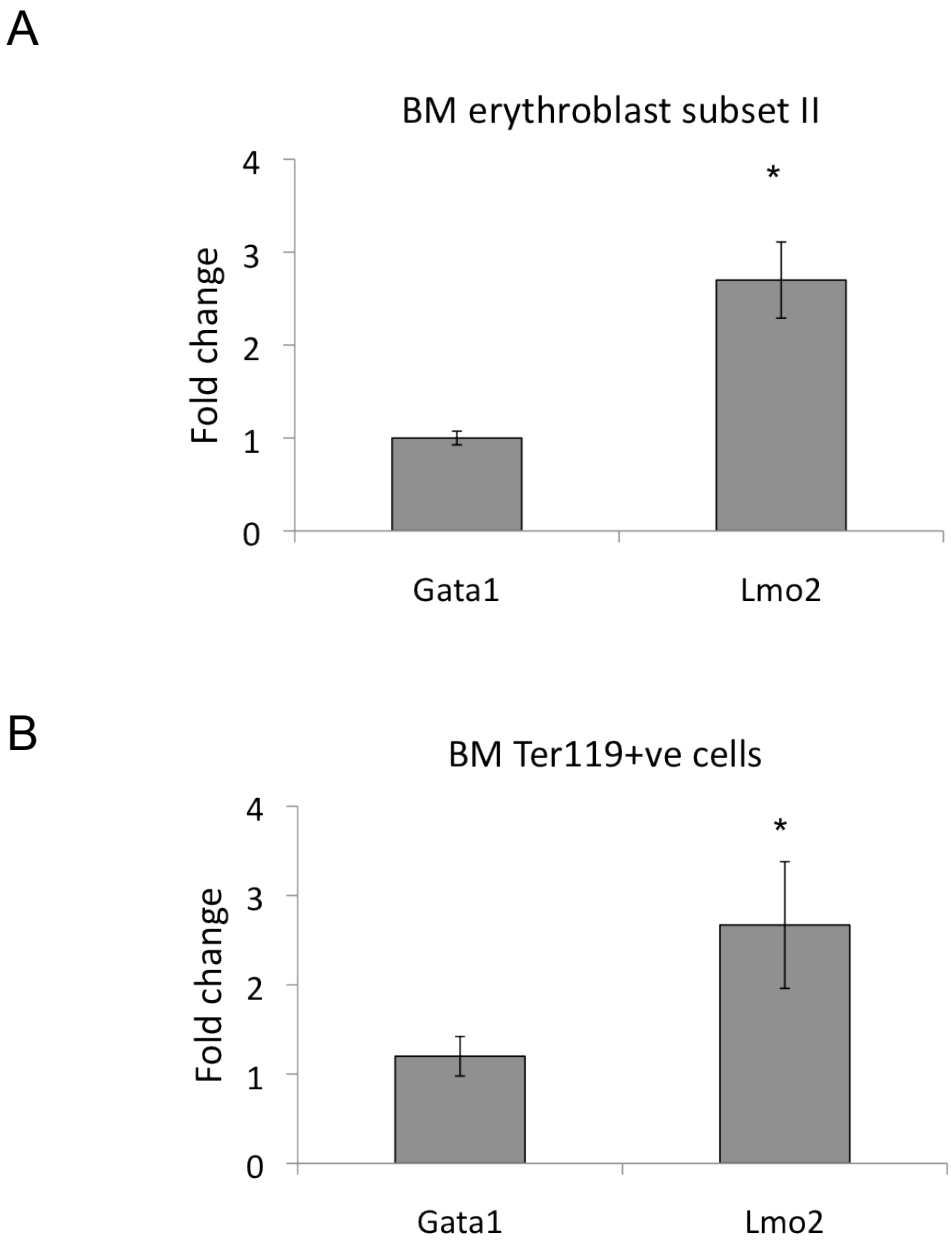

Figure 3.16 Fold change in expression of erythroid regulating genes in Dhh-/- cells compared to WT

Fold change in expression of *Gata1* and *Lmo2* between WT and Dhh-/- in population of erythroblast subset II were sorted by FACS (**A**) and Ter119+ve cells purified by magnetic beads (**B**) from WT and Dhh-/- bone marrow. Fold change in mRNA expression was analysed qRT-PCR and normalised to the levels of the housekeeping gene *ActB*. Error bars represent ± SEM. Data are representative of at least two independent experiments. *p<0.05, WT versus Dhh-/- for expression of *Gata1* and *Lmo2.*

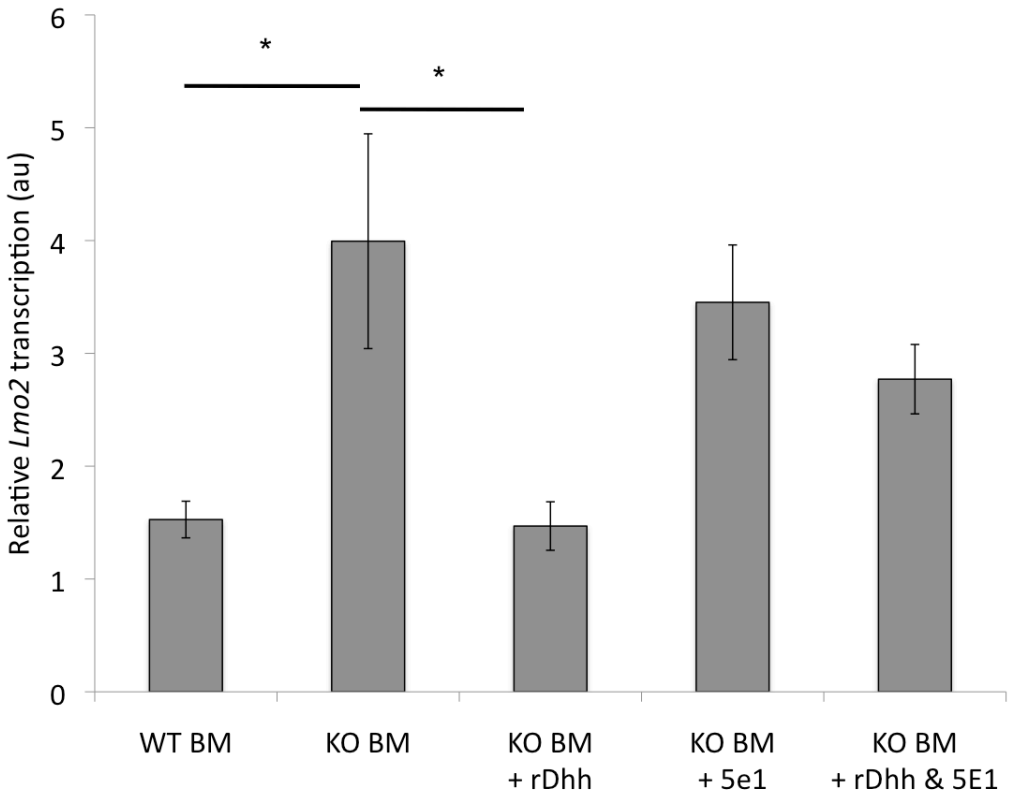

Figure 3.17 Transcription of *Lmo2* in Ter119 positive populations with different treatments

Bone marrow cells were isolated and cultured with rDhh or 5E1 or both reagents for 18 hours. Ter119+ve cells were purified by magnetic beads and the relative expression of *Lmo2* in response to the treatments was analyzed by qRT-PCR. The scale shows expression normalised to the levels of the housekeeping gene *ActB*. Error bars represent ± SEM. Data are representative of at least two independent experiments. *p<0.05 Dhh-/- BM versus WT BM; and Dhh-/- BM with rDhh versus Dhh-/- BM.

3.3 Discussion

Although many recent studies suggest Hh signalling is involved in the regulation of haematopoiesis, the role of Hh signalling proteins and their components in erythropoiesis is still unclear. In this study, we demonstrated a novel role of Dhh in regulating of erythropoiesis. We showed that it is required for the regulation of erythroid progenitor differentiation and that it acts as a negative regulator of erythropoiesis.

Analysis of Dhh-/- mice showed that in the absence of Dhh, normal erythroid development occurs in an accelerated fashion resulting in an accumulation of late stage erythroblasts both in the bone marrow and spleen. A negative regulatory role for a Hh protein family member has previously been described for Indian hedgehog (Outram et al. 2009). In this case, Hh signalling provides both positive and negative regulatory signals in order to maintain homeostatic control of the thymus. In terms of erythropoiesis, it was found that Shh positively regulates erythroid development, as addition of Shh promotes erythroid proliferation and resulted in expanded erythroid colonies (Detmer et al. 2000). Therefore, it is likely that the process of erythroid development may be controlled both by positive and negative regulatory signals with feedback between both sets of signals thus allowing a tight control of erythroid homeostasis, as seen in the case of the thymus (Outram et al. 2009).

In fact, the three Hh proteins sequences are highly conserved in vertebrates, and Hh proteins can act in the same tissues and have overlapping or redundant functions (Kumar et al. 1996). Although the overlapping functions of Hh proteins have not been well-studied, studies of Hh on T-cell development showed that the three Hh

proteins may have some differential functions and overlapping activities in order to regulate thymocyte differentiation (Crompton et al. 2007, Outram et al. 2009). Thus, it is possible that the Hh proteins may have differential regulatory roles and overlapping functions in controlling erythroid development to maintain homeostasis. More studies are needed to identify the role of other Hh proteins and the Hh signalling pathway components in erythropoiesis.

It is well known that the Hh signalling pathway is activated by binding of Hh proteins to Ptch and this relieves the Ptch mediated inhibition of Smo. This then allows Smo to regulate the activity of the Gli transcription factors, which in turn regulate expression of Hh target genes. Although Gli1 acts as an activator of transcription, it is not essential for the initiation of Hh signalling and is itself a target gene of the Hh signalling pathway (Crompton et al. 2007), thus it is important to point out that the transcription level of *Gli1* in a population of cells can also be read as an indicator of activation of Hh signalling. In our findings, the high expression level of *Gil1* in the population of late stage erythroblasts (subset III) suggested that the influence of Hh signalling on erythroblast differentiation may not be observed until the later stages of erythroid development. These findings are consistent with our observation of an increase in the number of late stage erythroblasts in the spleen and bone marrow in the Dhh-/- mice. Thus, here we show that Dhh may have a negative effect on erythroid differentiation, specifically in late stage erythroblasts and thus increase the total number of cells in the spleen in Dhh-/- mice.

Our data also demonstrated that loss of Dhh alters the differentiation of myeloid lineages, and results in decreased production of GMP and increased CMP and MEP

populations in Dhh-/- bone marrow. Furthermore, analysis of committed erythroid progenitors, BFU-E, also revealed an increased number of this population in Dhh-/-. These experiments indicate that Dhh is essential in haematopoiesis and negatively regulates erythroid development at multiple stages. We did not find evidence to support the hypothesis that the proliferation of erythroid lineages is increased. Thus the increased number of erythroblasts in the spleen and bone marrow that led to the enlarged spleen in Dhh-/- mice seemed to also be the result of an increased rate of differentiation from the early progenitors, CMP and MEP along the erythroid lineage. These findings are consistent with the regulatory functions of Gli1 in haematopoiesis, as Gli1 is essential for differentiation of myeloid progenitors. (Merchant et al. 2010)

Our data showed that Lmo2 is upregulated on loss of Dhh signalling in erythroid populations and down-regulated by treatment of Dhh-/- erythroblasts with rDhh. These experiments suggested that Lmo2 is a potential functional transcriptional target of Hh signalling, which is repressed by Dhh signalling, presumably by activation of an intermediate transcriptional repressor. Studies of Lmo2 have shown that it is required for erythroid differentiation and is expressed in the myeloid lineage and especially highly expressed in erythroid progenitors. Loss of Lmo2 cause defects in yolk sac erythropoiesis and leads to embryonic lethality (Hansson et al. 2007, Warren et al. 1994). Forced expression of Lmo2 leads to expansion of erythroid progenitors, thus suggesting that Lmo2 is a positive regulator of erythropoiesis (Hansson et al. 2007). In that study, overexpression of Lmo2 caused an increase in numbers of BFU-E, and reductions in granulocyte and macrophage progenitors, which is consistent with our findings in Dhh-/- mice (Hansson et al. 2007). Taken

together, the increased numbers and differentiation, and increased Lmo2 expression found in Dhh-/- erythroblasts consistent with the positive regulatory function of Lmo2, which may provide one possible mechanism for Dhh function in erythropoiesis.

3.4 Conclusion

In this chapter, we showed that Dhh plays a role in the regulation of erythroid development. Analysis of Dhh-/- mice revealed an increase in spleen size and late erythroblast population production in both the bone marrow and spleen. Moreover, analysis of the early haematopoietic progenitors showed that Dhh is involved in myeloid progenitor differentiation. Loss of Dhh resulted in a higher proportion of CMP, and the CMP were biased to differentiate into MEP rather than GMP, thus contributing to the expansion of the erythroid lineage in Dhh-/- mice. Analysis of gene expression in erythroblast subset II identified Lmo2 as a potential target gene of Dhh. Expression of Lmo2 was influence by Dhh *in vivo* and *in vitro*.

Chapter Four : Dhh in recovery post-irradiation and following acute anaemia recovery

Abstract

Stress erythropoiesis is a process, in which rapid expansion of erythrocytes in the spleen occurs in response to anaemia or hypoxia stimuli. Recent studies have suggested that Hh signalling is involved in regulation of stress erythropoiesis after PHZ-induced acute anaemia. However, the role of Dhh in stress erythropoiesis is still not clear. In this report, to investigate if loss of Dhh altered stress erythropoiesis, Dhh-/- mice were sub-lethally irradiated or treated with PHZ. These treatments aim to deplete mature haematopoietic cells or induce acute anaemia in order to study the dynamics of stress erythropoiesis during recovery. We found that Dhh plays a negative regulatory role in stress erythropoiesis in the spleen and is also involved in regulation of bone marrow regeneration. Analysis of Dhh-/- showed increased spleen size and accelerated erythropoiesis in the spleen after treatment by irradiation and PHZ, whereas the differentiation of myeloid progenitors in Dhh-/- bone marrow were reduced during recovery from PHZ-induced anaemia.

Declaration of Publication

Some data from the following chapter are taken a publication titled" Regulation of murine normal and stress-induced erythropoiesis by Desert Hedgehog" in Blood. 2012 May 17;119(20):4741-51. This manuscript was written by CI Lau and T Crompton. CI Lau and SV Outram are co-first authors in this paper.

4.1 Introduction

Under normal conditions, the bone marrow plays the main role in producing erythrocytes, however, the spleen serves as a reserve site for accelerated haematopoiesis and erythropoiesis in order to increase the number of erythrocytes under conditions of erythropoietic stress. In other words, erythroid progenitors in the spleen can proliferate and differentiate rapidly into mature erythrocytes in response to anaemia and hypoxia stimuli, a process referred to as stress erythropoiesis. It is critical to have efficient stress erythropoiesis to rapidly expand erythroid progenitors and erythrocytes in order to compensate for blood loss from clinical conditions, including radiotherapy, chemotherapy and anaemia. Animal models were widely used to study stress erythropoiesis, which is initiated by irradiation or cytotoxic drug treatment to cause suppression of haematopoiesis in the bone marrow, due in part, to apoptosis of haematopoietic cells and progenitors (Han et al. 2006).

There are several factors that have been identified as key regulators of stress erythropoiesis. They are, Erythropoietin (Epo), Stem cell factor (SCF), Bone Morphogenetic Protein 4 (BMP4) and hypoxia (Perry et al. 2007, Perry et al. 2009). It is suggested that acute anaemia leads to tissue hypoxia, which stimulates production of Epo, and induces expression of BMP4, whereas culturing spleen cells with SCF in hypoxic conditions significantly increases numbers of stress erythroid progenitors (Koury and Bondurant 1990, Perry et al. 2007). Interestingly, it has been suggested that BMP4 is not the only important component in stress erythropoiesis, and that its signal is induced by

Hh signalling and the interaction of these two signalling pathways is essential for maintenance of the stress erythropoiesis response pathway (Perry et al. 2009). In that study, treatment of bone marrow with Shh resulted in increased numbers of stress erythroid progenitors and induced BMP4 expression, which indicated that Shh signalling maintains BMP4 expression in response to the induction of stress erythropoiesis (Perry et al. 2009).

Furthermore, study of expression of Hh proteins in the erythroid compartment during the process of stress erythropoiesis in the spleen suggested that Dhh is involved in regulation of stress erythropoiesis. Splenocytes isolated from mice treated with Phenylhydrazine (PHZ) in order to induce anaemia were analyzed for expression of Shh, Ihh and Dhh (Perry et al. 2009). In the untreated mice, expression of Ihh in the spleen was similar to that of PHZ treated mice. Interestingly, Dhh was expressed at low levels in untreated mice, however, its expression was up-regulated in the mice that had received PHZ treatment and maintained at high level during the recovery from acute anaemia.

Objectives:

Although it has been suggested that Dhh signalling is involved in regulation of stress erythropoiesis, its functional role in erythropoiesis under stress conditions is still not clearly defined, and therefore further investigation is required.

To study stress erythropoiesis in Dhh-/- mice, WT and Dhh-/- mice were sub-lethally irradiated or treated with PHZ to deplete mature haematopoietic cells

and induce anaemia. This allowed us to study a synchronized wave of erythropoiesis during recovery.

4.2 Results

4.2.1 Increased spleen size in Dhh-/- mice after sub-lethal irradiation

In response to haematopoietic cell loss, stress erythropoiesis takes place in the spleen, where erythroid-lineage cells expand quickly to recover from the loss. To test the hypothesis that Dhh affects the rate of erythropoiesis during stress conditions, WT and Dhh-/- mice were sub-lethally irradiated to cause depletion of all haematopoietic cells, and bone marrow and the spleen were monitored during the recovery of RBC after irradiation.

Spleen cells were isolated and counted at day 7, 9 and 14 after irradiation. As shown in Figure 4.1A, after 14 days, the spleen size in Dhh-/-mice was much larger than that of WT control. Analysis of cell numbers in the spleen revealed spleen size in Dhh-/- mice was significantly increased by 1.5 fold ($p=0.046$) when compared to WT mice at day 14 after irradiation (Figure 4.1B).

4.2.2 Abnormal erythropoiesis in irradiated Dhh-/- mice

Furthermore, to confirm that the increased spleen size in Dhh-/- mice was due to an alteration of erythropoiesis, erythroblast subsets I-IV from the spleen of WT and Dhh-/- irradiated mice were isolated and analysed by FACS.

The results are shown in Figure 4.2. In the spleen of irradiated mice, after 7 days, the early populations of erythroblasts (subset I and II) were almost absent, indicating that these populations of erythroblasts in the spleen had not yet been replenished, and the late stage erythroblasts shown were radiation-resistant cells remaining from before the mice were irradiated (Figure 4.2A left panel).

At day 9, the early stage erythroblasts were markedly increased in Dhh-/- when compared to WT. After that, erythroblast subsets I-III were continuously expanded in the spleen of irradiated mice (Figure 4.2A left panel). At day 14 after irradiation, the relative percentage of the erythroblast subset I-IV populations in WT and Dhh-/- were analyzed. This analysis revealed a significant increase in erythroblast subset I ($p=0.003$) and II ($p=0.044$) in Dhh-/- mice compared to WT mice (Figure 4.2B).

Although stress erythropoiesis mainly occurs in the spleen, in general a higher number of early stage erythroblast populations were also observed in the bone marrow of irradiated Dhh-/- mice compared to WT (Figure 4.2A right panel). At day 7, the percentage of subset I and II in Dhh-/- was markedly more than that of WT and this was also the case on day 9. Dhh-/- mice produced a larger number of erythroblasts in the bone marrow after irradiation at day 14 (Figure 4.2A right panel). Analysis of the percentage of erythroblast populations in bone marrow showed a large variation between experiments (Figure 4.2C).

Given that granulocytes, macrophages and erythrocytes arise from the common myeloid progenitor, the proportion of Mac-1+ve and Gr-1+ve cells in bone marrow were also analysed at day 14 after irradiation. The Dhh-/- mice had significantly fewer cells that were committed to the macrophage lineage compared to WT ($p=0.0015$), while the granulocytes did not appear to be different. (Figure 4.3)

Overall, Dhh-/- mice showed more rapid erythropoiesis in the spleen after sub-lethal irradiation compared to WT, and they were both fully recovered to pre-irradiation status by day 21 (Figure 4.2A).

Thus, analysis of the progress of erythropoiesis in the spleen and bone marrow regeneration following irradiation indicate that there is a negative regulatory role for Dhh during replenishment of erythrocytes, and in particular, a requirement for Dhh is observed in early erythroid development.

4.2.3 Dhh-/- mice showed increased stress-erythropoiesis after induction of acute anaemia

To focus on stress erythropoiesis in the spleen, acute anaemia was induced in WT and Dhh-/- mice by Phenylhydrazine (PHZ) treatment, which causes denaturation of haemoglobin, and thus results in depletion of erythrocytes only (Shetlar and Hill 1985). Stress erythropoiesis and the recovery wave following acute anaemia were monitored over time.

Firstly, peripheral RBC counts before and after the PHZ treatment were examined for a period of 14 days. The RBC counts of both WT and Dhh-/- mice had greatly decreased 2 days after the treatment, and were gradually decreasing from day 2 to day 5. At day 7, WT mice had reached their lowest RBC counts, while the Dhh-/- mice had started to recover from the loss, and mean RBC counts showed a significant increase ($p=0.01$) compared to WT. Then, the RBC counts of both mice recovered steadily and returned to the level of untreated mice by day 14. (Figure 4.4A)

In addition, the percentages of reticulocytes in peripheral blood were also analysed to monitor the synchronized wave before and after PHZ treatment. The reticulocyte count is also an indicator of anaemia and a measurement of the rate of erythropoiesis. While the acute anaemia is on-going, the numbers of

erythrocytes and reticulocytes will be expanded in response, to compensate for the loss of RBC.

As mentioned in chapter 3, the percentage of reticulocytes was significantly increased from 1.2 in WT mice to 1.6 in Dhh-/- mice (Figure 3.8B). After the PHZ treatment at day 2, the percentage of reticulocytes had dramatically increased in both mice, which indicates that the mice were recovering from RBC loss by producing a large number of erythrocytes. Then, the percentage of reticulocytes continuously increased during day 2 to day 5, and reached its peak at 25% and 33% in WT and Dhh-/- mice, respectively. Mirroring the RBC count, the number of erythrocytes in Dhh-/- had increased to replenish the loss at day 7, and thus the reticulocyte percentage dropped steadily from day 7 to 14 until the RBC counts were fully recovered. On the other hand, the reticulocyte count of WT remained steady at 23% to 28% during day 5 to day 9 and then fell to 5% at day 14. The percentage of reticulocytes at day 9 was significantly decreased from 26% in WT to 16% in Dhh-/- ($p=0.045$). The results indicate Dhh-/- mice needed less time to recover from acute anaemia compared to WT. (Figure 4.4B)

All in all, the RBC count and the analysis of the percentage of reticulocytes revealed that the Dhh-/- mice had accelerated erythropoiesis after PHZ-induced acute anaemia.

4.2.4 Dhh-/- mice showed increased stress-erythropoiesis in the spleen

In Figure 4.5, the spleens of WT and Dhh-/- mice are shown at day 5, day 9 and day 14 after injection of PHZ (Figure 4.5A) in comparison with WT and Dhh-/- spleen under normal conditions (Figure 4.5B). Both spleens were grossly

enlarged and had darker coloration at day 5 after PHZ treatment, indicating that the mice were producing large numbers of RBC from the spleen in response to the acute anaemia, and that thus stress erythropoiesis was induced. On day 9 after treatment, Dhh-/- spleen size was greatly reduced and smaller than that of WT. At day 14, both spleens returned to the average size of untreated mice.

In addition, to confirm if increased erythropoiesis is responsible for the changes in spleen size before and after acute anaemia, histology of these spleens was assessed. Sections of PHZ-treated and untreated spleen were stained with haematoxylin and eosin dye. The two main compartments, red pulp and white pulp, were identified. The red pulp is mainly comprised of erythrocytes and it stained red, while the white pulp area contains lymphocytes and therefore stains densely dark (Figure 4.6A). The ratio of red pulp to white pulp area and percentage of red pulp area were analysed and presented in table 4.1.

Before PHZ treatment, Dhh-/- spleens had visibly more red pulp then that of WT (Figure 4.6 A,B), and the ratio of red pulp/white pulp and the percentage of red pulp were increased from 1.4 in WT to 2.1 in Dhh-/- and 59% in WT and 68% in Dhh-/-, respectively. During day 5 to day 9, the red pulp percentages, as well as the red pulp/white pulp ratio were greatly increased and remained high in both WT and Dhh-/- (Figure 4.6 C-H). At day 14, consistent with the higher recovery rate follow acute anaemia observed in Dhh-/- mice, the red pulp/ white pulp ratio and red pulp percentage was reduced to 2.5 and 71% in Dhh-/-respectively, while they still remained high at 3.7 and 79% in WT (Figure 4.6I,J).

4.2.5 Increased early erythroid subsets and erythroid progenitors in Dhh-/- mice during stress-erythropoiesis

To investigate which stage of erythropoiesis was affected by loss of Dhh and thus led to the abnormal spleen histology and erythropoiesis in Dhh-/- mice, we analysed the erythroblast and the erythroid progenitors isolated from the bone marrow and the spleen during stress erythropoiesis by flow cytometry (Figure 4.7).

Five days after the PHZ injection, both WT and Dhh-/- mice had an enormously expanded population of erythroblast subset II in the spleen, and the percentage increased from 3-8% in normal conditions to over 50% in PHZ treated mice (Figure 3.9, 4.7 left panel).

At day 9, Dhh-/- had only 18% and 4% in erythroblast subset II and III respectively, while WT mice showed 25% and 8% in these two populations (Figure 4.7 left panel). These results were consistent with the decreased proportion of reticulocytes and smaller size of spleen observed in Dhh-/- mice, after PHZ treatment at day 9. The Dhh-/- spleen showed reduced erythropoiesis as it had a higher recovery rate of acute anaemia and thus percentages of the early erythroblast subset in Dhh-/- were already in decline, while they still remained high in WT.

Moreover, an increase in erythropoiesis was also observed in Dhh-/- bone marrow after PHZ treatment compared to WT (Figure 4.7 right panel). At day 5, the proportion of erythroblast subset II was increased from 37% in WT to 47% in Dhh-/-, and only 0.9% and 1% of erythroblast subset IV were found in WT and Dhh-/-, respectively. Interestingly, erythroblast subset II still remained high in

both mice at day 9 after treatment, and the percentage of subset IV were increased to 10% in both mice. Towards the end of the recovery period, after 14 days, an increased percentage of erythroblast subset II was observed in both mice compared to normal conditions (Figure 3.10, 4.7 right panel). There were 35% in WT and 39% in Dhh-/- after treatment compared to 31% in WT and 27% in Dhh-/- in normal conditions.

To investigate whether the early erythroid progenitors were influenced by loss of Dhh during stress erythropoiesis, the proportion of myeloid progenitors were assessed 7 days after PHZ treatment. The populations of CMP, GMP and MEP were defined by the expression of CD34 and FcγRII/III, after gating on Sca-1^{-}c-kit^{+} as seen in Figure 3.14**.** Interestingly, the relative proportion of MEP in the Dhh-/- spleen was significantly increased (Figure 4.8A), whereas it was significantly decreased in bone marrow, when compared to WT (Figure 4.8B). Moreover, the progenitors of other lineages of myeloid cells, the GMP, showed results that mirrored this as the GMP proportions were reduced significantly in the spleen in Dhh-/-, while they were raised in bone marrow (Figure 4.8). Given that the percentage of GMP were altered in Dhh-/-, the proportion of macrophages and granulocytes in the spleen and bone marrow were examined. However, there were no differences between WT and Dhh-/- (Figure 4.9). On the other hand, the percentage of neutrophils was significantly reduced in the Dhh-/- bone marrow compared to WT (Figure 4.10).

Taken together, analysis of the spleen and the proportion of erythroblast subsets, as well as myeloid progenitors, revealed that Dhh-/- mice had abnormal erythropoiesis in the spleen after induction of acute anaemia. Loss of Dhh

increased the MEP populations and enhanced erythrocyte regeneration, thus leading to the higher rate of recovery during stress erythropoiesis.

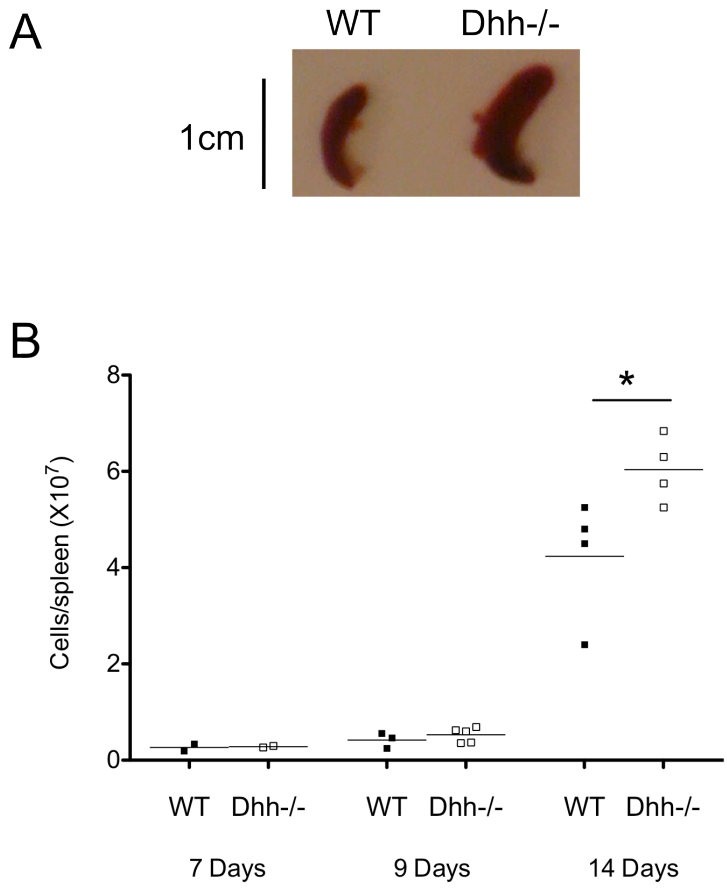

Figure 4.1 Spleen size of irradiated WT and Dhh-/- mice.

(**A**) Photograph shows typical spleen from WT and Dhh-/- mice at day-14 after irradiation. (**B**) Scatter plot shows the total spleen cell numbers isolated from individual WT and Dhh-/- mice at day 7, day 9 and day 14 after radiation. The mean for each group is indicated with a line. (n=2 for experiment at day 7; n=5 for experiment at day 14; n=4 for experiment at day 14) *p<0.05; WT versus Dhh-/- .

.

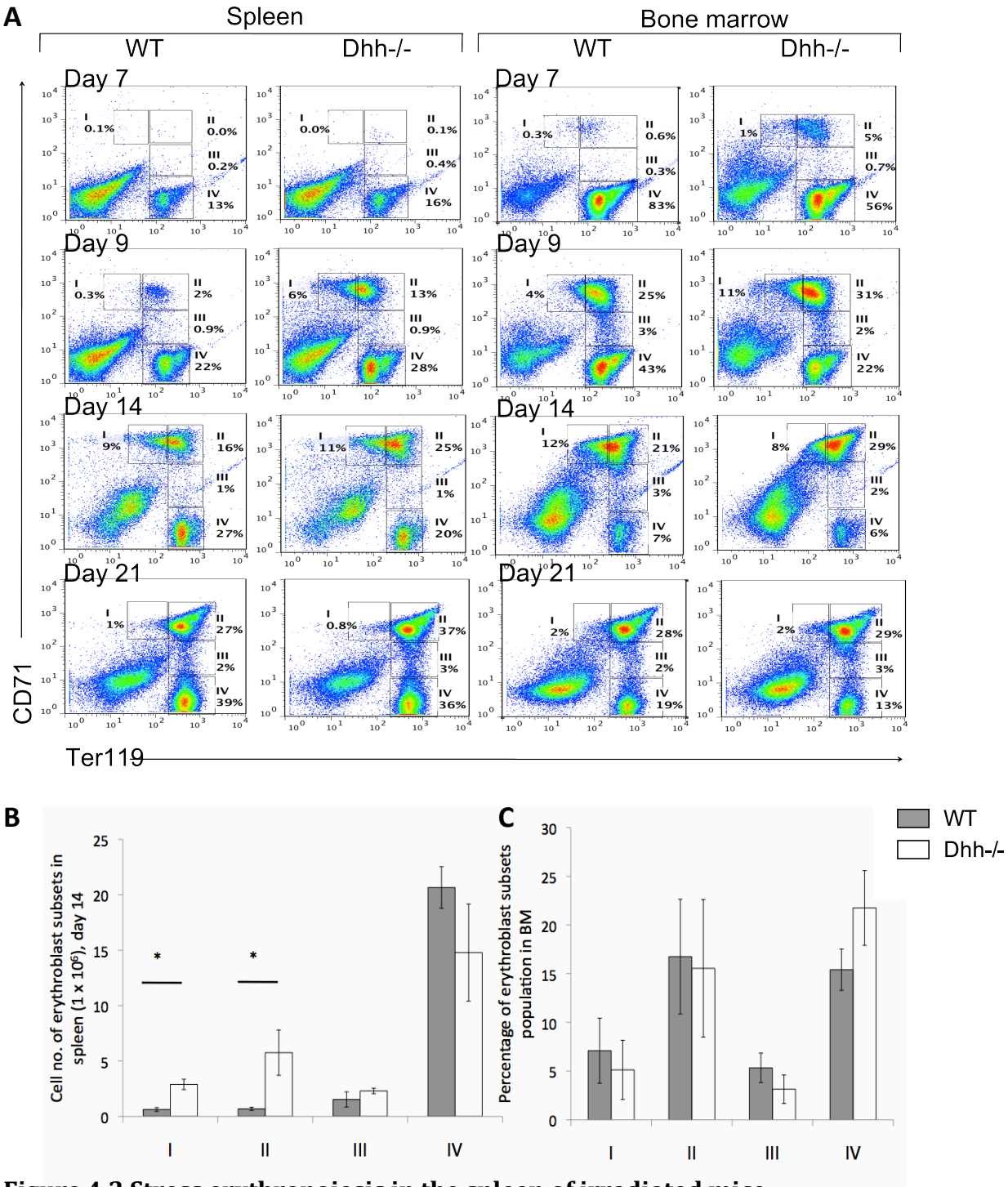

Figure 4.2 Stress erythropoiesis in the spleen of irradiated mice

(**A**) The dot plots show CD71 and Ter119 staining. Splenocytes and bone marrow cells isolated from WT and Dhh-/- irradiated mice at day 7, day 9, day 14 and day 21 after radiation. Four erythroblast populations (I-IV) were identified. Bar charts show the mean cell number of erythroblast populations (I-IV) in spleen (**B**) and bone marrow (**C**) of irradiated mice after 14 days of radiation. Error bars represent ± SEM. (n=2 for experiment at day 7; n=5 for experiment at day 14; n=4 for experiment at day 14; n=2 for experiment at day 21) *p<0.05; WT versus Dhh-/-.

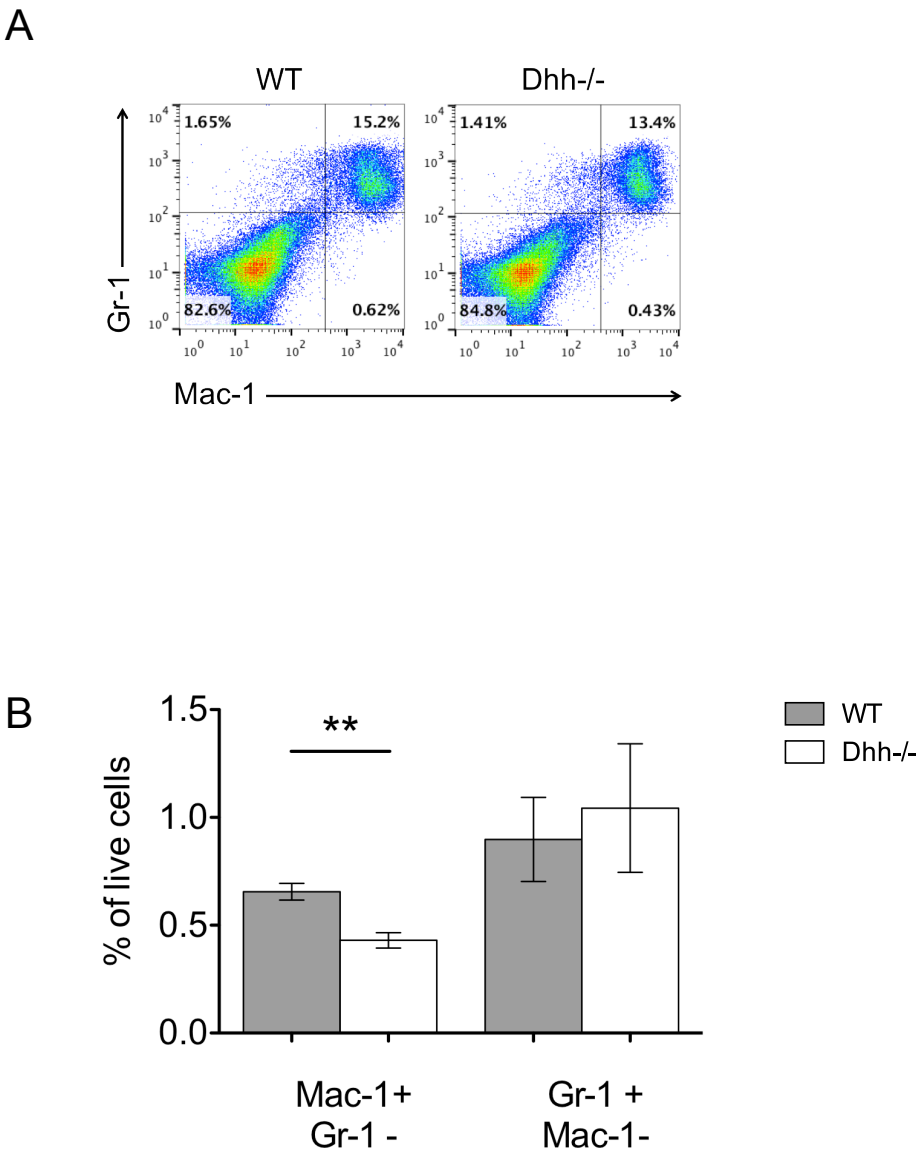

Figure 4.3 Macrophage and Granulocyte composition in WT and Dhh-/- bone marrow

(**A**) The dot plots show staining against Gr-1 and Mac-1 on bone marrow cells isolated from WT and Dhh-/- mice on day 14 after irradiation. (**B**) Histogram shows the mean percentage of macrophages (Mac-1+Gr-1-) and granulocytes (Gr-1+Mac-1-) in bone marrow. Error bars represent ± SEM. (n=5 of each genotype) **p<0.01 WT versus Dhh-/-.

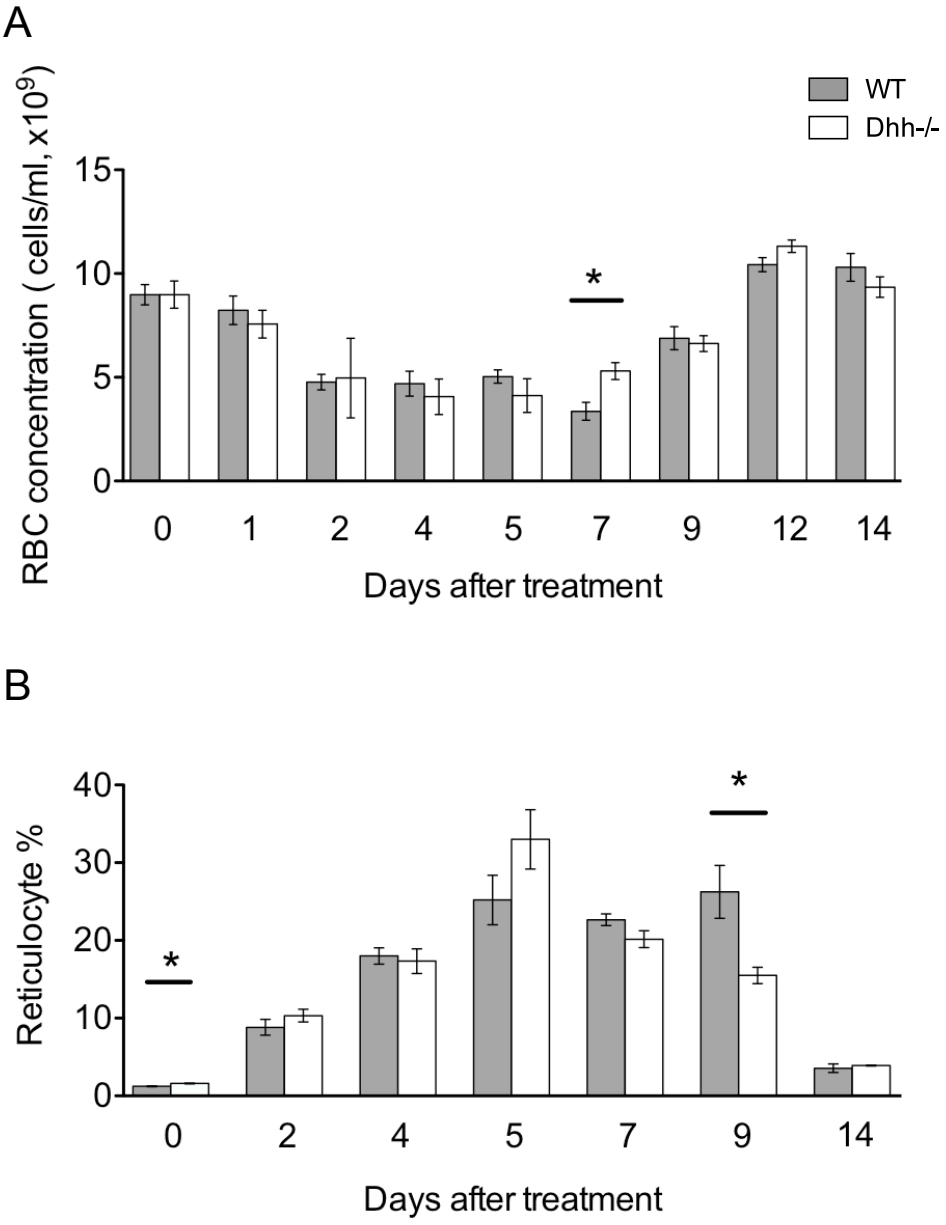

Figure 4.4 RBC concentration and percentage of reticulocytes in peripheral blood in WT and Dhh-/- mice

Bar charts show the mean of RBC concentration (**A**) and percentage of reticulocytes (**B**) in WT and Dhh-/- mice obtained from tail tips before and after PHZ treatment. Error bars represent ± SEM. (n=3 for each genotype) *p<0.05, WT versus Dhh-/-.

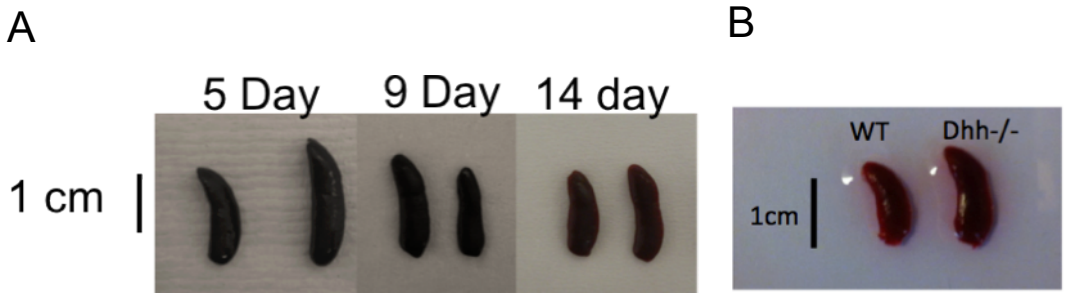

Figure 4.5 Spleen size of PHZ treated WT and Dhh-/- mice

Photographs show typical spleens from WT and Dhh-/- mice at day-5, 9 and 14 after injection of PHZ (**A**) and spleens from WT and Dhh-/- mice without treatments (**B**) as comparison. (n=1 for each time point)

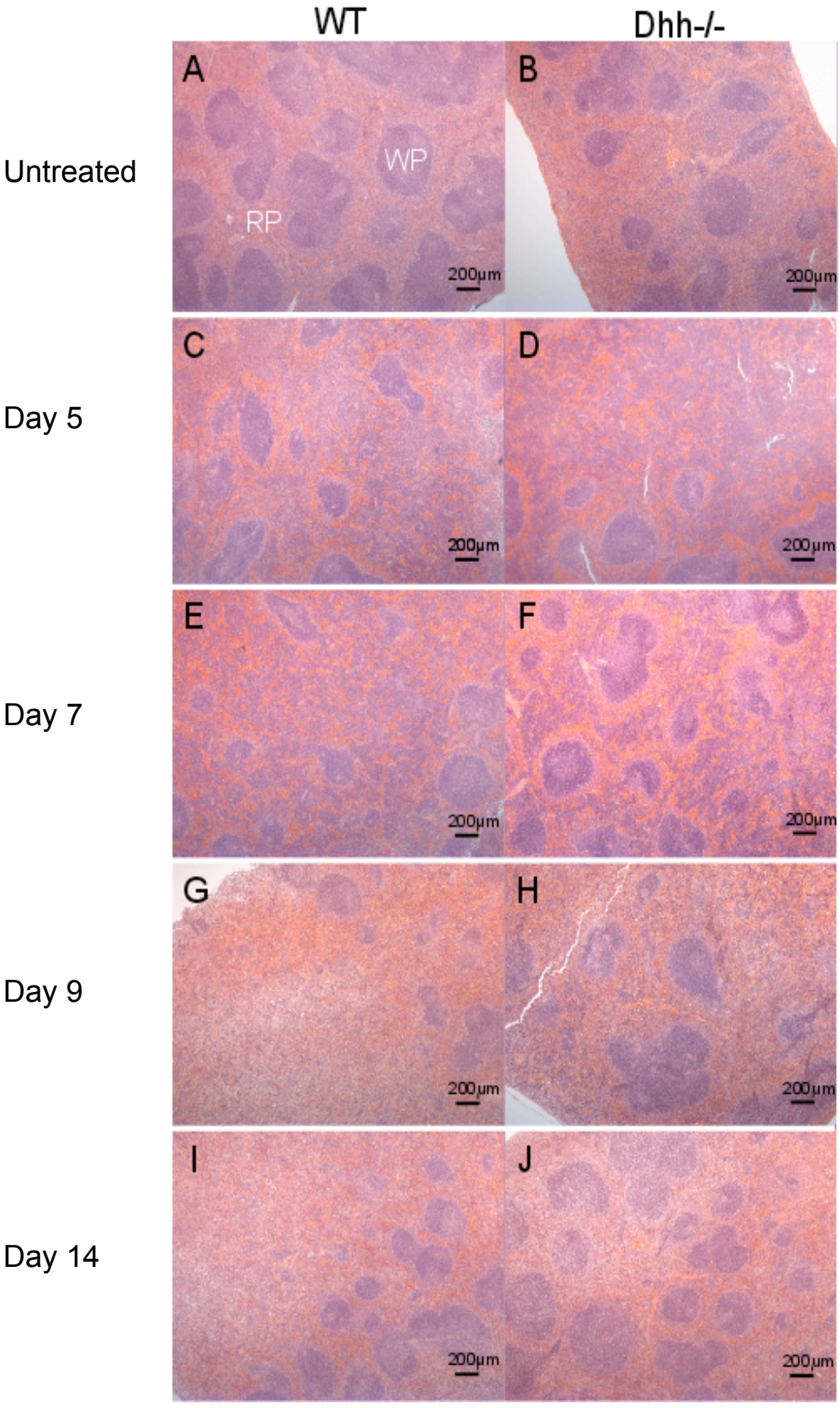
WT
Dhh-/-
Untreated
Day 5
Day 7
Day 9
Day 14
A
B
C
D
E
F
G
H
I
J
WP
RP
200μm

Figure 4.6 Histology of WT and Dhh-/- spleen before and after PHZ treatment

Representative spleen sections show changes in histology in WT and Dhh-/- spleen after treatment with PHZ. Parafin embedded spleen sections were stained with hematoxylin and eosin, to identify white pulp (WP) areas, which stained deeper purple, and red pulp (RP) areas, which stained pink. Typical WP and RP are illustrated in (**A**). Left-hand column (**A**,**C**,**E**,**G**,**I**) shows typical histology in WT spleens and right-hand column (**B**,**D**,**F**,**H**,**J**) shows typical histology in Dhh-/- spleen, without treatment (**A**-**B**) and during a time course following induction of stress-erythropoiesis following PHZ-treatment, on day 5 (**C**-**D**), 7 (**E**-**F**), 9 (**G**-**H**), and 14 (**I**-**J**). (n=1 for each time point)

	Red pulp/White/pulp		Red pulp %	
	WT	Dhh-/-	WT	Dhh-/-
Day 0	1.4	2.1	59	68
Day 5	5.2	4.8	84	83
Day 7	4.8	6.2	83	86
Day 9	5.0	4.9	83	83
Day 14	3.7	2.5	79	71

Table 4.1 The ratio of red pulp/white pulp and percentage of red pulp in control and PHZ-treated WT and Dhh-/- spleen

Red pulp and white pulp and entire surface area of longitudinal sections of paraffin embedded spleen from WT and Dhh-/- mice, untreated (day 0) and at time points after PHZ-treatment. Ratio of red pulp and white pulp and percentage of red pulp were quantified using ImageJ software. (n=1 for each time point)

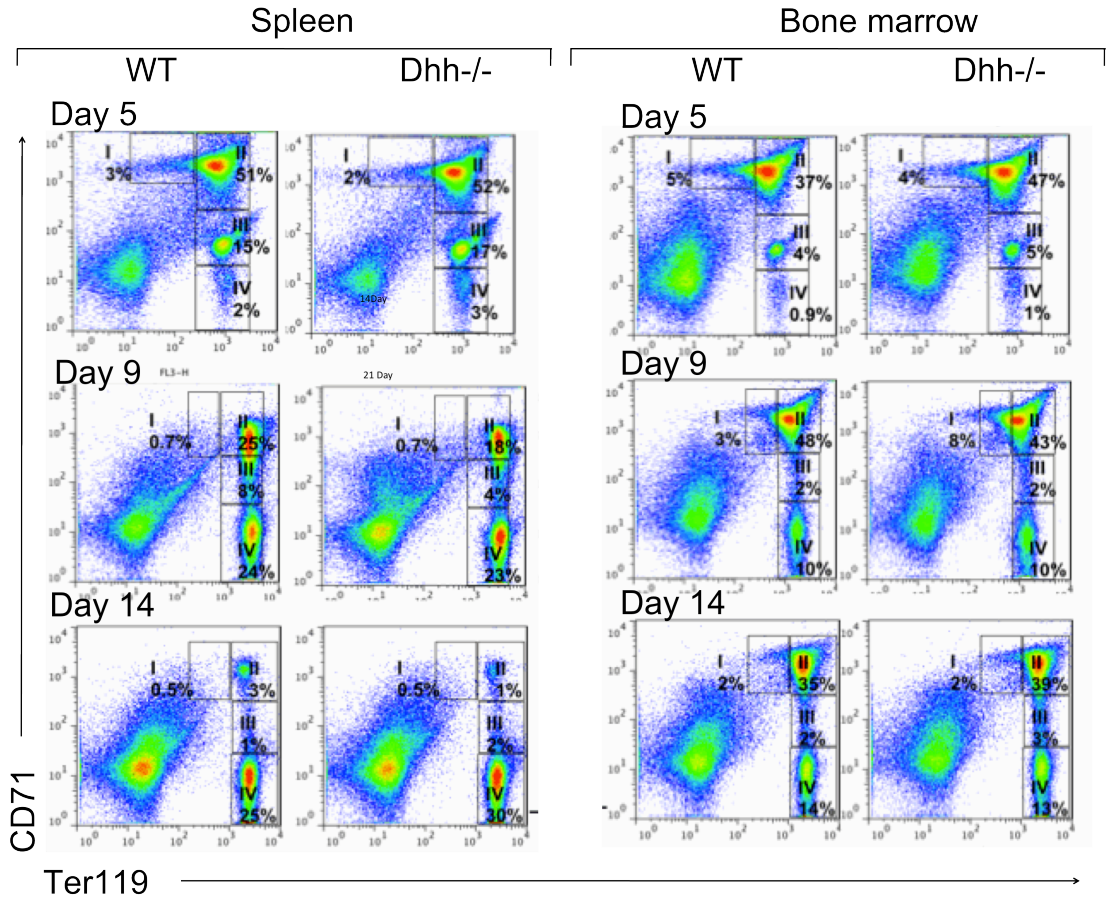

Figure 4.7 Stress erythropoiesis in the spleen and bone marrow of PHZ treated mice

Dot plots show CD71 and Ter119 staining from WT and Dhh-/- mice at day 5, day 9, and day 14 after PHZ injection. Four erythroblasts populations (I-IV) were identified. (n=1 for each time point)

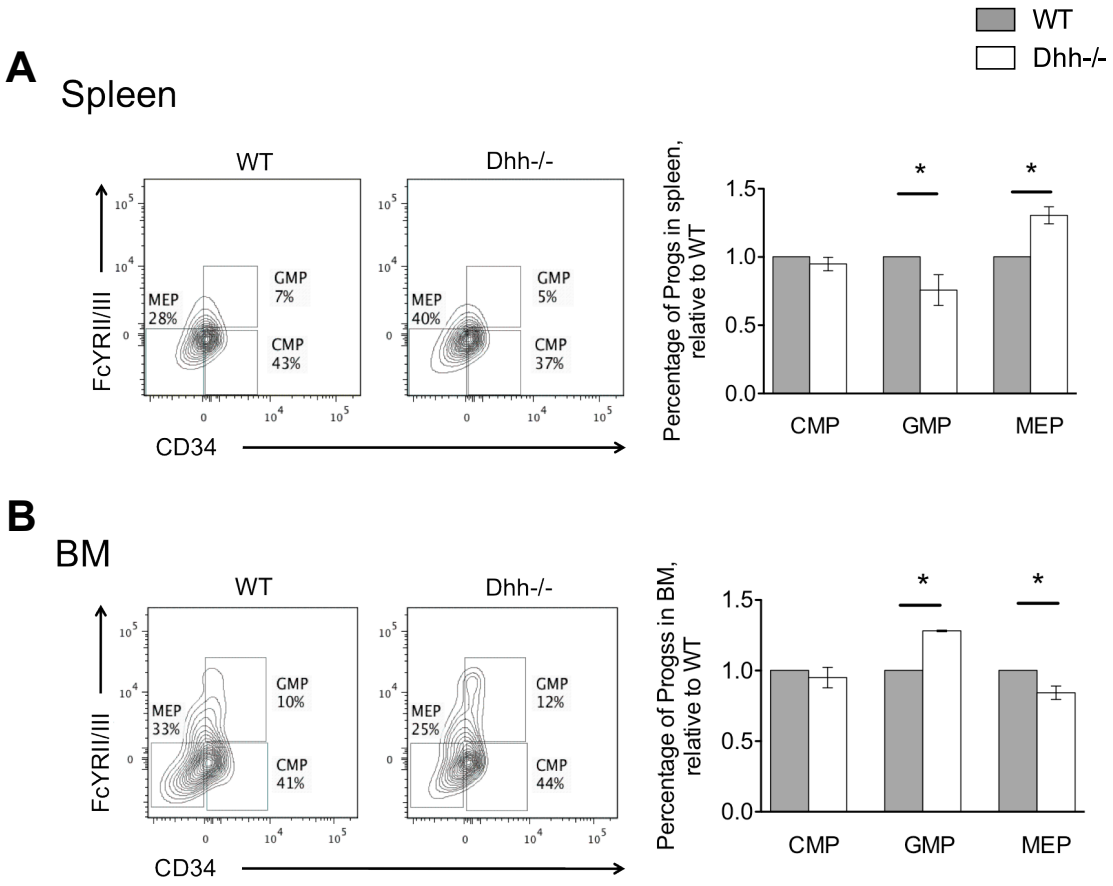

Figure 4.8 Myeloid progenitors in spleen and bone marrow 7 days after PHZ treatment

The dot plots show populations of FcϒRII/III^{+}CD34^{+}(GMP), FcϒRII/III^{-}CD34^{+} (CMP) and FcϒRII/III $^{-}$ CD34^{-}(MEP), in the spleen (**A**) and bone marrow (**B**) after gating on the myeloid progenitors (Lin^{-}Sca-1^{+}C-kit^{+}(Prog)). Bar charts show relative percentage of CMP, GMP and MEP in the spleen (**A**) and bone marrow (**B**). In each experiment, the average value of the WT is set to 1, to allow comparison between experiments. Error bars represent ± SEM. (n=3 for each genotype) *p<0.05 WT versus Dhh-/-.

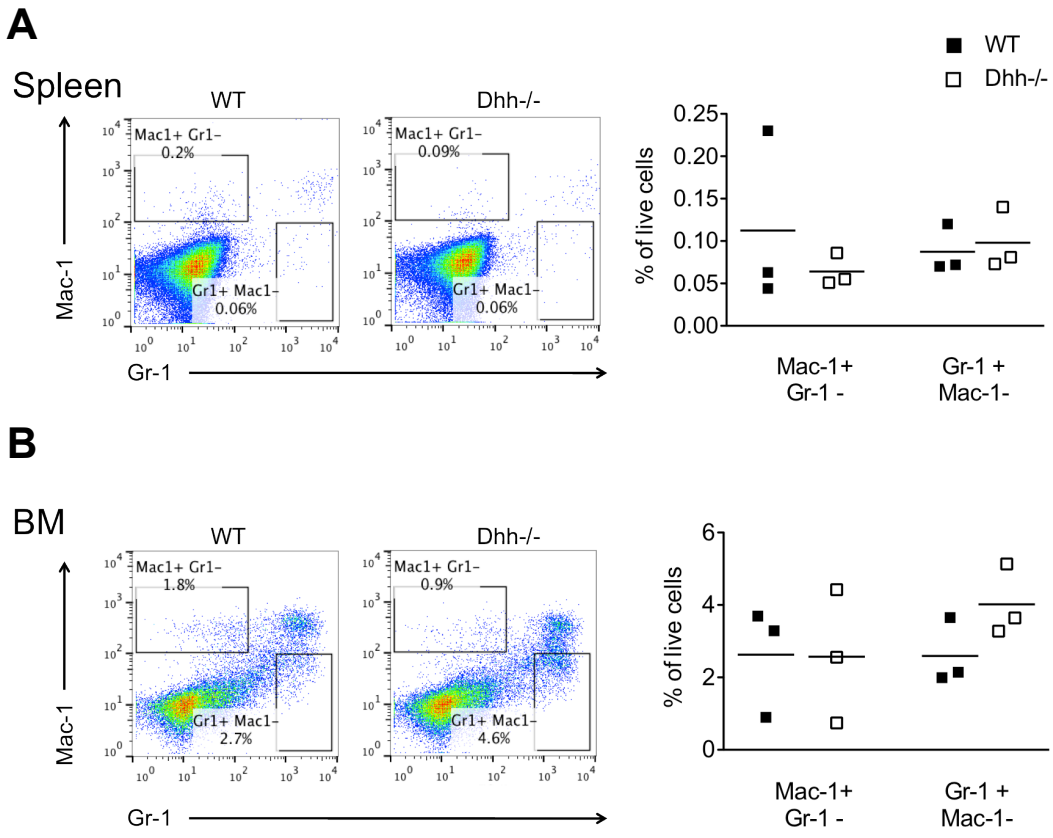

Figure 4.9 Percentage of macrophages and granulocytes in spleen and bone marrow 7 days after PHZ treatment

Dot plots show staining against Gr-1 and Mac-1 in the spleen (**A**) and bone marrow (**B**) isolated from WT and Dhh-/- mice. Scatter plots show the percentage of Mac-1+Gr-1- and Gr-1+Mac-1- in individual WT and Dhh-/- spleen (**A**) and bone marrow (**B**). The mean for each group is indicated with a line. (n=3 for each genotype)

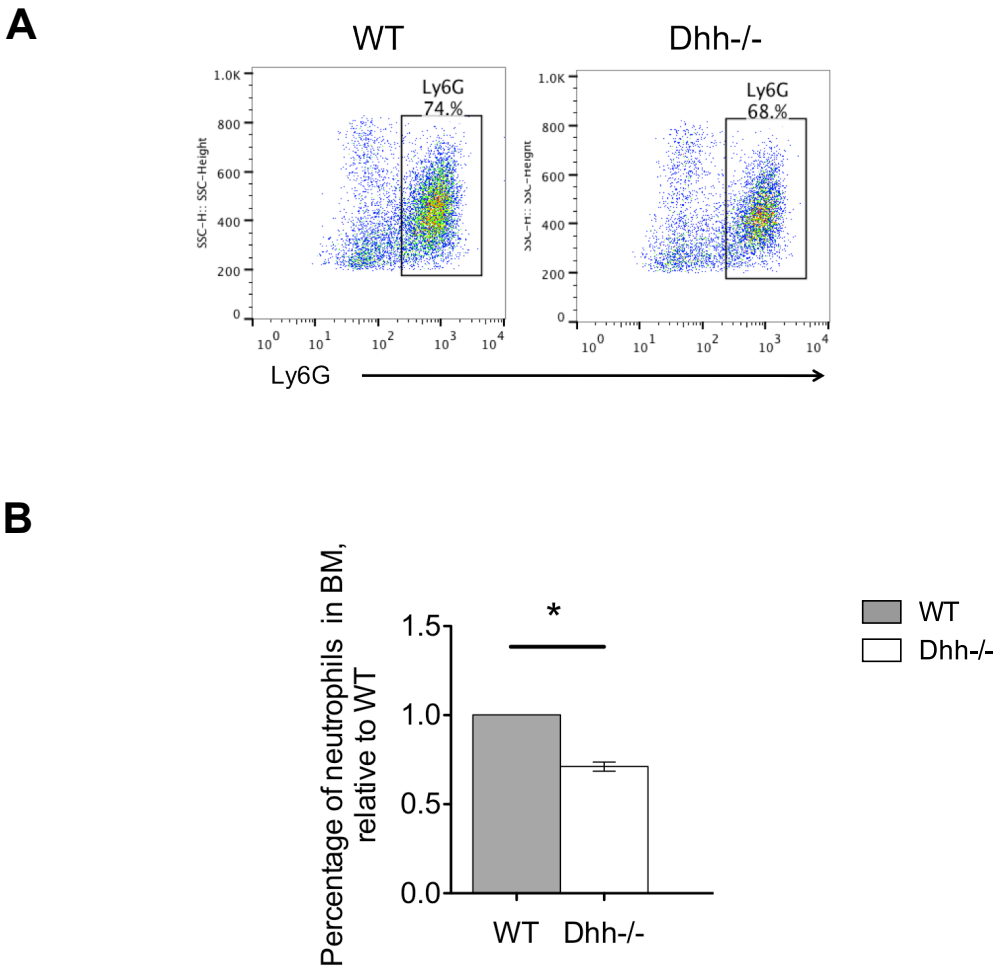

Figure 4.10 Percentage of neutrophils in bone marrow 7 days after PHZ treatment

(**A**) The dot plots show the proportion of neutrophils (Ly6G+) in bone marrow after gating on granulocytes (Gr-1+) isolated from WT and Dhh-/- mice. (**B**) Bar chart shows the mean percentage of neutrophils in Dhh-/- bone marrow, relative to WT. In each experiment, the average value of the WT is set to 1, to allow comparison between litters. Error bars represent ± SEM. *p<0.05 WT versus Dhh-/-. (n=3 for each genotype)

4.3 Discussion

Following chemotherapy or radiotherapy, humans, as well as mice, may experience bone marrow regeneration and stress erythropoiesis to replenish the HSCs and erythrocytes. Use of mouse models to induce bone marrow regeneration and stress erythropoiesis by sub-lethal irradiation or treatment with drugs to induce anaemia, can help to better understand the regulation of haematopoiesis and erythropoiesis.

Here we showed that loss of Dhh resulted in acceleration of erythropoiesis in the spleen and altered haematopoiesis in the bone marrow during recovery from irradiation and PHZ-induced acute anaemia. It is the first study to reveal that Dhh is essential in bone marrow regeneration and stress erythropoiesis *in vivo*.

Our findings are consistent with previous reports. Study of Ptch-1+/- mice revealed that Hh signalling is involved in positively regulating haematopoietic regeneration (Trowbridge et al., 2006). Study of conditional deletion of Smo mice also showed that Smo-deficient cells were unable to respond to BMP4 and failed to recover normally after PHZ-induced acute anaemia (Perry et al. 2009). In addition, it has been demonstrated that Shh is essential for expansion of stress erythroid progenitors, and that Shh functions in association with BMP4, in response to stress erythropoiesis in the spleen (Perry et al. 2009). That group also proposed that either Ihh or Dhh act together with BMP4 to promote the development of stress erythroid progenitors. Given the fact that BMP4 and Dhh are coexpressed in non-hematopoietic stromal cells in the spleen, and that the

expression of Dhh is maintained at high levels after PHZ-induced erythropoiesis, it is possible that Dhh, among the Hh proteins, is associated with BMP4 in the stress erythropoiesis pathway. BMP4 is also a key regulator of haematopoiesis in bone marrow and it has been found that regeneration of haematopoietic cells was defected in BMP4-deficient mice (Goldman et al. 2009). The altered numbers of myeloid progenitors observed in Dhh-/- bone marrow after PHZ-induced acute anaemia suggested that Dhh is involved in haematopoietic regeneration in bone marrow. The ability to influence haematopoietic regeneration of Dhh and BMP4 indicates that these two signalling may interact with each other in the bone marrow micro-environment to regulate haematopoiesis. Further studies will need to be carried out to test these hypotheses.

Given the different expression levels of Hh proteins in the spleen that were found before and during the process of stress erythropoiesis (Perry et al. 2009), it will be also interesting to examine the expression of Hh signalling components in bone marrow during the recovery from irradiation.

4.4 Conclusion

In this chapter, we showed that Dhh is involved in regulation of stress erythropoiesis. Analysis of the kinetics of erythropoiesis in the Dhh-/- spleen and bone marrow following treatment by irradiation and PHZ revealed that Dhh acts as a negative regulator in stress erythropoiesis. Increased spleen size and accelerated erythropoiesis in Dhh-/- mice was observed after irradiation and PHZ-induced anaemia. Loss of Dhh affected not only the differentiation of the erythroid lineage, but myeloid progenitors were also altered. The proportions of macrophages and GMP were decreased in Dhh-/- bone marrow, revealing that Dhh is involved in the regulation of differentiation of myeloid progenitor populations during recovery after PHZ-induced acute anaemia.

Chapter Five : Hh signalling pathway in embryonic erythropoiesis

Abstract

Precise regulation of haematopoiesis is crucial during embryogenesis. Although the role of Hh signalling in embryonic development has been known for decades, the precise function of the Hh signalling pathway in erythropoiesis during embryonic development is still not clear. In this study, the role of Dhh, Smo and Gli3 in haematopoiesis, especially erythropoiesis in murine fetal liver were examined. Analysis of Dhh mutant embryos did not reveal altered haematopoiesis in the fetal liver. However, conditional deletion of Smo in the haematopoietic lineage resulted in a decreased proportion of early haematopoietic progenitors, whereas mice carrying one copy of Gli3 showed an increased proportion of GMP and decreased proportion of MEP relative to WT. Moreover, Gli3+/- embryos also exhibited a reduction in the erythroblast population compared to WT.

5.1 Introduction

5.1.1 Murine fetal haematopoiesis

After birth, haematopoiesis takes place mainly in the bone marrow, and this continues throughout life. During embryonic development, however, the sites that produce haematopoietic cells shift to various places. In mammals, two major haematopoietic phases have been defined. The first haematopoietic wave, named primitive haematopoiesis, occurs in the yolk sac at E7 in mice. Primitive erythroid progenitors (EryP) are the main and earliest population produced at this stage, whereas rare primitive macrophage and megakaryocyte progenitors are also detected in the yolk sac (Palis et al. 1999, Tober et al. 2007, Xu et al. 2001). This is followed by the second wave, definitive haematopoiesis, which begins within the aorta-gonads-mesonephros (AGM) region at E10 (Medvinsky and Dzierzak 1996). Although the initial production of haematopoietic stem cells (HSC) is detected in the AGM region, the HSC produced at this stage are incapable of differentiating into different lineages (Godin et al. 1999). Instead, the HSC seed the fetal liver at around E11 to give rise to multipotent haematopoietic cells. In the fetal liver, the HSC are then expanded and differentiate into different haematopoietic lineages, including myeloid, T-cell, and B-cell precursors. (Ema and Nakauchi 2000, Ema et al. 1998, Gunji et al. 1991) (Figure 1.1)

The fetal liver then acts as a major site of haematopoiesis during mid- to late-gestation development. When HSC seed the fetal liver, the differentiation of the erythroid lineage begins. BFU-E are detected as early as E11.5, the number of erythroblasts are then greatly induced, and erythropoiesis reaches a peak at

E12.5 (McGrath et al. 2011, Tada et al. 2006). Haematopoiesis is then subsequently shifted to the thymus for T-cells and spleen from mid-gestation, and to the bone marrow before birth and throughout postnatal life (Rieger and Schroeder 2012). (Figure 1.1)

5.1.2 Primitive and definitive erythropoiesis

The term primitive haematopoiesis refers to haematopoiesis derived from primitive haematopoietic progenitors that develop from the yolk sac in early development, while definitive haematopoiesis generates all haematopoietic lineages, except the primitive progenitors, in the fetus, and after birth. The erythroid progenitors generated from these two different phases are different in a number of important characteristics.

The primitive erythroid progenitors (EryP) are generated exclusively in the yolk sac, only for a very brief period between E7 and E9, and arise from unique erythroid-restricted precursors, the primitive erythroid-colony forming cells (EryP-CFC) (Keller et al. 1993, Palis et al. 1999). In contrast, definitive erythroid progenitors (EryD) can be found in the fetal liver, spleen and bone marrow, and they are derived from BFU-E and CFU-E progenitors. The two erythroid lineages also differ in size and express distinct forms of haemoglobin. EryP are much larger than EryD, and express both embryonic and adult haemoglobins, while EryD express only adult forms of haemoglobins (Kingsley et al. 2006, Wong et al. 1986)

It has been long believed that the EryP that are circulating retain their nuclei during murine embryonic development (Palis and Yoder 2001). However, a number of studies have demonstrated that EryP are only nucleated during early-gestation, and that they eventually enucleate between E12.5 and E16.5 and continue to circulate throughout development up until the end of gestation and even for a few days after birth (Fraser et al. 2007, Kingsley et al. 2004).

5.1.3 The role of Hh signalling in primitive and definitive haematopoiesis

It has been found that Ihh and Dhh are expressed in the yolk sac (Farrington et al. 1997), whereas many Hh pathway components are expressed in the fetal liver, including Ihh, Dhh, Ptch1, Smo and Gli (Cridland et al. 2009, Dyer et al. 2001). These expression patterns, and the fact that Hh signalling plays an important role in development during embryogenesis, therefore, suggest that Hh signalling may also be involved in haematopoiesis during embryonic development.

Among the three mammalian Hh ligands (Shh, Ihh and Dhh). Ihh has been relatively well studied in embryonic haematopoiesis, and several studies have reported that Ihh is required for differentiation and proliferation in both primitive and definitive haematopoiesis. Byrd (2002) found that loss of Ihh in the yolk sac resulted in defects in blood island formation and led to the failure of vasculogenesis and haematopoiesis in the embryo (Byrd et al. 2002). Moreover, Ihh-/- mice developed defective erythropoiesis in the fetal liver, led to mid-gestation anaemia which may be responsible for partial embryonic

death (Cridland et al. 2009). Activation of the Hh signal by stimulation with recombinant Ihh proteins demonstrated that Ihh induced the initiation of primitive haematopoiesis, whereas blocking of Hh activity by anti-Hh antibodies resulted in inhibition of initiation of haematopoiesis (Dyer et al. 2001). Similarly, cell number and proliferation of human primitive haematopoietic progenitors were enhanced by stimulation with either Shh or Dhh proteins (Bhardwaj et al. 2001). These studies suggest that Hh ligands and activation of the Hh signalling pathway are required for regulation of primitive and definitive haematopoiesis during embryogenesis.

Ptch and Smo are important Hh pathway mediators, and therefore, the role of these two Hh pathway components in haematopoiesis has also been investigated by various groups. Mice with loss of one copy of Ptch have increased numbers of HSC and progenitors, and Ptch+/- fetal liver cells displayed enhanced regenerating ability and self-renewal properties of short-term HSC compared with WT (Dierks et al. 2008, Trowbridge et al. 2006). These findings are consistent with a recent study of Smo in HSC, suggesting that loss of Smo impairs the self-renewal ability of HSC (Zhao et al. 2009).

In contrast, other studies which used conditional deletion of Smo mice in haematopoietic cell lineages to analyse the effects of Smo on adult haematopoiesis and HSC self-renewal ability and homeostasis showed contradictory results. It was found that deletion of Smo did not lead to defects in normal HSC differentiation and homeostasis, suggesting that loss of Smo did not impact on definitive haematopoiesis (Gao et al. 2009, Hofmann et al. 2009).

The studies above have focused on the functions of up-stream modulators of the Hh pathway, including Hh ligands, Ptch and Smo. However, investigation of the down-stream effectors may give a better understanding of the function of Hh signalling. Thus, there are also studies on the role of Gli genes in haematopoiesis. The Gli transcription factors are the main effectors of Hh signalling. Gli1 is a positive regulator of Hh-mediated transcription, while Gli3 acts as an inhibition of Hh-mediated transcription (Marigo et al. 1996, Ruiz i Altaba 1998). Recent studies in adult mice showed Gli1 and Gli3 are involved in regulation of HSC differentiation and human pluripotent stem cell development respectively (McIntyre et al. 2013, Merchant et al. 2010).

In summary, 1) Ihh acts as a positive regulator in definitive erythropoiesis in fetal liver, 2) increased Hh activity by endogenous or recombinant Hh proteins can stimulate primitive haematopoietic progenitor proliferation and HSC self-renewal ability, 3) Gli transcription factors are involved in HSC development.

In many respects, the fact that Hh signalling plays a role in haematopoiesis has been widely established in the last decade. However, the precise role of Hh signalling in haematopoiesis during embryonic development is still unknown. Thus, more studies are needed to determine the functions of each Hh component in embryonic haematopoiesis.

Objectives:

In the last two chapters, we reported that Dhh is involved in the control of erythroid development, and haematopoiesis under normal and stressed

conditions. In this chapter, we will test if Dhh influences erythropoiesis in the mouse embryo. In addition, we will investigate the role of a main Hh component, Smo, in embryonic and adult erythropoiesis, and a downstream target of the Hh signalling pathway, Gli3, in embryonic erythropoiesis.

5.2 Results

5.2.1 Loss of Dhh did not alter embryonic erythropoiesis

Fetal liver acts as a major site of haematopoiesis during mid- to late-gestation development. Dhh is expressed in the fetal liver (Cridland et al. 2009). In order to determine whether Dhh is involved in the regulation of embryonic haematopoiesis and erythropoiesis, the Dhh+/- mice were inter-crossed to produce WT, Dhh+/- and Dhh-/- embryos. Since there were no visual differences between the different genotypes of embryo, genotying was performed by PCR, as shown in chapter 3 (Figure 3.6).

Given that haematopoiesis in the murine fetal liver begins on E14.5, fetal liver cells between E14.5 and E15.5 were isolated and analysed. There were no differences in fetal liver cell number between Dhh+/-, Dhh-/- and WT (Figure 5.1A). The proportions of haematopoietic progenitors and erythroblast subsets from Dhh+/- and Dhh-/- fetal liver, were assessed and shown relative to WT, to allow comparison between littermates. Again, no significant differences between groups were detected in both progenitors and erythroblast subsets (Figure 5.1B, C, D).

5.2.2 Conditional deletion of Smo impairs haematopoietic cell differentiation

Smo is an important mediator of Hh signalling. Conflicting results have been reported regarding the role of Smo in the regulation of haematopoiesis. Smo-

null embryos die at E9 due to severe developmental defects, including patterning of somite, heart and gut (Zhang et al. 2001). Thus, to study whether loss of Smo altered haematopoiesis during embryogenesis, mice conditionally deficient of Smo were generated by crossing $Smo^{flox/flox}$ mice with vav-cre mice to inactivate Smo in all haematopoietic cells. The $Smo^{flox/flox}$ vav-cre+ (Smo KO) mice were analysed and compared with $Smo^{flox/flox}$ vav-cre- (Smo WT) littermates. To determine genotypes of Smo WT and Smo KO littermates, PCR was performed. Figure 5.2 shows an agarose gel with PCR products that were amplified from genomic DNA extracted from Smo WT and Smo KO embryo tail.

To study embryonic erythropoiesis, haematopoietic cells from E14.5 Smo WT and Smo KO fetal liver were isolated and analysed. Although there were no differences observed in fetal liver size between the Smo WT and Smo KO (Figure 5.3A), the relative proportions of haematopoietic stem cells (LSK) and myeloid progenitors (Prog) were clearly decreased in the Smo KO compared to Smo WT littermates. The relative percentage of LSK were significantly decreased in Smo KO ($p=0.04$) (Figure 5.3B). The proportions of CMP, GMP and MEP were similar in Smo WT and Smo KO mice (Figure 5.3C). The relative percentages of the erythroblast subsets showed no significant difference between the two groups (Figure 5.3D).

5.2.3 Abnormal haematopoiesis in Gli3 mutant embryos

It has been found that the Gli3 transcription factor acts as positive or negative regulator of Hh signalling, dependent on the absence or presence of Hh signals.

In the absence of Hh, a truncated form of Gli3 is produced which binds Gli binding sites and prevents the transcription of Hh target genes. It is thus able to inhibit the activation of Hh-mediated transcription. In the presence of Hh signals, Gli3 functions as a transcriptional activator. (Ruiz i Altaba 1999, Sasaki et al. 1999) In addition, Gli3 acts to repress Shh transcription in some tissues. The fact that the Gli3-mutants and Shh-mutants have opposing phenotypes and that Gli3-mutant tissues show higher levels of Hh pathway activation than WT, confirm that Gli3 acts mainly as a transcriptional repressor of Hh signalling (te Welscher et al. 2002).

Gli3 is considered to be important in development. Mice deficient in Gli3 die before or shortly after birth with severe birth defects, including brain malformations and polydactyly (Schimmang et al. 1992). Mice heterozygous for mutation of Gli3 appear normal and viable, but with an extra digit formed in the anterior side of the limb (Schimmang et al. 1992).

Recently, the role of Gli3 in thymocyte development has been established. It was found that Gli3 is expressed in thymus stromal cells and regulates thymocyte development in the fetal thymus (Hager-Theodorides et al. 2005, Hager-Theodorides et al. 2009). However, the role of Gli3 in erythropoiesis and haematopoiesis during embryogenesis has not been studied. We tested if Gli3 plays a role in erythropoiesis and haematopoiesis in the fetal liver by analyzing mice with heterozygous (Gli3+/-) and homozygous (Gli3-/-) mutation for Gli3 compared with their WT littermates.

The Gli3 mutant mice were genotyped by their characteristic extra toe and polydactyly phenotypes (Figure 5.4). There were no differences in the size of fetal liver between Gli3+/-, Gli3-/- and WT (data not shown). The haematopoietic progenitors and erythroblast subsets were analysed and shown relative to WT. Again, no significant differences between groups were detected in the early haematopoietic progenitors (Figure 5.5B). In contrast, the frequency of GMP and MEP showed significant changes between WT and Gli3+/- on E17.5. The relative percentage of GMP was increased by 50% in Gli3+/-, while the percentage of MEP was reduced 15% in Gli3+/- compared to WT littermates (GMP, p= 0.026; MEP, p=0.038). Furthermore, analysis of the percentage of erythroid subsets revealed that Gli3+/- had less mature erythroblasts at this stage (p=0.014) (Figure 5.5C).

5.2.4 Loss of Smo in the adult did not influence haematopoiesis

Although loss of Smo in haematopoietic cells did not affect embryonic erythropoiesis, the early stages of haematopoiesis were altered (Figure 5.3). Thus, we continued to investigate if Smo deletion influenced haematopoiesis in conditional Smo KO adult mice.

To assess the role of Smo in the regulation of adult haematopoiesis, bone marrow cells from Smo WT and Smo KO mice were isolated and the proportion of the LSK and myeloid progenitors were analysed. There were no significant differences shown in the percentage of LSK and all myeloid progenitor populations (CMP, GMP and MEP) between WT and Smo KO mice (Figure 5.6A, B). The percentage of erythroblast subsets isolated from bone marrow and

spleen, as well as the size of spleen, were also investigated, and likewise, showed no significant differences between groups (Figure 5.6C-E).

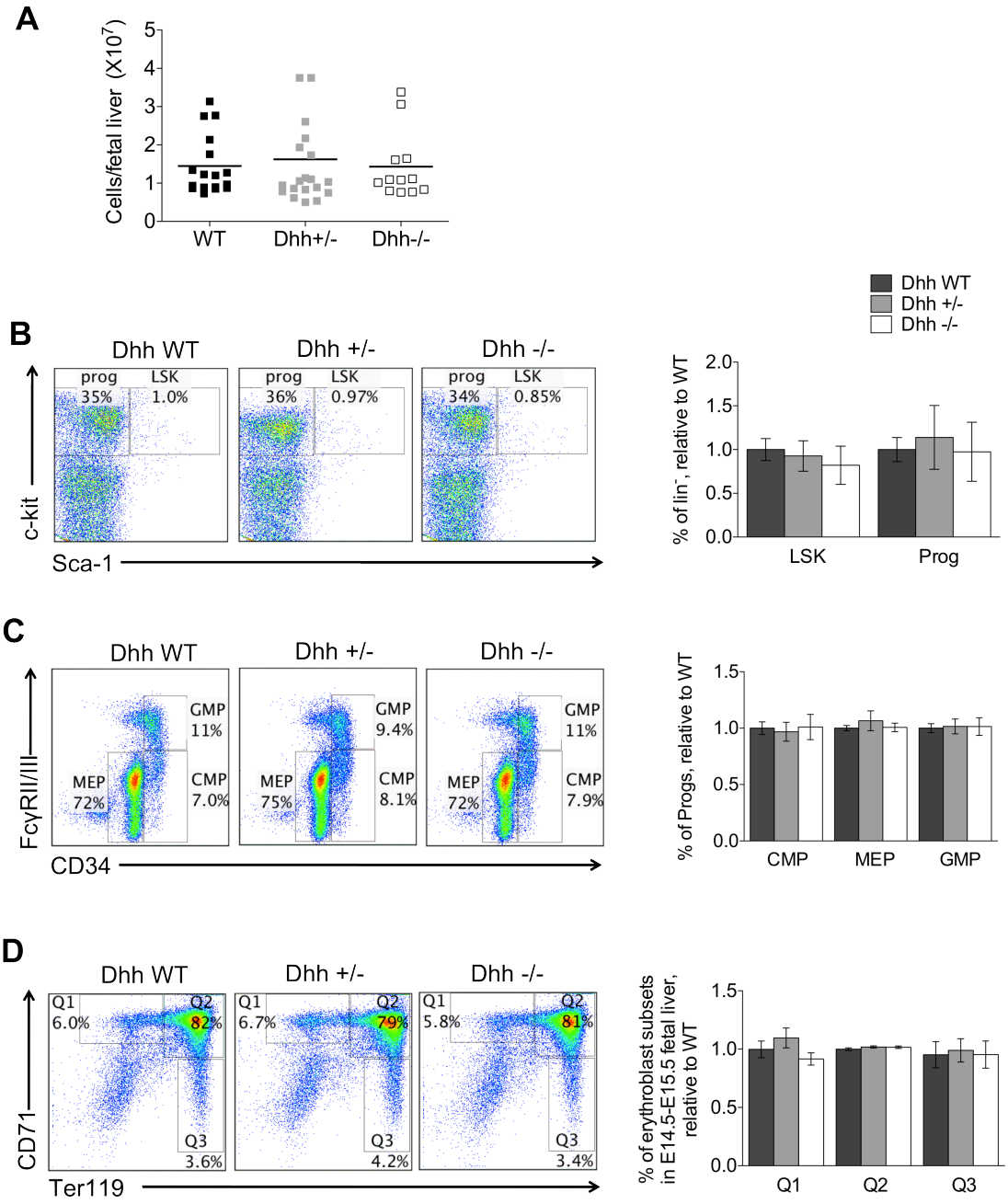
A
Cells/fetal liver (X10^7)
WT
Dhh+/-
Dhh-/-
B
Dhh WT
Dhh +/-
Dhh -/-
prog
LSK
35%
1.0%
36%
0.97%
34%
0.85%
c-kit
Sca-1
% of lin-, relative to WT
LSK
Prog
C
GMP
11%
MEP
72%
CMP
7.0%
GMP
9.4%
MEP
75%
CMP
8.1%
GMP
11%
MEP
72%
CMP
7.9%
FcγRII/III
CD34
% of Progs, relative to WT
CMP
MEP
GMP
D
Q1
6.0%
Q2
82%
Q3
3.6%
Q1
6.7%
Q2
79%
Q3
4.2%
Q1
5.8%
Q2
81%
Q3
3.4%
CD71
Ter119
% of erythroblast subsets in E14.5-E15.5 fetal liver, relative to WT
Q1
Q2
Q3

Figure 5.1 Erythroblast subsets and progenitors in Dhh mutant E14.5-E15.5 fetal liver

(**A**) Scatter graph shows the cell number of each individual WT, Dhh+/- and Dhh-/- E14.5-E15.5 fetal liver. The mean of each group is indicated with a line. (**B**) Fetal liver cells were analyzed by mutliparameter flow cytometer to identify the hematopoietic stem cells Lin^{-} Sca-1 $^{+}$ C-kit^{+} (LSK) and the myeloid progenitors, Lin^{-} $Sca\text{-}1^{-}$ C-kit^{+} (Prog). Bar chart shows relative percentage of LSK and Prog within the lineage negative compartment in WT, Dhh+/- and Dhh-/- mice. (**C**) The Prog population is subdivided by expression of CD34 and FcϒRII/III which results in FcϒRII/III $^{+}$CD34 $^{+}$(GMP), FcϒRII/III^{-} CD34 $^{+}$ (CMP), FcϒRII/III $^{-}$ $CD34^{-}$ (MEP). Bar chart shows relative percentage of CMP, GMP and MEP within the myeloid progenitor compartment in WT, Dhh+/- and Dhh-/- embryos. (**D**) Three populations of erythroblast subsets were identified by expression of CD71 and Ter119 in fetal livers. Bar chart shows relative percentage of erythroblasts population (Q1-Q3) in WT, Dhh+/- and Dhh-/- mice. In each experiment (litter) the average value of the WT is set to 1 so as to allow comparison between litters. Error bars represent ± SEM.

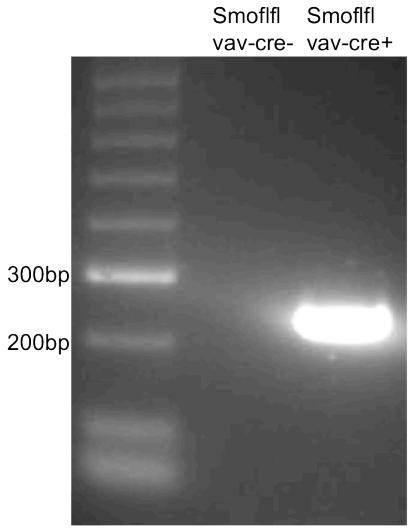

Figure 5.2 PCR genotyping for Vav-cre

PCR of genomic DNA for $Smo^{flox/flox}$ Vav-cre- (WT) and $Smo^{flox/flox}$ Vav-cre+ (Smo KO) mutated bands ran on a 1% agarose gel visualized using U.V.

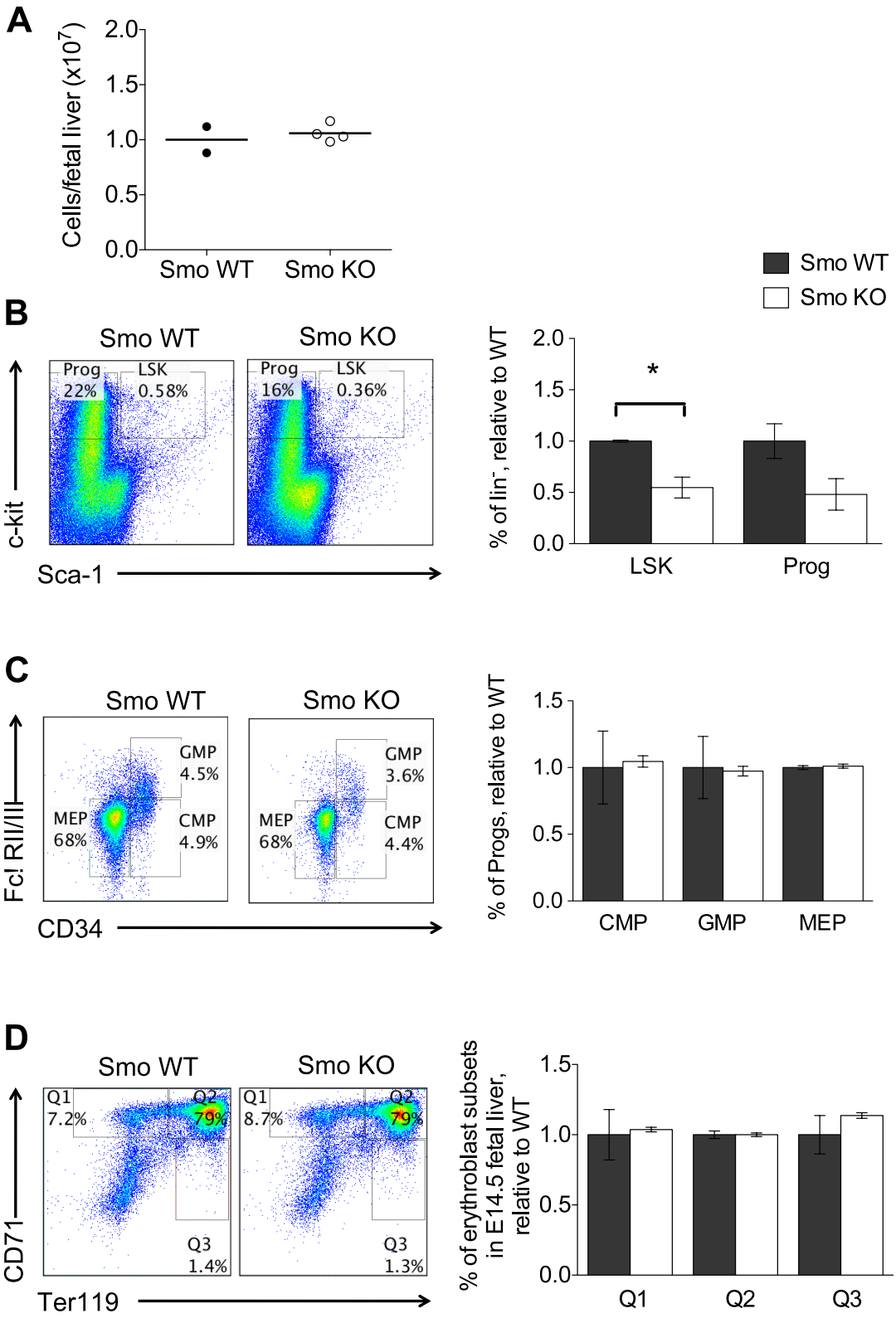
A
Cells/fetal liver (x10^7)
2.0
1.5
1.0
0.5
0.0
Smo WT
Smo KO
B
Smo WT
Smo KO
Prog
22%
LSK
0.58%
Prog
16%
LSK
0.36%
c-kit
Sca-1
Smo WT
Smo KO
% of lin⁻, relative to WT
2.0
1.5
1.0
0.5
0.0
*
LSK
Prog
C
Smo WT
Smo KO
GMP
4.5%
MEP
68%
CMP
4.9%
GMP
3.6%
MEP
68%
CMP
4.4%
FcI RII/III
CD34
% of Progs, relative to WT
1.5
1.0
0.5
0.0
CMP
GMP
MEP
D
Smo WT
Smo KO
Q1
7.2%
Q2
79%
Q3
1.4%
Q1
8.7%
Q2
79%
Q3
1.3%
CD71
Ter119
% of erythroblast subsets in E14.5 fetal liver, relative to WT
1.5
1.0
0.5
0.0
Q1
Q2
Q3

Figure 5.3 Erythroblast subsets and progenitors in WT and Smo KO E14.5 fetal liver

(**A**) Scatter plot shows the cell number of each individual WT and Smo KO E14.5 fetal liver. The mean of each group is indicated with a line. (**B**) Fetal liver cells were analyzed by mutliparameter flow cytometer to identify the hematopoietic stem cells $Lin^{-}Sca\text{-}1^{+}C\text{-}kit^{+}$ (LSK) and the myeloid progenitors, $Lin^{-}Sca\text{-}1^{-}C\text{-}kit^{+}$ (Prog). Histogram shows relative percentage of LSK and Prog within the lineage negative compartment in WT and Smo KO mice. (**C**) The Prog population is subdivided by expression of CD34 and FcϒRII/III which results in $FcϒRII/III^{+}CD34^{+}$ (GMP), $FcϒRII/III^{-}CD34^{+}$ (CMP), and $FcϒRII/III^{-}CD34^{-}$ (MEP). Histogram shows relative percentage of CMP, GMP and MEP within the myeloid progenitor compartment in WT and Smo KO mice. (**D**) Three populations of erythroblast subsets were identified by expression of CD71 and Ter119 in fetal livers. Histogram shows relative percentage of erythroblasts population (Q1-Q3) in WT and Smo KO mice. In each experiment (litter) the average value of the WT is set to 1 so as to allow comparison between litters. Error bars represent ± SEM. (WT, n=2; Smo KO, n=4) *$p<0.05$ WT versus Smo KO.

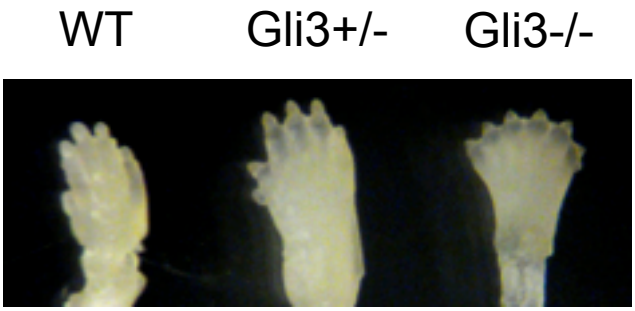

Figure 5.4 Forelimb of Gli3 mutant

Picture shows forelimbs of E17.5 Gli3+/- and Gli3-/- compared to WT. The forelimb of a typical Gli3+/- forms an extra digit in the anterior side of the limb. The Gli3-/- forelimb is polydactylous.

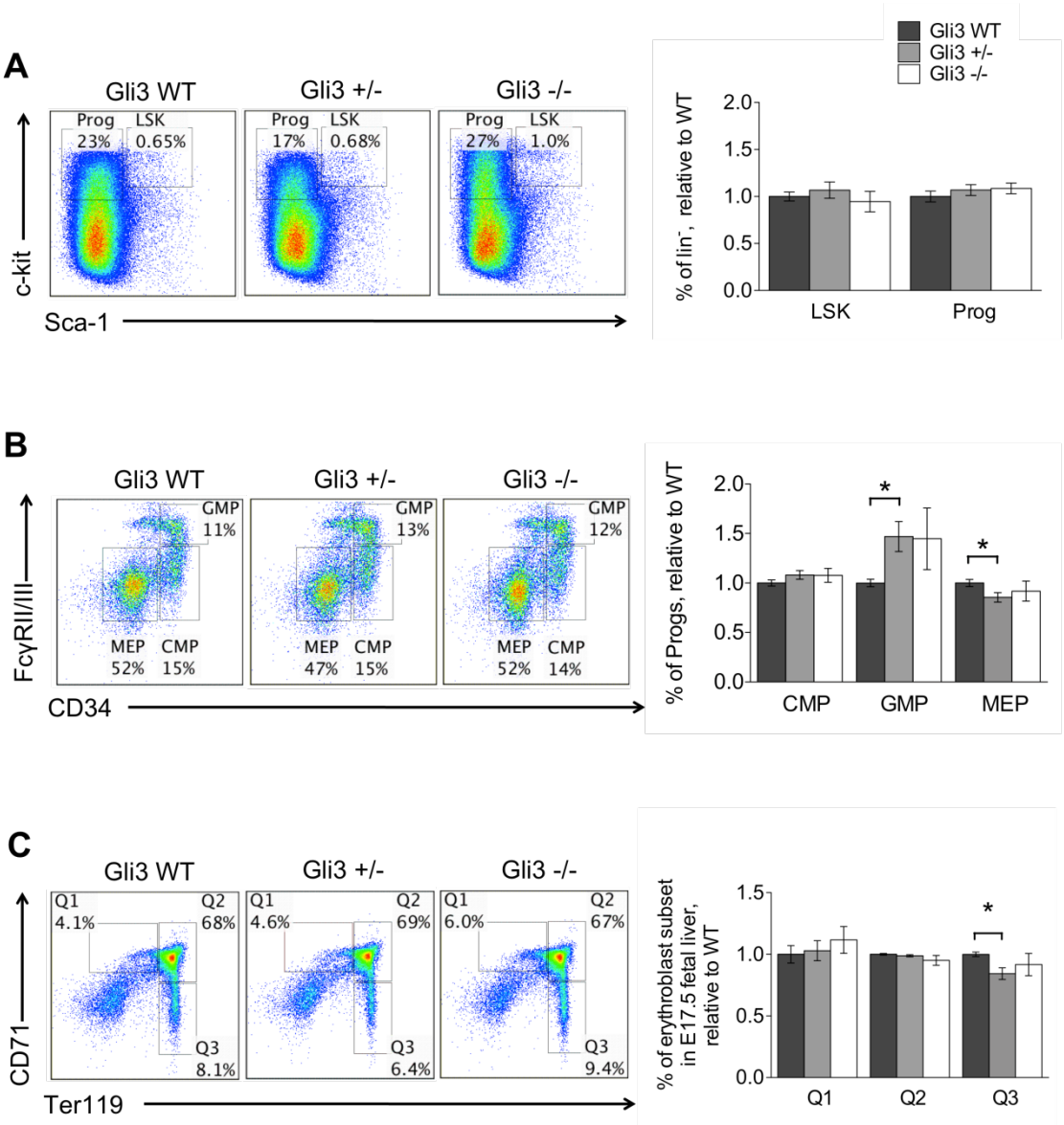
A
Gli3 WT
Gli3 +/-
Gli3 -/-
Prog
LSK
23%
0.65%
17%
0.68%
27%
1.0%
c-kit
Sca-1
Gli3 WT
Gli3 +/-
Gli3 -/-
% of lin- relative to WT
2.0
1.5
1.0
0.5
0.0
LSK
Prog
B
Gli3 WT
Gli3 +/-
Gli3 -/-
GMP
11%
13%
12%
MEP
52%
47%
52%
CMP
15%
15%
14%
FcγRII/III
CD34
% of Progs, relative to WT
2.0
1.5
1.0
0.5
0.0
*
*
CMP
GMP
MEP
C
Gli3 WT
Gli3 +/-
Gli3 -/-
Q1
4.1%
4.6%
6.0%
Q2
68%
69%
67%
Q3
8.1%
6.4%
9.4%
CD71
Ter119
% of erythroblast subset in E17.5 fetal liver, relative to WT
1.5
1.0
0.5
0.0
*
Q1
Q2
Q3

Figure 5.5 Erythroblast subsets and progenitors in Gli3 mutant E17.5 fetal liver

(**A**) Fetal liver cells were analyzed by mutliparameter flow cytometer to identify the hematopoietic stem cells Lin^- $Sca\text{-}1^+$ $C\text{-}kit^+$ (LSK) and the myeloid progenitors, Lin^- $Sca\text{-}1^-$ $C\text{-}kit^+$ (Prog). Histogram shows relative percentage of LSK and Prog within the lineage negative compartment in WT, Gli3+/- and Gli3-/- embryos. (**B**) The Prog population is subdivided by expression of CD34 and FcϒRII/III which results $Fc\gamma RII/III^+CD34^+$ (GMP), $Fc\gamma RII/III^-CD34^+$ (CMP), and $Fc\gamma RII/III^-CD34^-$ (MEP). Histogram shows relative percentage of CMP, GMP and MEP within the myeloid progenitor compartment in WT, Gli3+/- and Gli3-/- embryos. (**C**) Three populations of erythroblast subsets were identified by expression of CD71 and Ter119 in fetal livers. Histogram shows relative percentage of erythroblasts population (Q1-Q3) in WT, Gli3+/- and Gli3-/- mice. In each experiment (litter) the average value of the WT is set to 1 so as to allow comparison between litters. Error bars represent ± SEM. (WT, n=14; Gli3+/-, n=23; Gli3-/-, n=10) *$p<0.05$, WT versus Gli3+/-.

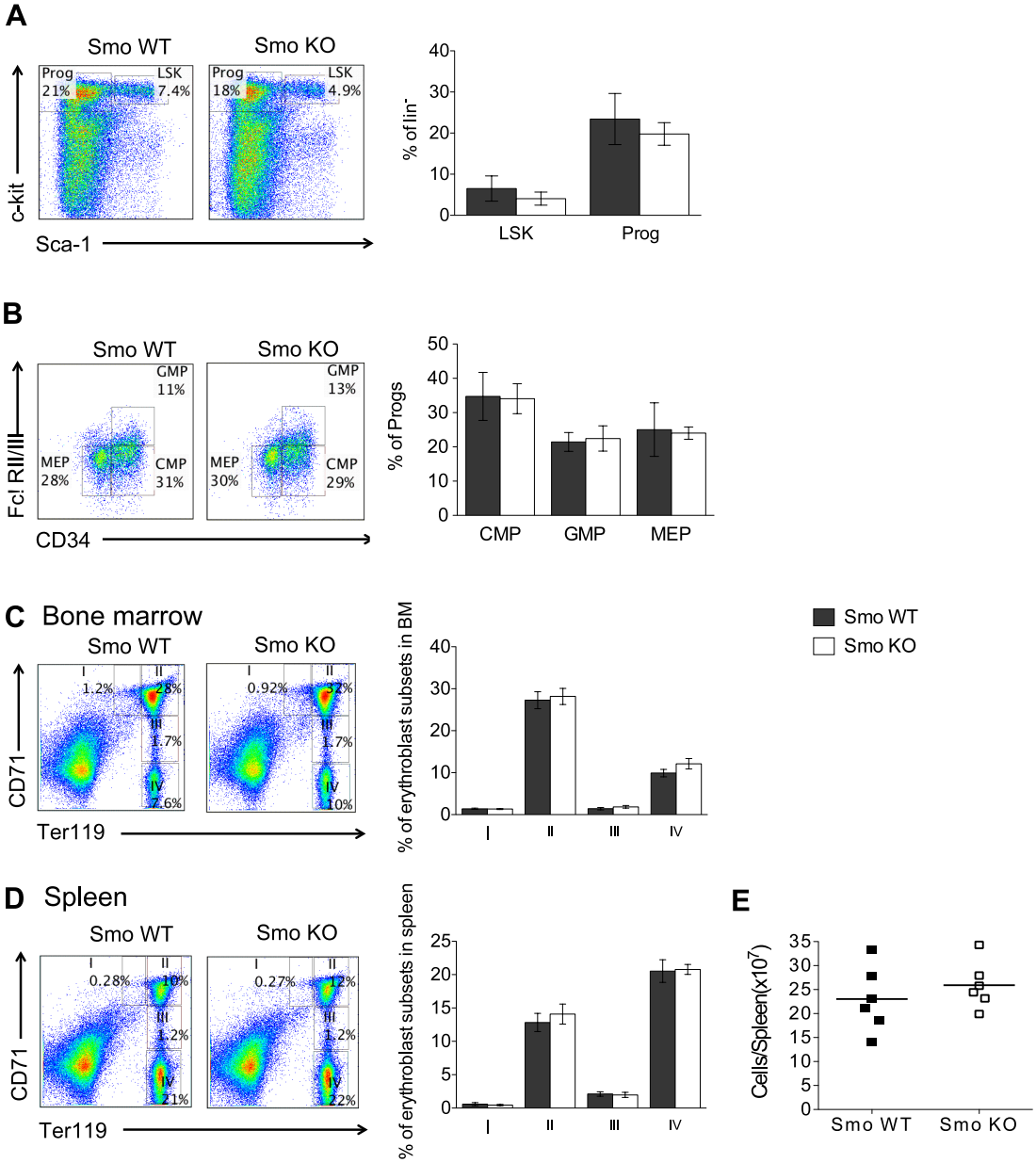
A
Smo WT
Smo KO
Prog
21%
LSK
7.4%
Prog
18%
LSK
4.9%
c-kit
Sca-1
% of lin-
40
30
20
10
0
LSK
Prog
B
Smo WT
Smo KO
GMP
11%
MEP
28%
CMP
31%
GMP
13%
MEP
30%
CMP
29%
Fcl RII/III
CD34
% of Progs
50
40
30
20
10
0
CMP
GMP
MEP
C Bone marrow
Smo WT
Smo KO
I
1.2%
II
28%
III
1.7%
IV
2.6%
I
0.92%
II
27%
III
1.7%
IV
10%
CD71
Ter119
% of erythroblast subsets in BM
40
30
20
10
0
I
II
III
IV
Smo WT
Smo KO
D Spleen
Smo WT
Smo KO
I
0.28%
II
10%
III
1.2%
IV
21%
I
0.27%
II
12%
III
1.2%
IV
22%
CD71
Ter119
% of erythroblast subsets in spleen
25
20
15
10
5
0
I
II
III
IV
E
Cells/Spleen(x10^7)
35
30
25
20
15
10
5
0
Smo WT
Smo KO

Figure 5.6 Erythroblast subsets and progenitors in WT and Smo KO mice

(**A**)Bone marrow cells were analyzed by mutliparameter flow cytometer to identify the hematopoietic stem cells Lin- Sca-1 + C-kit+ (LSK) and the myeloid progenitors, Lin- Sca-1- C-kit+ (Prog). Histogram shows percentage of LSK and Prog within the lineage negative compartment in WT and Smo KO mice. (**B**) The Prog is subdivided by expression of CD34 and FcϒRII/III which results FcϒRII/III + CD34 +(GMP), FcϒRII/III- CD34 + (CMP), and FcϒRII/III-CD34- (MEP). Histogram shows percentage of CMP, GMP and MEP within the myeloid progenitor compartment in WT and Smo KO mice. The dot plots show Ter119 and CD71 staining of bone marrow cells (**C**) and splenocytes (**D**) isolated from WT and Smo KO mice, and four erythroblast populations (I-IV) were identified. Histograms show percentage of erythroblasts population (I-IV) in WT and Smo KO bone marrow (**C**) and spleen (**D**). (**E**) Scatter plot shows the cell number of each individual WT and Smo KO spleen. The mean of each group is indicated with a line. Error bars represent ± SEM. (n=6 for each genotype)

5.3 Discussion

In the last two chapters, we showed that Dhh is required for the regulation of erythropoiesis in both normal erythropoiesis and during stress conditions. However, our analysis suggested that Dhh is not involved in definitive haematopoiesis in the fetal liver, as analysis of Dhh+/- and Dhh-/- did not show significant differences in haematopoietic progenitors and erythroid population compared to WT littermates. In contrast, recent studies demonstrated that mice deficient in Ihh showed impairment of definitive erythropoiesis in the fetal liver (Cridland et al. 2009). Interestingly, Ihh and Dhh share similar expression patterns in haematopoietic-related tissues, as they are both expressed in the fetal liver and non-haematopoietic cell in bone marrow and spleen (Cridland et al. 2009, Hegde et al. 2008). These observations suggest a functional redundancy between these two Hh ligands in haematopoiesis. Ihh may compensate for the loss of Dhh in definitive erythropoiesis during embryonic development.

In the last decade, a growing body of evidence demonstrated that Hh ligands and activation of the Hh signalling pathway are required in regulation of haematopoiesis, however, data from recent studies are inconclusive and have reported conflicting results. Our investigation showed that conditional deletion of Smo in haematopoietic cells using the Vav-cre promoter led to a reduction of haematopoietic cell differentiation in the fetal liver, while conditional loss of Smo did not alter HSC differentiation in adult mice. Our findings are similar

with the study of Zhao (2009), which used the same mice model and demonstrated that Smo is required in HSC functions, but the conditional Smo-deficient adult mice exhibited no defects in haematopoiesis. On the other hand, two studies analysed mice with conditional loss of Smo, implied that Hh signalling is dispensable for haematopoietic function (Gao J. et al. 2009, Hofmann et al. 2009). It is important to point out that inducible Mx-1-cre transgenic mice were used in these two studies to delete Smo in haematopoietic cells in adulthood. Mx-1 were expressed in most of haematopoietic cells, while Vav were active in both haematopoietic cells and endothelial cells during early development in mice. Therefore, inactivation of Smo in different phases in these studies may explain the contradictory findings on the function of Smo in haematopoiesis, and that Smo may regulate the haematopoietic lineage in primitive and early definitive haematopoiesis during embryo development, but be dispensable in haematopoiesis in adult life.

Earlier studies have demonstrated that Gli1 expression was increased in Gli3+/- and Gli3-/- fetal thymus (Hager-Theodorides et al. 2009), thus indicating that loss of Gli3 led to an increase of Hh signalling. In out study, Gli3+/- fetal liver showed fewer MEP populations compared to WT. The finding is opposing to the phenotype of Ihh-/- fetal liver, in which an increased percentage of MEP was found (Cridland et al. 2009). These studies thus suggest that Gli3 might also act as a Hh repressor in the fetal liver. Interestingly, the Gli3-/- embryo did not appear to show any effects on haematopoietic cell development. More studies will be needed to understand the function of Gli3 on haematopoiesis and the

transcriptional difference between Gli3+/- and Gli3-/-, but the phenotype of the Gli3+/- suggests that the effect is due to a change in expression levels of a Gli3 target gene rather then an global influence of increased Hh pathway activation.

5.4 Conclusion

In this chapter, our analysis of Dhh+/- and Dhh-/- embryos did not reveal a significant difference in embryonic haematopoiesis and erythropoiesis in the fetal liver compared to WT. In contrast, mice conditionally deficient in Smo showed significantly decreased percentage of the LSK population in the E14.5 fetal liver. However, no differences were observed in erythropoiesis between Smo WT and Smo KO adult mice. We also investigate if Gli3 is involved in embryonic erythropoiesis. Analysis of E17.5 Gli3+/- and Gli3-/- fetal liver showed that the proportion of GMP was increased, while the proportion of MEP was decreased in Gli3+/- compared to WT. The late erythroblast population in Gli3+/- is also decreased relative to WT.

Chapter Six : The role of Foxa1 and Foxa2 in T-cell development

Abstract

The Foxa1 and Foxa2 transcription factors are essential for mouse development. Foxa2 has been identified as a downstream target gene of the Hh signalling pathway in thymocyes. However, the role of Foxa1 and Foxa2 in the regulation of the immune system have yet been determined. In this study, we used mice with conditional deletion of Foxa1 and/or Foxa2 in mature T-cells to study if Foxa1 and/or Foxa2 are involved in T-cell differentiation and function. We found that both Foxa1 and Foxa2 are required in T-cell development. Further studies found that CD4 T-cell differentiation was reduced in conditional Foxa2 KO mice. In the periphery, Foxa2-deficient T-cells displayed reduced T-cell activation and proliferation, and an increased production of Th2 cytokines. Gene expression analysis showed loss of Foxa2 influences Hh activation.

6.1 Introduction

6.1.1 Role of Hh signalling in regulation of T-cell development

Recent studies have shown that Hh signalling is involved in haematopoiesis and that it also plays a role in the immune system. Our laboratory has focused on the role of Hh signalling pathway in T-cell development for the last decade. We found that Hh signalling is involved in regulation of T-cell differentiation at various stages.

In mice, gene transcription of the Hh signalling components, including *Shh*, *Ihh*, *Ptch*, *Smo*, *Gli1*, *Gli2* and *Gli3*, were detected by qRT-PCR in the adult and fetal thymus, suggesting that Hh signalling operates in thymocyte development in the thymus during embryogenesis and in adult life. (Outram et al. 2000)

Analysis of Shh and Gli3 mutants has shown that the Hh signal is important for early T-cell development, where it plays a role in the expansion and differentiation of DN progenitors. The transition from DN1 to DN2 cell was severely hindered in Shh-/- and Gli3-/- mice (Hager-Theodorides et al. 2005, Shah et al. 2004). The role of Hh signalling in the regulation of early thymocyte differentiation also was confirmed by analysis of conditional Smo-deficient mice. Deletion of Smo in T-cells lineage caused disruption of early T-cell progenitors and an increase in apoptotic death in DN2 and DN3 cells (El Andaloussi et al. 2006).

Furthermore, treatment of mouse fetal thymus organ cultures (FTOCs) with rShh protein has shown that Hh signalling negatively regulates thymocyte differentiation and arrested development at the DN3 stage, whereas neutralising of Hh signal with Hh inhibitor, 5E1, enhanced production of DP populations (Outram et al. 2000). However, a positive regulatory role of Shh in DN to DP differentiation has been demonstrated in other studies. Analysis of Shh-/- thymi showed increased apoptosis of DN4 cells, which led to reduction in DP populations (Shah et al. 2004). Gli3 was also found to be required at the transition from DN to DP cell. Analysis of Rag1-/-Gli3-/- E15.5 FTOC treated with anti-CD3 showed an accumulation of DN cells and reduced number of DP in cultures, thus indicating that Gli3 positively regulates differentiation of DN to DP thymocytes. (Hager-Theodorides et al. 2005)

Studies have also demonstrated Hh signalling is involved in later stages of T-cell development. In Shh-/- FTOC, differentiation of DP to CD4SP was greatly increased and the ratio of SP/DP was increased compared to WT controls, suggesting that loss of Shh resulted in increased differentiation from DP to SP (Rowbotham et al. 2007). Study of Gli2ΔC_2 transgenic mice further confirmed this hypothesis. Gli2ΔC_2 mice express a repressor form of Gli2, which leads to a constitutive inhibition of Hh-dependent transcription in T-lineage cells. In other words, the mouse model is mimicking the effect of lack of Hh signal in T-cells. In the absence of Hh signalling, the proportion of CD4SP was increased in the Gli2ΔC_2 thymus and peripheral lymphoid organs (Furmanski et al. 2013, Rowbotham et al. 2008). In contrast, analysis of Gli2ΔN_2 transgenic mice has

shown the opposing effect. The truncated from of Gli2 in Gli2ΔN$_2$ mice acts as an activator of Hh-dependent transcription, and hence, Hh signalling was constitutively activated in T-lineage cells. A reduction in the proportion of CD4 T-cells was observed in Gli2ΔN$_2$ thymus, spleen and lymph node (LN), whereas the percentages of DP and CD8 T-cells were significantly increased in the Gli2ΔN$_2$ thymus (Rowbotham et al. 2007).

6.1.2 Role of Hh signalling in regulation of T-cell activation and effector cell differentiation

By using the mouse model (Gli2ΔC$_2$ and Gli2ΔN$_2$), in which Hh signalling is repressed or activated in T-cells, we have shown that Hh signalling influences peripheral T-cell activation. In Gli2ΔC$_2$ splenocytes, expression of the T-cell activation markers CD69 and CD25 were increased after stimulation with anti-CD3 and anti-CD28 antibodies, whereas T-cell activation was inhibited in Gli2ΔN$_2$ splenocytes by the same treatment (Rowbotham et al. 2007, Rowbotham et al. 2008).

Furthermore, gene expression analysis revealed that Hh-dependent transcription effects differentiation of peripheral CD4 T-cell subsets (Furmanski et al. 2013). In that study, splenocytes from Gli2ΔC$_2$ and Gli2ΔN$_2$ mice, were stimulated with anti-CD3 and anti-CD28 antibodies for 6 hours, RNAs from stimulated cells, as well as resting cells were then isolated and validated for gene expression by microarray analysis. It was found that conditions where Hh signal is repressed (Gli2ΔC$_2$), the Th2-related genes were downregulated and expression of Th1 genes were increased, whereas when Hh signal is activated

(Gli2ΔN_2), the expression of Th2 cytokines were upregulated and Th1-related transcription was reduced. (Furmanski et al. 2013)

Activation of the Hh pathway has also been shown to influence the function of CD4 Th2 effector cells *in vivo*. When mild allergic asthma was induced in Gli2ΔN_2 mice by dosing with house dust mite (HDM), production of Th2 cytokines (IL4 and IL13) and recruitment of eosinophils were increased, compared with that of WT control mice. Moreover, the proportion of CD4 T-cells that expressed IL4 and IL13 in Gli2ΔN_2 lung were increased compared to WT following HDM treatment. (Furmanski et al. 2013)

In the Th1/Th2 skewing experiment, analysis of intracellular levels of Gata3 and Tbet indicated that Hh signals promote Th2 differentiation. Gata3 acts as a transcriptional regulator central in Th2 differentiation, whereas Th1 differentiation is controlled by expression of Tbet. Gli2ΔN_2 CD4 T-cells had higher Gata3 expression in both neutral and Th2-skewed condition whereas expression of Tbet was decreased in Gli2ΔN_2 cells compared with WT cells.

Taken together, these findings suggested that Hh signals influence transcription required for Th2 cell differentiation, resulting in increased production of Th2 cytokines, which may led to increase asthma pathogenesis. (Furmanski et al. 2013)

6.1.3 Fox protein family

The forkhead box (FOX) proteins are a family of transcription factors, which display a wide variety of functions in cellular and biological processes, including cell growth, survival and cell fate (Jackson et al. 2010).

The *fox* gene was first discovered in *Drosophila* by analysis of the mutant. The mutation caused homeotic transformations during embryogenesis, with defects in head involution that resulted in a spiked head structure, which thus led to the name *fork head* gene (Weigel et al. 1989). Shortly afterwards, a novel group of transcription factors, hepatocyte nuclear factor3s (HNF3) were identified in the liver in mice (Lai et al. 1990). These transcription factors contained the unique winged-helix DNA-binding domains (Forkhead domains) (Lai et al. 1991, Weigel and Jackle 1990).

Since then, there are more than 100 members of the Fox family of transcription factors have been identified and are now classified into 18 subfamilies (A to R) The Fox protein family shares a winged-helix protein structure, the DNA-binding domain of which consists of 110 amino acids, that is highly conserved from yeast to human (Jackson et al. 2010).

6.1.4 Foxa protein

The Foxa protein family has three members, which were previously named HNF-3α, HNF-3β, HNF-3γ, and are now called Foxa1, Foxa2, Foxa3 respectively. The three members are highly conserved and closely related to each other. Foxa1 shares 95% amino acid sequence identity and Foxa2 shares 90%, with

Foxa3 within the DNA-binding domain (Clark et al. 1993). For the sequences outside the DNA-binding region, Foxa1 and Foxa2 have about 30% identity, while Foxa3 is highly divergent to Foxa1 and Foxa2 in these sequences (Lai et al. 1991).

The Foxa genes are widely expressed during murine embryogenesis, and in the adult. In the early embryo, Foxa2 is the first gene among the family to be expressed. Foxa2 mRNA is expressed at E6.5 in the node and the three germ layers, which subsequently give rise to all organs during organogenesis. Following that, activity of Foxa1 is detected in the midbrain floorplate, notochord and endoderm at E7.5. The areas where Foxa1 is expressed are mostly parallel to that of Foxa2 throughout embryonic development, except that Foxa1 is more extensively expressed in the notochord and the gut (Monaghan et al. 1993, Sasaki and Hogan 1993). On the other hand, Foxa3 expression is restricted to the endoderm-derived organs, such as liver, pancreas and gut, during embryogenesis (Monaghan et al. 1993). Furthermore, expression of both Foxa1 and Foxa2 is maintained in a wide range of adult organs, including lung, pancreas, stomach, liver, intestine and thymus while Foxa3 is expressed in liver, stomach, intestine, heart, ovary and testis (Besnard et al. 2004, Kaestner et al. 1994, Rowbotham et al. 2009).

The expression pattern and sequence similarity of Foxa proteins may explain their overlapping and divergent roles in embryonic development and adult cells. During embryogenesis, Foxa2 is required for the normal development of notochord, floorplate and endoderm, therefore Foxa2-deficient embryos exhibit

severe defects in these areas and die at E10-11 (Weinstein et al. 1994). In contrast, Foxa1 and Foxa3 null mice develop normally and appear normal at birth, which demonstrates that they are not vital during early mouse development (Friedman and Kaestner 2006). Both Foxa1 and Foxa3 KO mice develop hypoglycaemia, and Foxa1 KO mice have defects in regulation of glucose homeostasis and die postnatally (Shih et al. 1999). Foxa3 KO mice suffer from hypoglycaemia when fasting, and have a normal lifespan (Shen et al. 2001).

Foxa proteins are closely related to one another, with highly conserved DNA-binding domains and they are co-expressed in various tissues. This suggests that they may either functionally compete with each other, or that one of them may be able to compensate for the loss of another one. The compensatory roles for Foxa1 and Foxa2 have been demonstrated in development and in the regulation of multiple adult tissues (Lee et al. 2005, Wan et al. 2005).

In the liver, Foxa proteins are crucial for the initiation of liver development. It has been found that null mutation of Foxa1 and Foxa2 in the embryo inhibited liver bud formation and suppressed the expression of the earliest liver marker gene alpha-fetoprotein (Afp) (Lee et al. 2005). In contrast, embryos deficient for either Foxa1 or Foxa2 alone showed normal hepatic development (Lee et al. 2005).

A similar compensatory role of Foxa1 and Foxa2 has also been found in lung development. Loss of both Foxa1 and Foxa2 from respiratory epithelium caused

defects in branching morphogenesis and inhibited epithelial cell proliferation and differentiation, while ablation of either Foxa gene alone did not alter the expression of lung differentiation markers or interfere with lung architecture (Wan et al. 2005).

Further evidence that Foxa1 and Foxa2 can cooperate comes from development of the pancreas, which is blocked when both factors are missing. Interestingly, Foxa2 is a more potent regulator of pancreatic cell differentiation, as loss of Foxa1 alone did not have an impact on pancreatic size, while the pancreatic mass was greatly reduced when Foxa2 was removed. (Gao N. et al. 2008)

6.1.5 Foxa proteins and Hh signalling

It has been suggested that Hh signalling is regulated by Foxa proteins in many different tissues and *Foxa* is a potential Shh target gene. For instance, Foxa2 is required for secretion of Shh in the notochord, to stimulate the differentiation of the floorplate, and expression of Foxa2 is maintained by a positive feedback loop through Hh signalling (Jeong and Epstein 2003, Sasaki et al. 1997). Likewise, expression of Foxa1 is correlated with activities of Hh. In one study, Foxa1 null mice showed elevated Shh expression in prostate epithelium when compared with WT (Gao N. et al. 2005). That observation suggested that Hh is negatively regulated by Foxa1.

Foxa2 is not only a target gene of Hh in the floorplate, it is also a Hh target gene in thymocytes. A study using transgenic mice (Gli2ΔC_2), in which Hh signalling is constitutively repressed in T-cells showed that Foxa2 expression is

downregulated in thymocytes during the transition from DN to DP, and that Hh signalling is required to maintain physiological levels of Foxa2 expression. That experiment suggested that Hh signalling effectively maintains expression of Foxa2 during pre-TCR signal transduction (Rowbotham et al. 2009).

Objectives:

The functional relationship between Foxa proteins and Hh signalling is complex, and the functions of the Foxa family in regulating T-cell development and differentiation have not been studied. In this chapter, the functions of Foxa1 and Foxa2 in T-cell development and differentiation will be investigated, as well as their role in regulating Hh signalling.

Given that Foxa1 and Foxa2 are closely related to one another, with almost identical DNA-binding domains, we hypothesized that Foxa1 and Foxa2 may play compensatory roles in thymocyte development and differentiation in cooperation with Hh signalling.

In this chapter, the following objectives will be completed:

1) Mice conditionally deficient for Foxa1 and/or Foxa2 in mature thymocytes will be used to test if Foxa1 and/or Foxa2 influence late T-cell development and differentiation, and peripheral T-cell function and to test if Foxa1 and Foxa2 can compensate for one another during T-cell development,

2) To test if deletion of Foxa1 and/or Foxa2 altered Hh signalling activities, expression of Hh target genes will be studied.

6.2 Results

6.2.1 Expression of Foxa1 and Foxa2 in WT mice

In order to investigate whether Foxa1 and Foxa2 influence T-cell development, qRT-PCR was first carried out to test if Foxa1 and Foxa2 are expressed in the lymphoid organs. We found that *Foxa1* and *Foxa2* are expressed at similar levels in the thymus and spleen in C57BL/6 adult mice (Figure 6.1).

To study the expression pattern of Foxa1 and Foxa2 in developing thymocytes, DN1 to DN4, DP, CD4SP and CD8SP thymocytes were sorted by FACS from C57BL/6 adult mice. During thymopoiesis, both *Foxa1* and *Foxa2* were expressed throughout development with highest expression in the earliest thymocytes population, DN1. Following that, the *Foxa1* and *Foxa2* expression stayed high in DN2. From DN3 to DP, the expression patterns of *Foxa1* and *Foxa2* were opposite to each other. DN3 had relatively low expression of *Foxa1* while *Foxa2* was expressed at high levels in DN3. A similar finding was observed in the DN4 and DP populations, where expression of *Foxa1* in DN4 was higher than that in DP thymocytes, but in contrast, *Foxa2* was expressed higher in DP than DN4 cells. However, both *Foxa1* and *Foxa2* were expressed more highly in CD4SP than in CD8SP thymocytes (Figure 6.2).

6.2.2 Breeding strategy for conditional KO mice

Since Foxa1 KO mice die shortly after birth, and Foxa2 KO mice are embryonic lethal, we used a CD4-cre transgene and Foxa1 and/or Foxa2 floxed mice to

inactivate Foxa1 and/or Foxa2 in thymocytes. Mice were generated by crossing CD4-cre transgenic mice with single or double mutants of Foxa1$^{flox/flox}$ and/or Foxa2$^{flox/flox}$ mice. The use of CD4-cre should excise floxed alleles from all T-lineage populations from the DP stage onwards.

Given that Foxa1 and Foxa2 have compensatory roles in many different tissues, and, they are co-expressed in the developing thymocytes, mice single or double conditional KO for Foxa1 and/or Foxa2 were investigated.

In this thesis, the conditional deletion of Foxa1 and/or Foxa2 will be referring to "Foxa KO". In all experiments, Foxa KO will be compared with their WT counterparts.

6.2.3 Genotyping of Foxa1 and Foxa2 conditional knockout mice by PCR

Genomic DNA was extracted and genotyped by PCR analysis in order to distinguish between WT and Foxa KO littermates. WT and floxed alleles of Foxa1 and Foxa2 were shown in Figure 6.3 A and B, respectively. In sample 1 and 4, only WT alleles were amplified, so therefore, it was genotyped as Foxa1 and Foxa2 WT. Sample 2 and 5 showed PCR products from both WT and floxed alleles were generated, and indicates that they were Foxa1$^{flox/WT}$ and Foxa2 $^{flox/WT}$ mice. Sample 3 and 6 amplified only floxed allele PCR products, therefore, they were genotyped as Foxa1$^{flox/flox}$ and Foxa2 $^{flox/flox}$ mice.

Mice conditionally deficient of Foxa1 and/or Foxa2 were generated by crossing Foxa1$^{flox/flox}$ and/or Foxa2 $^{flox/flox}$ mice with CD4-cre mice to inactivate Foxa1 and/or Foxa2 in T-cells from the DP stage onwards. The Foxa$^{flox/flox}$ CD4-cre + (Foxa KO) mice were analysed and compared with Foxa$^{flox/flox}$ CD4-cre – (Foxa WT) littermates. To determine genotypes of Foxa WT and Foxa KO littermates, PCR was performed. Figure 6.3C shows an agarose gel with PCR products that were amplified from genomic DNA extracted from Foxa WT and Foxa KO tail.

6.2.4 QRT-PCT to confirm ablation of Foxa1 and Foxa2 in CD4 expressing cells.

To confirm the deletion of Foxa1 and Foxa2 in the T-cell lineage, expression of these two genes were studied in CD4SP and CD8SP thymocytes. As shown in Figure 6.4 and 6.5, *Foxa1* and *Foxa2* are efficiently deleted in Foxa1a2 KO CD4SP and CD8SP thymocytes when compared to the WT control.

6.2.5 Role of Foxa1 in thymocyte development

To assess the effect of conditional deletion of Foxa1 on thymocyte development, Foxa1$^{flox/flox}$ CD4-cre+ (Foxa1 KO) mice were analysed and compared with Foxa1$^{flox/flox}$ CD4-cre-(WT) littermates. The number of thymocytes was similar in WT and Foxa1 KO mice (Figure 6.6A). Thymocytes were isolated and stained with anti-CD4 and anti-CD8 to study the differentiation of mature thymocytes from DP to SP stage. The proportion of CD4SP and CD8SP T-cells showed no significant difference between Foxa1 KO and WT mice (Figure 6.6B-C). The number of CD4 and CD8 T-cells in spleen and lymph node (LN) were also

investigated, and likewise showed no significant difference between groups (Figure 6.7C-6.8C).

To further investigate if Foxa1 influenced the transition from DP to SP, the CD4:CD8 ratio in thymus, spleen and LN were analysed and are shown relative to WT (Figure 6.6D, 6.7D, 6.8D). In LN, the relative CD4:CD8 ratio in the Foxa1 KO was 10% lower that than in WT (p=0.009)(Figure 6.8D).

Overall, loss of Foxa1 from T-cells did not greatly affect T-cell development in the thymus, but had an influence in the peripheral CD4/CD8 proportions.

6.2.6 Role of Foxa2 in thymocyte development

To examine the function of Foxa2 in T-cell development, $Foxa2^{flox/flox}$ mice were crossed with CD4-cre transgenic mice to generate $Foxa2^{flox/flox}$ CD4-cre+ (Foxa2 KO), in which the $Foxa2^{flox/flox}$ CD4-cre- act as WT control littermates.

The number of thymocytes was compared between WT and Foxa2 KO mice, and as for conditional Foxa1 KO mice, no significant difference in thymocyte number was found (Figure 6.9A). Similarly, the proportions and ratio of CD4SP and CD8SP populations in the thymus appeared normal when compared between WT and Foxa2 KO littermates (Figure 6.9B-C).

Although conditional Foxa2 deficiency did not influence cell numbers in spleen and LN (Figure 6.10A, 6.11A), the percentages of mature T-cells were greatly reduced in these two peripheral lymphoid organs in conditional Foxa2 KO mice. The percentages of CD4 and CD8 T-cells in the Foxa2 KO spleen are shown

relative to WT littermates (Figure 6.10B-C). We found 20% fewer CD4+ cells in the Foxa2 KO spleen compared to that of WT ($p<0.005$)(Figure 6.10C).

Foxa2 KO mice also exhibited decreases in the percentages of CD4+ and CD8+ T-cells in the LN (CD4+ $p=0.003$, CD8+ $p=0.03$) (Figure 6.11B-C). Interestingly, the CD4:CD8 ratio were relatively low in Foxa2 KO mice in both spleen and LN compared to that of WT (Figure 6.10D, 6.11D).

Thus, deletion of Foxa2 in mature T-cells reduced numbers of CD4+ T-cells in peripheral lymphoid organs.

6.2.7 Thymocyte development in conditional Foxa1 and Foxa2 double KO mice

Since Foxa1 and Foxa2 have been found to have compensatory roles in many different tissues, and they are co-expressed in the thymus and developing thymocytes, mice deficient for both Foxa1 and Foxa2 were also investigated, by analysis of $Foxa1^{flox/flox}$ $Foxa2^{flox/flox}$ CD4-cre – (WT) and $Foxa1^{flox/flox}$ $Foxa2^{flox/flox}$ CD4-cre + (Foxa1a2 KO) littermates.

In the thymus, the cell number was not significantly different between WT and conditional Foxa1a2 KO mice (Figure 6.12A). However, change in thymocyte development in conditional Foxa1a2 KO was observed. This analysis revealed a significant decrease in CD4SP in Foxa1a2 KO mice compared to WT mice ($p=0.024$) (Figure 6.12B-C). In addition, the CD4:CD8 ratio in the Foxa1a2 KO thymus was 15% lower than that in WT ($p=0.005$)(Figure 6.12D).

Similar results in the Foxa1a2 KO spleen and LN were observed. The number of cells recovered from spleen and LN were similar in WT and Foxa1a2 KO mice (Figure 6.13A, 6.14A), but Foxa1a2 KO mice exhibited reduced proportions of peripheral CD4+ compared to WT controls. The percentage of CD4+ T-cells was significantly decreased in Foxa1a2 KO spleen ($p=0.011$) (Figure 6.13C). In addition, the CD4:CD8 ratio in the Foxa1a2 KO mice was 25% lower than that in WT ($p=0.0008$) (Figure 6.13D).

In the LN, percentages of CD4+ T-cells were also decreased in Foxa1a2 KO compared to that of WT but this difference was not statistically significant ($p=0.064$) (Figure 6.14C). The Foxa1a2 KO LN also showed a 20% reduction in CD4:CD8 ratio when compared to WT ($p=0.0016$) (Figure 6.14D).

In summary, the double KO of Foxa1 and Foxa2 had reduced numbers of CD4+ T-cells, and reduced CD4:CD8 ratios in thymus, spleen and LN. The altered CD4:CD8 ratio, and decrease in numbers of CD4SP population in the thymus, and CD4+ T-cells in peripheral lymphoid organs, suggested that lineage commitment or homeostasis is altered and leads to fewer CD4 T-cells that differentiate from DP, and/or fewer CD4 T-cells surviving and expanding.

Interestingly, conditional deletion of both Foxa1 and Foxa2 has more profound effect on the thymus that deletion of Foxa1 or Foxa2 alone, suggesting that both Foxa1 and Foxa2 are involved in the regulation of T-cell development in the thymus. However, Foxa1 and Foxa2 did not function equally in controlling T-cell differentiation. Loss of Foxa1 had less impact than loss of Foxa2 on the

reduction of CD4 T-cells. Thus, although both Foxa proteins are required for T-cell development, Foxa2 is more potent that Foxa1, and Foxa2 appeared to compensate for deficiency of Foxa1 in T-cells, but not vice versa.

6.2.8 Foxa2 controls T-cell maturation

As mentioned above, there were fewer CD4+ T-cells in the periphery in Foxa2 KO mice compared to WT. To investigate the maturation status of these thymocytes before they leave the thymus and migrate to periphery, the expression of maturity markers HSA and Qa2 on DP, CD4SP and CD8SP thymocyte in thymus were assessed. As the DP cell differentiates, its surface expression of HSA and Qa2 changes from HSA^{hi} and $Qa2^{low}$ to HSA^{low} in DP and $Qa2^{hi}$ in SP cells.

The expression of HSA and Qa2 on DP, CD4 and CD8 cells in Foxa2 KO was measured compared to WT littermates (Figure 6.15A). There was a significant decrease in the percentage of DP and CD4SP thymocytes that expressed Qa2 in Foxa2 KO compared to WT ($p=0.03$), whereas HSA expression was significantly increased on Foxa2 KO DP compared to that of WT, although the differences in percentage were small ($p=0.04$)(Figure 6.15B-C). A similar result was observed in CD4SP T-cells, in which a lower percentage of CD4SP expressed Qa2 ($p=0.016$), although HSA expression was similar in WT and Foxa2 KO (Figure 6.15D-E). On the other hand, the Foxa2 KO CD8SP T-cells had no altered Qa2 and HSA expression (Figure 6.15F-G.).

Overall, this analysis suggested that Foxa2 KO DP cells were less capable differentiating to single positive T-cells than WT. In addition, fewer CD4SP T-cells expressed Qa2 suggesting that they were less mature, and is consistent with the fact that there were fewer CD4+ T-cells in the spleen and LN in Foxa2 KO mice, compared to WT.

6.2.9 Influence of Foxa2 on TCR signal was not detected

The strength of TCR signal is critical in determining the outcome of repertoire selection during thymocyte development, and influences CD4/CD8 lineage commitment in the thymus (Kappes and He 2005). The TCR is associated with the CD3 molecules to form a TCR complex, which regulates T-cell differentiation, activation and proliferation. Cell surface expression of CD5 can be used to measure TCR signal strength, which is correlated to the intensity of CD5 cell surface expression on T-cells (Azzam et al. 2001).

To study if deletion of Foxa2 in DP cells influences TCR expression and its signal strength, the intensity of CD3 and CD5 expression on the thymocyte surface were investigated (Figure 6.16). There was no difference in expression of CD3 and CD5 on DP, CD4SP and CD8SP thymocytes between groups and therefore we found no evidence that Foxa2 effected TCR signal strength (Figure 6.16).

6.2.10 Foxa2 regulates proliferation of T-cells

To investigate if Foxa2 has a role in regulating proliferation, which leads to the reduction of T-cells, CD4SP and CD8SP T-cells in WT and Foxa2 KO thymus were sorted by FACS to analyse the cell cycle status by PI staining.

In this analysis, the three major phases of cell cycle status G0/G1;S;G2/M, were identified and compared between WT and Foxa2 KO CD4 and CD8 T-cells. For CD4 T-cells, 79% of WT were in G0/G1 phase, while 83% were found in this phase in Foxa2 KO CD4 cells, indicating that more CD4 T-cells in Foxa2 KO were resting, compared to WT. In WT, 20% of cells were going through S+G2/M (9%in S, 11%in G2/M) phase, compared to only 14% in S+G2/M (7% in S, 7% in G2/M) in Foxa2 KO (Figure 6.17A). In CD8 T-cells, comparison of cell status showed similar results. Foxa2 KO CD8 T-cells had more cells in G0/G1 phase and fewer cells in S+G2/M phase, compared to their WT counterparts (Figure 6.17B).

Overall, the cell cycle analysis indicated that Foxa2 is involved in the regulation of T-cell proliferation in the thymus.

6.2.11 Foxa2 influences differentiation of regulatory T-cells (Treg)

Given that the numbers of T-cells were decreased in Foxa2 KO spleen and LN compared with WT, the percentages of the Treg population was analysed to test if Foxa2 is involved in Treg development. Splenocytes and LN cells from WT and Foxa2 KO mice were isolated and the Treg population was analyzed by expression of CD25 and Foxp3.

In the spleen, there was a significant increase in the percentage of the CD4+CD25+Foxp3+ population (Treg) detected in the Foxa2 KO mouse relative to WT (p=0.029)(Figure 6.18). The Treg population in Foxa2KO LN was also significantly higher than that found in WT littermates (p=0.015) (Figure 6.19)

In conclusion, conditional deletion of Foxa2 from T-cells resulted in an increase in the peripheral Treg population.

6.2.12 Foxa2 influences T-cell activation

To study the role of Foxa2 in T-cell activation, splenocytes isolated from WT and Foxa2 KO mice were stimulated with anti-CD3 and anti-CD28 antibodies. The cell surface expression of the early activation marker CD69 was assessed by flow cytometry at 4, 18 and 40 hours after stimulation in culture (Figure 6.20A (CD4 T-cells), 6.21A (CD8 T-cells)), whereas the later activation marker CD25 was assessed at 18 and 40 hours after treatment (Figure 6.20C (CD4 T-cells), 6.21C (CD8 T-cells)).

According to the cell surface expression of CD69 and CD25, Foxa2 deficient T-cells exhibited reduced T-cell activation when compared with WT. After stimulation, expression of CD69 and CD25 on CD4 T-cells in Foxa2 KO were decreased compared to WT (Figure 6.20B). The changes were more obvious at later time points, when both of the markers were clearly decreased in Foxa2 KO CD4 T-cells. The difference in expression of CD25 between Foxa2 KO CD4 T-cells and WT CD4 T-cells was significant 40 hours after activation (p=0.02) (Figure 6.20D).

A similar pattern was observed in CD8 T-cells, where activation seemed to be lower in Foxa2 KO CD8 T-cells, compared with WT. However, there was no significant reduction found in the expression of either the early activation marker CD69 or the later activation marker CD25 between the two groups (Figure 6.21).

Taken together these experiments showed that T-cell activation was inhibited in Foxa2-deficient T-cells and thus suggested a positive regulatory role for Foxa2 in T-cell activation.

6.2.13 Proliferation of Activated T-cells is inhibited in Foxa2 KO splenocytes

Carboxyfluorescein diacetate succinimidyl ester (CFSE) assays were used to assess the rate of proliferation of activated T-cells. Splenocytes isolated from WT and Foxa2 KO mice were labelled with CFSE and stimulated with anti-CD3 and anti-CD28 to measure the numbers of cell divisions after 72 hours in culture.

The FACS profiles for the CFSE staining of unstimulated and stimulated T-cells are shown in Figure 6.22 and 6.23. Without stimulation, a spontaneous division was observed in both CD4 and CD8 WT T-cells after culture for 72hrs while the Foxa2 KO cells did not show this (Figure 6.22A, 6.23A).

T-cells had undergone four to five divisions following a stimulus with anti-CD3 and anti-CD28 as shown in the FACS profiles (Figure 6.22B, 6.23B). The total proliferation of both CD4 and CD8 T-cells isolated from Foxa2 KO were lower

than that of WT. From the FACS profile of CD4 cells, WT peaked at the 4th division and started the 5th division, while Foxa2 KO cells peaked at the 3rd division and very few reached the 5th division (Figure 6.22B-C). A Similar pattern was observed in CD8 T-cells (Figure 6.23B-C).

Furthermore, to test if Foxa2 is involved in cell survival, Annexin V was used to measure the apoptosis of T-cells. Activated splenocytes were treated as above for 40 hours, cells were stained with Annexin V and gated on CD4 and CD8 T-cells. In Foxa2 KO CD4 T-cells, expression of Annexin V was significantly increased, with a mean of 27% compared to mean of 14% in the WT (p=0.02) (Figure 6.24A). Similarly, an increase in apoptosis was observed in Foxa2 KO CD8 T-cells. Annexin V staining was greatly increased, with mean of 32% in Foxa2 KO compared to mean of 20% in WT (p=0.035)(Figure 6.24B).

Overall, Foxa2 KO deficient T-cells had a higher rate of apoptosis.

6.2.14 Cytokine staining revealed Foxa2KO CD4 T-cells are more Th2-like

Given that Foxa2 deficient CD4 T-cells showed reduced activation compared to that of WT, we tested if Foxa2 is also involved in the regulation of differentiation and effector functions of activated T-cell subsets, by detection of intracellular cytokines in peripheral T-cells *ex vivo.* Expression of IL4, IL13 and IL17 in CD4 T-cells, and expression of IL2, IFNγ in CD8 T-cells were examined by flow cytometry, 4 hours following stimulation with PMA, inomycin and brefeldin A treatment.

There was no difference in the expression of IL2 and IFNγ in both CD4 and CD8 T-cells between WT and Foxa2 KO (Figure 6.25A,B,F,G). Likewise, the analysis of IL17 expression on CD4 T-cells did not show any differences between the two groups (Figure 6.25E). Thus, deletion of Foxa2 did not appear to drive CD4+ T-cells to differentiate into Th1 and Th17 subsets. Interestingly, the proportion of CD4 T-cells that produce Th2 cytokines was increased in Foxa2 KO mice: percentages of IL4 and IL13 were increased overall, with 1.8% and 1.75% respectively compared to 1.3% and 1% in WT (Figure 6.25D,E). The increase in IL13 was statistically significant (p=0.04) (Figure 6.25E).

6.2.15 Foxa1 and Foxa2 act as direct target genes of Hh signalling in the thymocytes

Hh signalling plays an essential role in T-cell development. In thymocytes, Foxa2 expression is maintained by Hh signalling during pre-TCR signal transduction. In order to investigate if Shh signalling directly influences the expression of Foxa1 and/or Foxa2 at later stages of thymocyte development, we performed WT E17.5 FTOC, treated with rShh for 2 days to investigate if transcription of Foxa1 and Foxa2 would change with increased Hh signal. Expression of *Foxa1* and *Foxa2* was examined by qRT-PCR and compared with untreated control.

Firstly, to confirm whether the Hh signalling was activated by treatment with rShh, induction of expression of the Hh target gene, Ptch1, was verified. Expression of *Ptch* was increased in rShh treated thymi lobe compared to the untreated control (Figure 6.26A). Then, examination of Foxa1 and Foxa2

expression was carried out. Both *Foxa1* and *Foxa2* were upregulated in the culture stimulated with rShh (Figure 6.26B,C). These experiments suggested that activation of Hh signalling upregulated expression of *Foxa1* and *Foxa2*.

6.2.16 Foxa2-deficient mice showed elevated Hh signalling in the thymus

The interaction of Foxa proteins and Hh signalling has not been well understood. Foxa2 is required to maintain Hh expression in the neural tube during development, whereas loss of Foxa1 raised Shh activities in prostate epithelial cells (Gao N. et al. 2005, Sasaki et al. 1997).

Of interest, we examined the level of Hh signalling in the Foxa2 KO thymus, by qRT-PCR analysis of *Ptch* expression. *Ptch* was upregulated in the Foxa2 KO thymus compared to WT.(Figure 6.27)

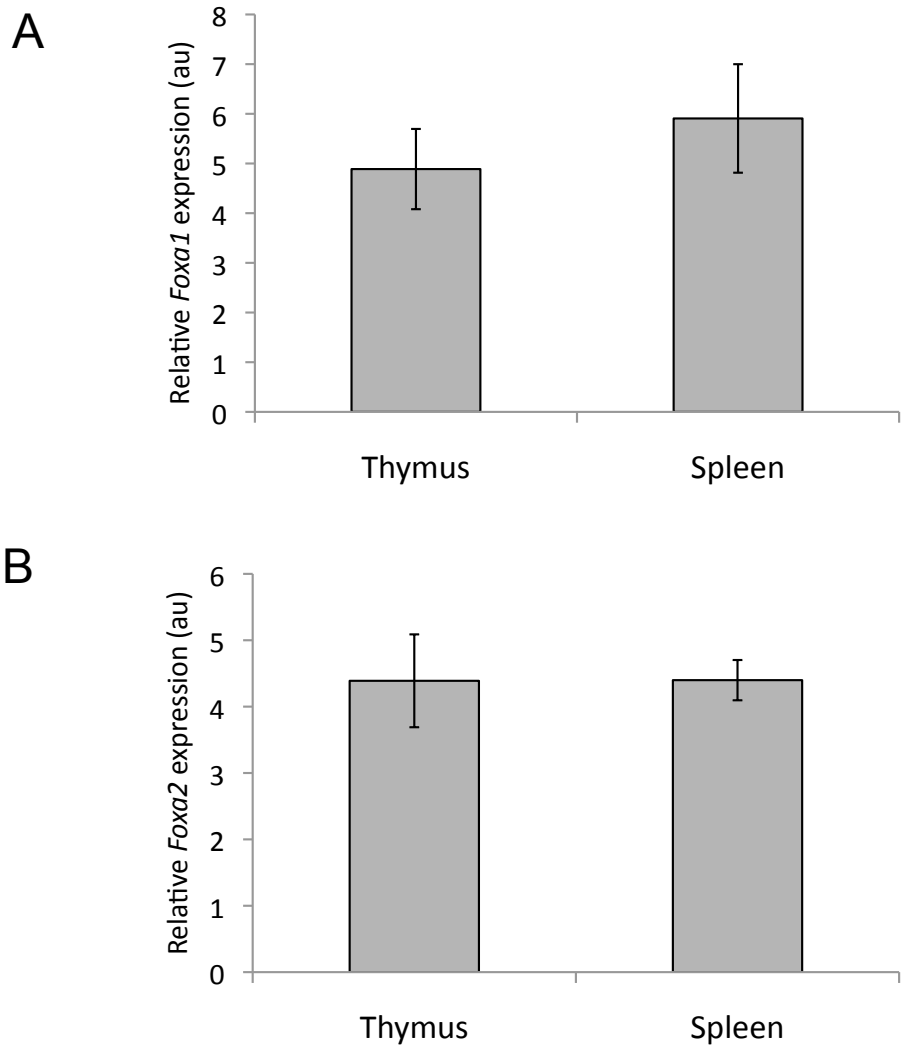

Figure 6.1 *Foxa1* and *Foxa2* are expressed in thymus and spleen in WT mice

Bar chart to show relative *Foxa1* (**A**) and *Foxa2* (**B**) expression in the thymus and spleen in WT mice. The scale shows expression normalised to the level of the housekeeping gene *HPRT*. Error bars represent ± SEM. Data are representative of at least two independent experiments.

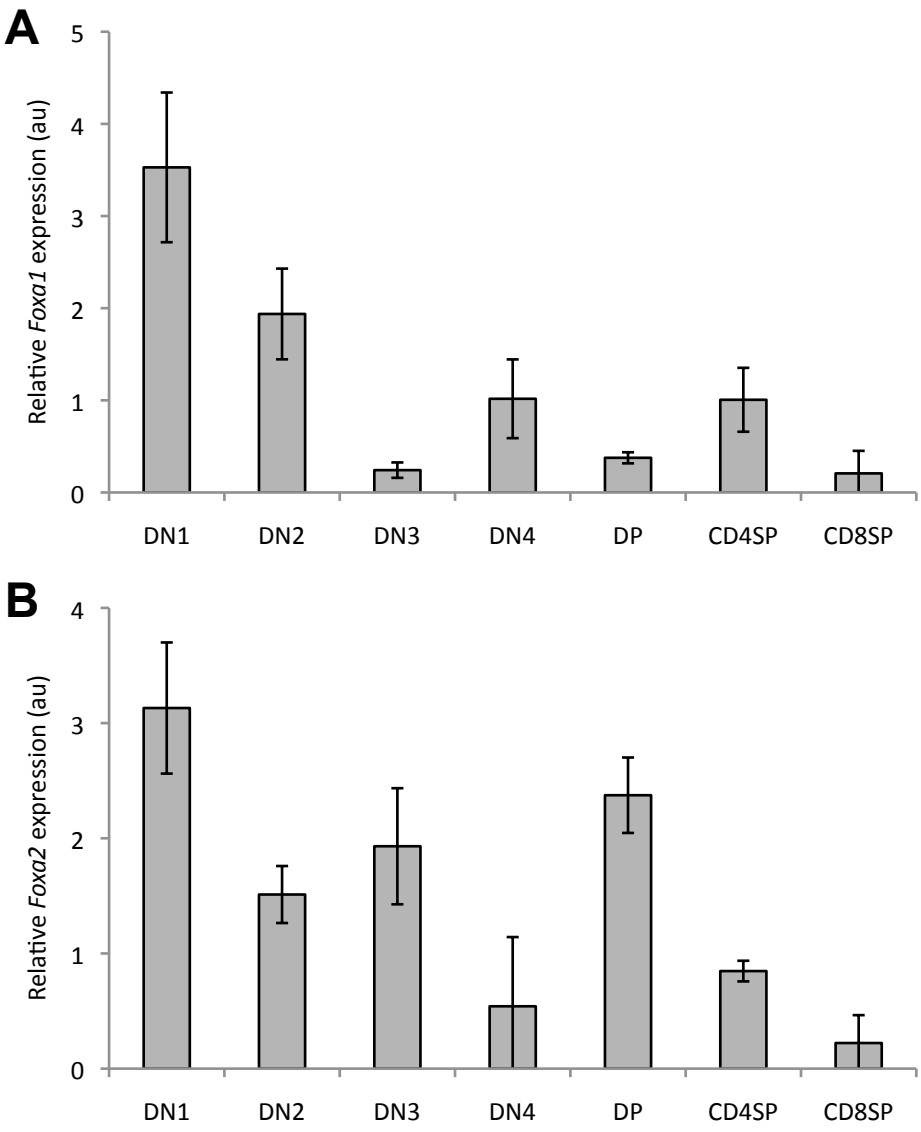

Figure 6.2 *Foxa1* and *Foxa2* are expressed in developing thymocytes

Bar chart to show relative *Foxa1* (**A**) and *Foxa2* (**B**) expression in DN1 (CD44+CD25), DN2 (CD44+CD25+), DN3 (CD44-CD25+), DN4 (CD44-CD25-), DP (CD4+CD8+), CD4SP (CD4+CD8-) and CD8SP (CD8+CD4-) thymocytes. The scale shows expression normalised to the level of the housekeeping gene *HPRT*. Error bars represent ± SEM. Data are representative of at least two independent experiments.

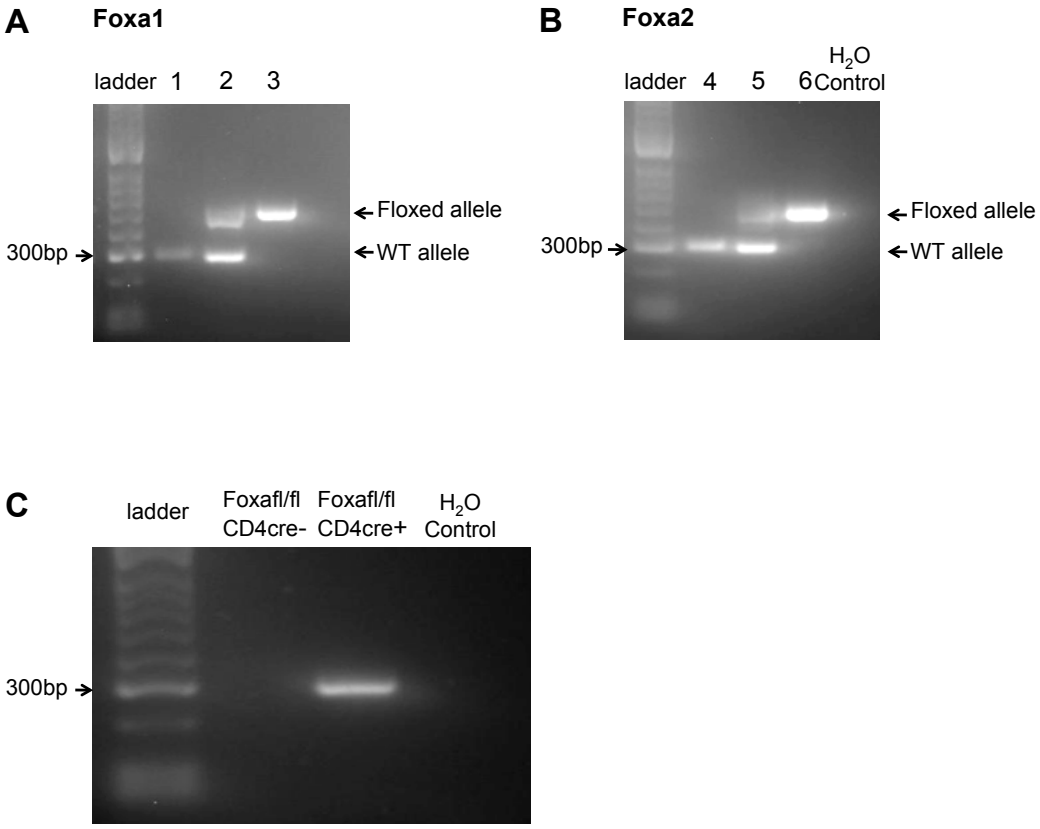

Figure 6.3 Genotyping of conditional KO mice

PCR of genomic DNA for Foxa1 (**A**) and Foxa2 (**B**) WT and floxed allele, and CD4-cre (**C**) ran on 1% agarose gel visualized using U.V.

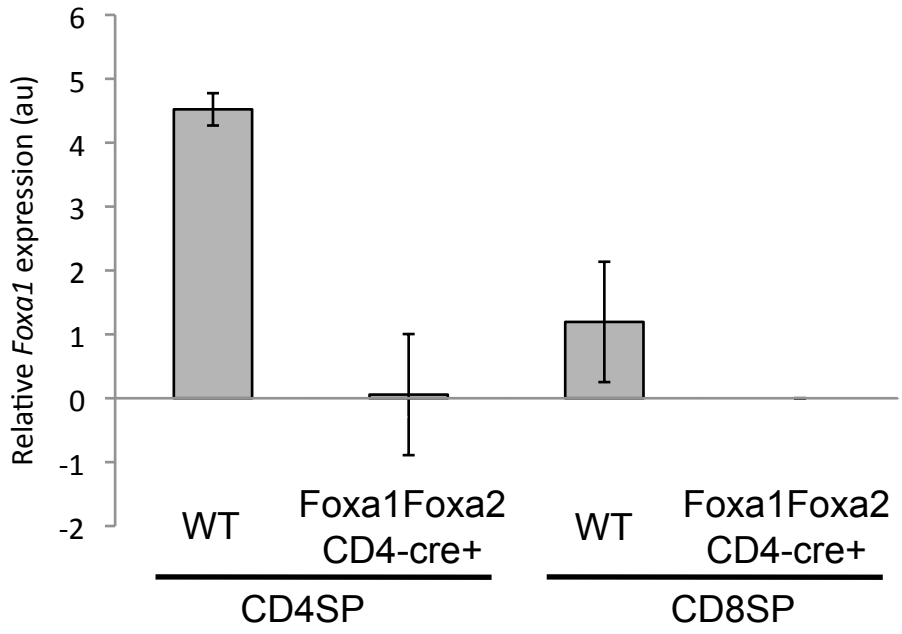

Figure 6.4 Relative expression of *Foxa1* in conditional KO mice

Bar chart shows relative expression of *Foxa1* in CD4 and CD8 T-cells of Foxa1a2 KO mice compared with WT. The scale shows expression normalised to the level of the housekeeping gene *HPRT*. Error bars represent ± SEM. Data are representative of at least two independent experiments.

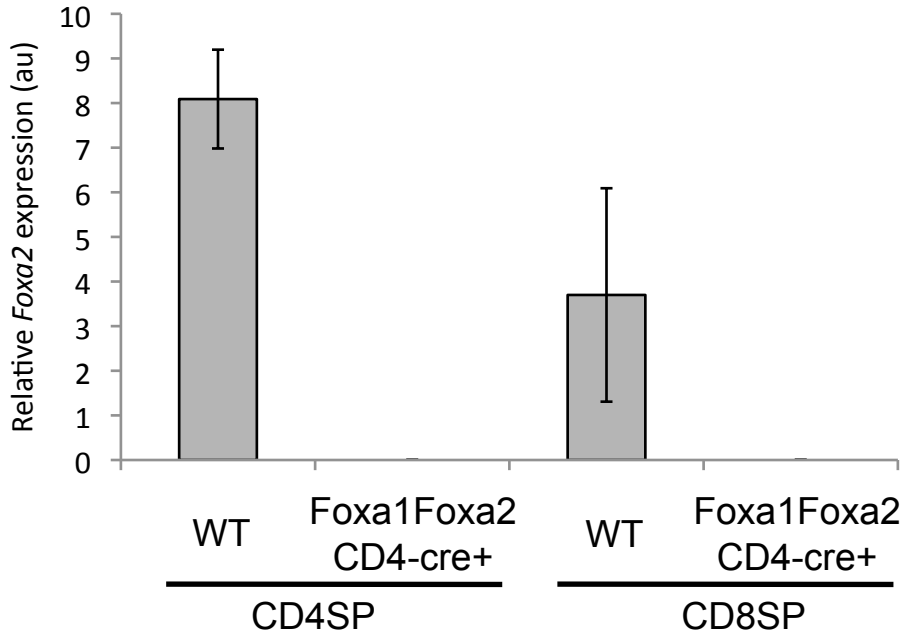

Figure 6.5 Relative expression of Foxa2 in conditional KO mice

Bar chart shows relative expression of *Foxa2* in CD4 and CD8 T-cells of Foxa1a2 KO mice compared with WT. The scale shows expression normalised to the level of the housekeeping gene *HPRT*. Error bars represent ± SEM.Data are representative of at least two independent experiments.

Foxa1 KO - Thymus

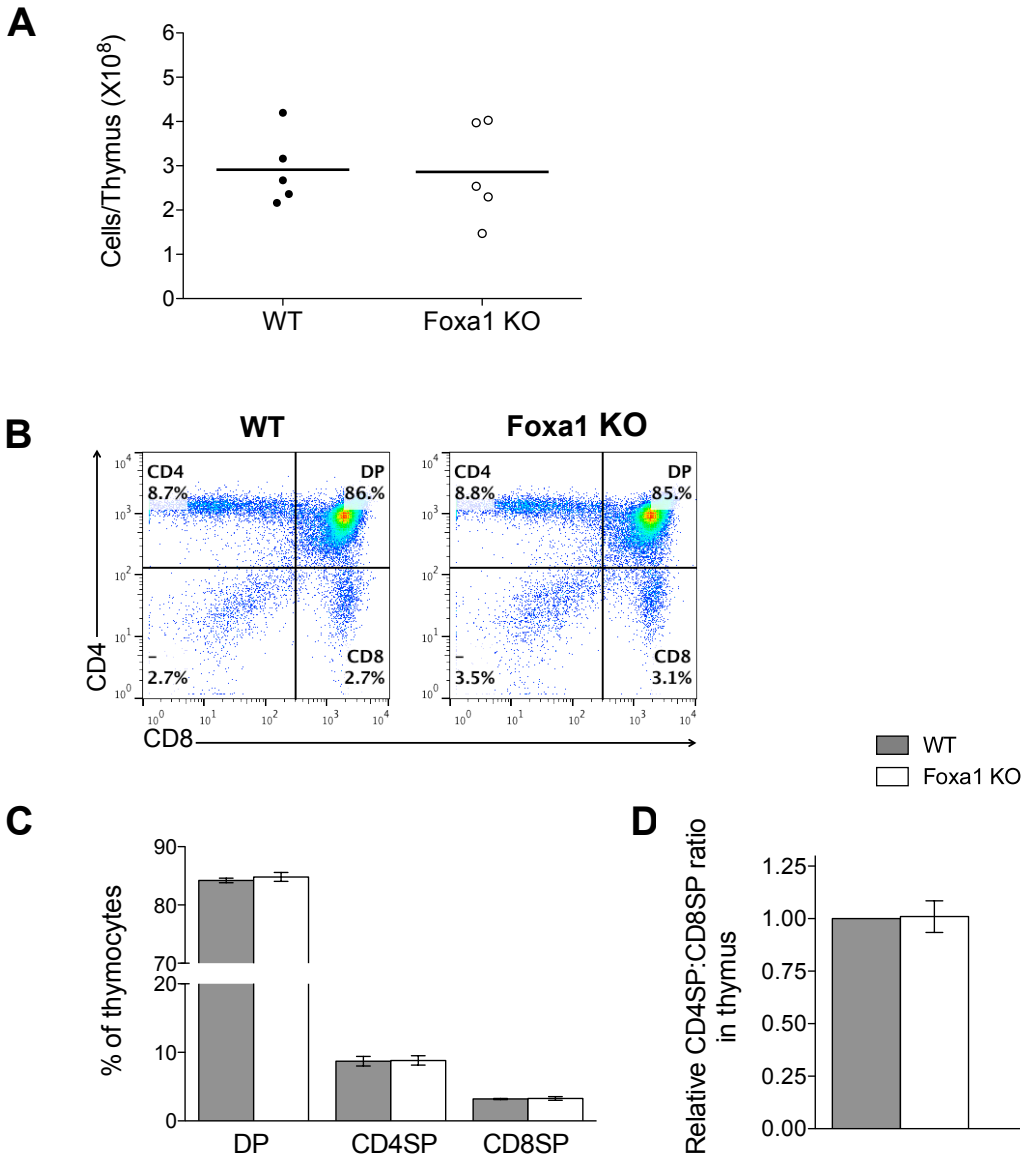

Figure 6.6 Thymocyte development in WT and Foxa1 KO mice

(A) Scatter plot shows thymocyte numbers isolated from WT and Foxa1 KO mice. The mean for each group is indicated with a line. **(B)** The dot plots show representative facs profiles of developing thymocytes isolated from WT and Foxa1 KO thymus stained with anti-CD4 and anti-CD8. Bar charts show **(C)** percentage of DP, CD4SP and CD8SP and **(D)** relative CD4:CD8 ratio in WT and Foxa1 KO thymus. Error bars represent ± SEM. (n=5 for each genotype)

Foxa1 KO - Spleen

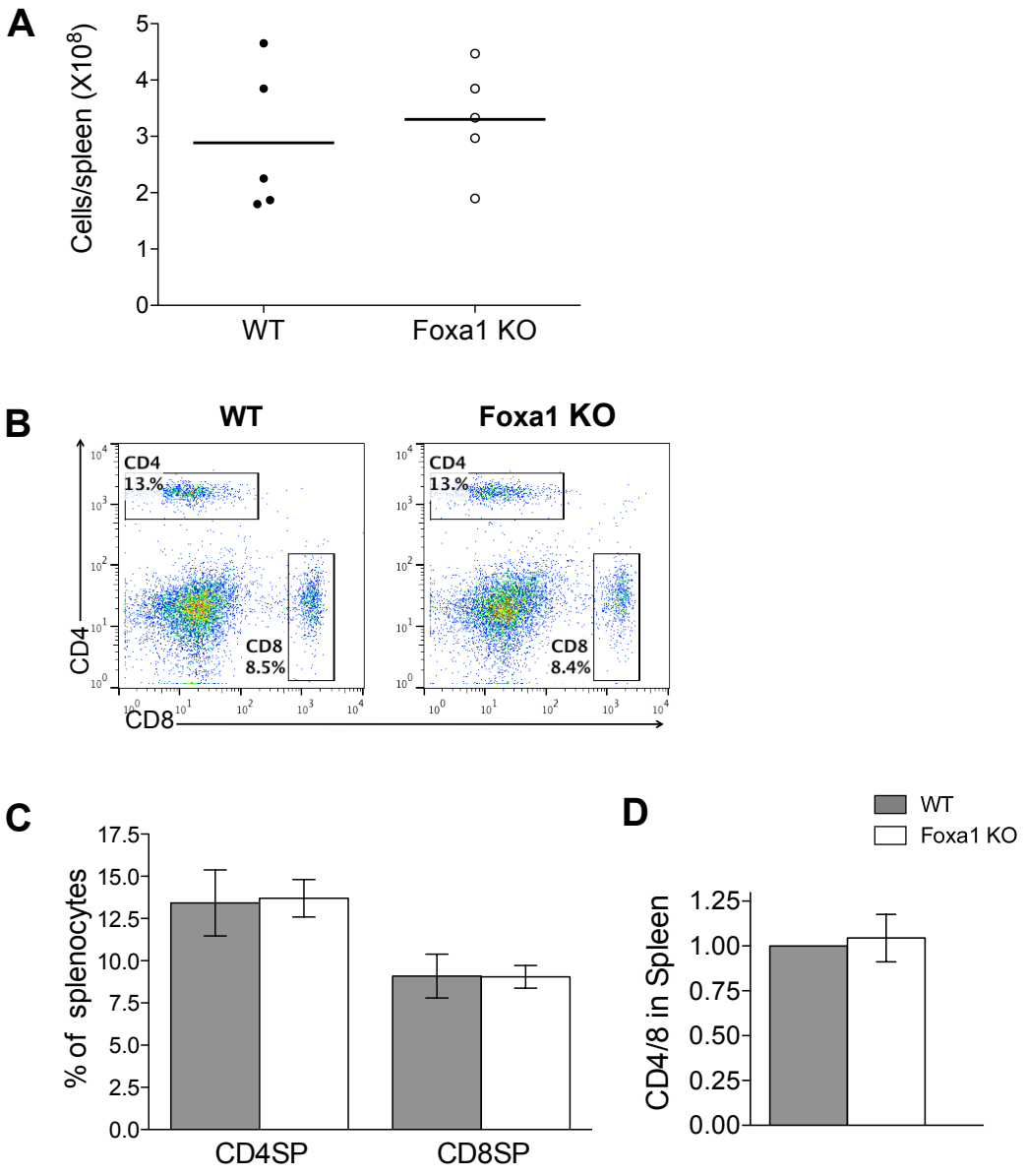

Figure 6.7 T-cell populations in WT and Foxa1 KO spleen

(A) Scatter plot shows spleen cell numbers isolated from WT and Foxa1 KO mice. The mean for each group is indicated with a line. **(B)** The dot plots show representative facs profile of splenocytes isolated from WT and Foxa1 KO spleen stained with anti-CD4 and anti-CD8. Bar charts show **(C)** percentage of CD4SP and CD8SP and **(D)** relative CD4:CD8 ratio in WT and Foxa1 KO spleen. Error bars represent ± SEM. (n=5 for each genotype)

Foxa1 KO - LN

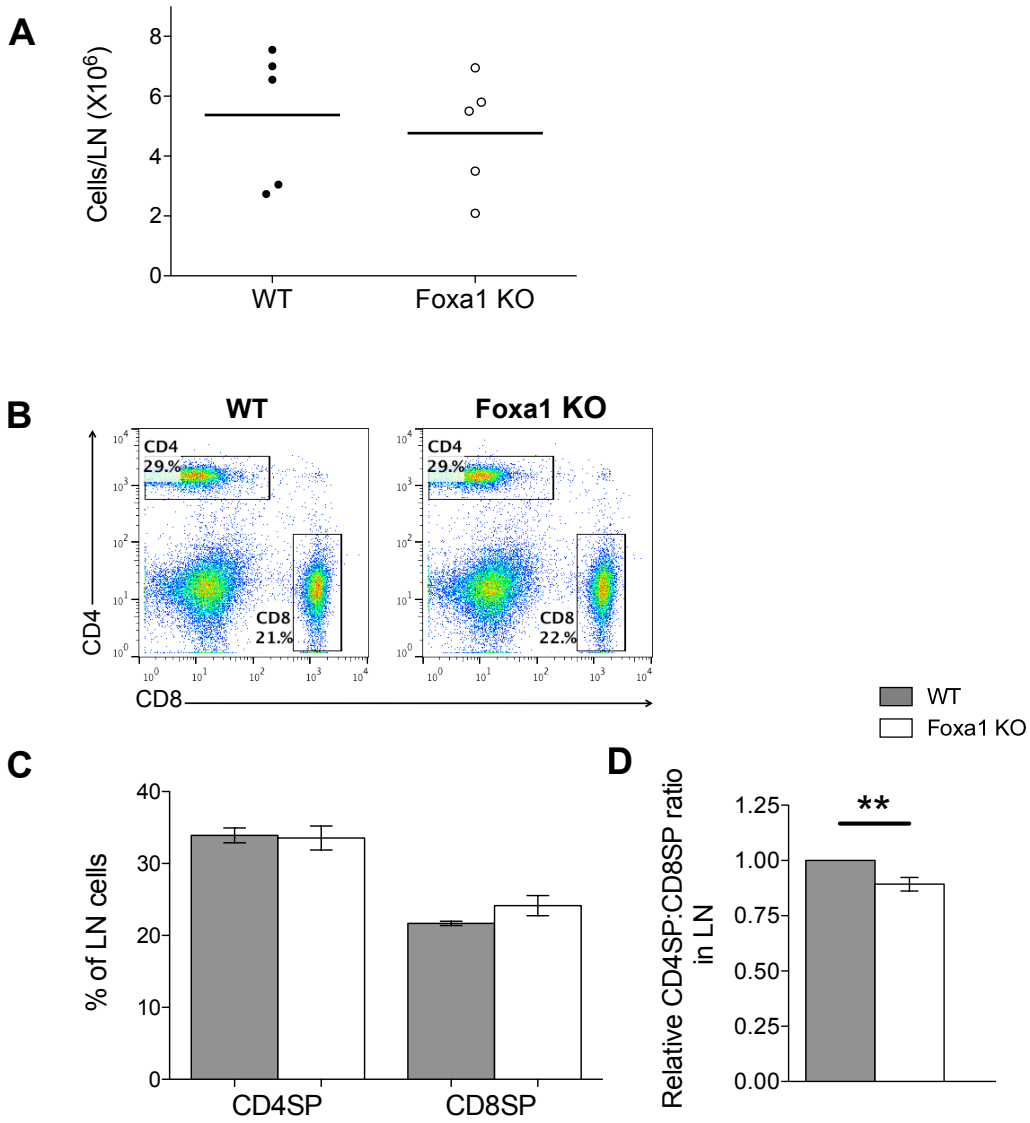

Figure 6.8 T-cell populations in WT and Foxa1 KO LN

(A) Scatter plot shows LN cell numbers isolated from WT and Foxa1 KO mice. The mean for each group is indicated with a line. **(B)** The dot plots show representative facs profiles of LN cells isolated from WT and Foxa1 KO LN stained with anti-CD4 and anti-CD8. Bar charts show **(C)** percentage of CD4SP and CD8SP and **(D)** relative CD4:CD8 ratio in WT and Foxa1 KO LN. Error bars represent ± SEM. (n=5 for each genotype) **p<0.01; WT versus Foxa1 KO .

Foxa2 KO - Thymus

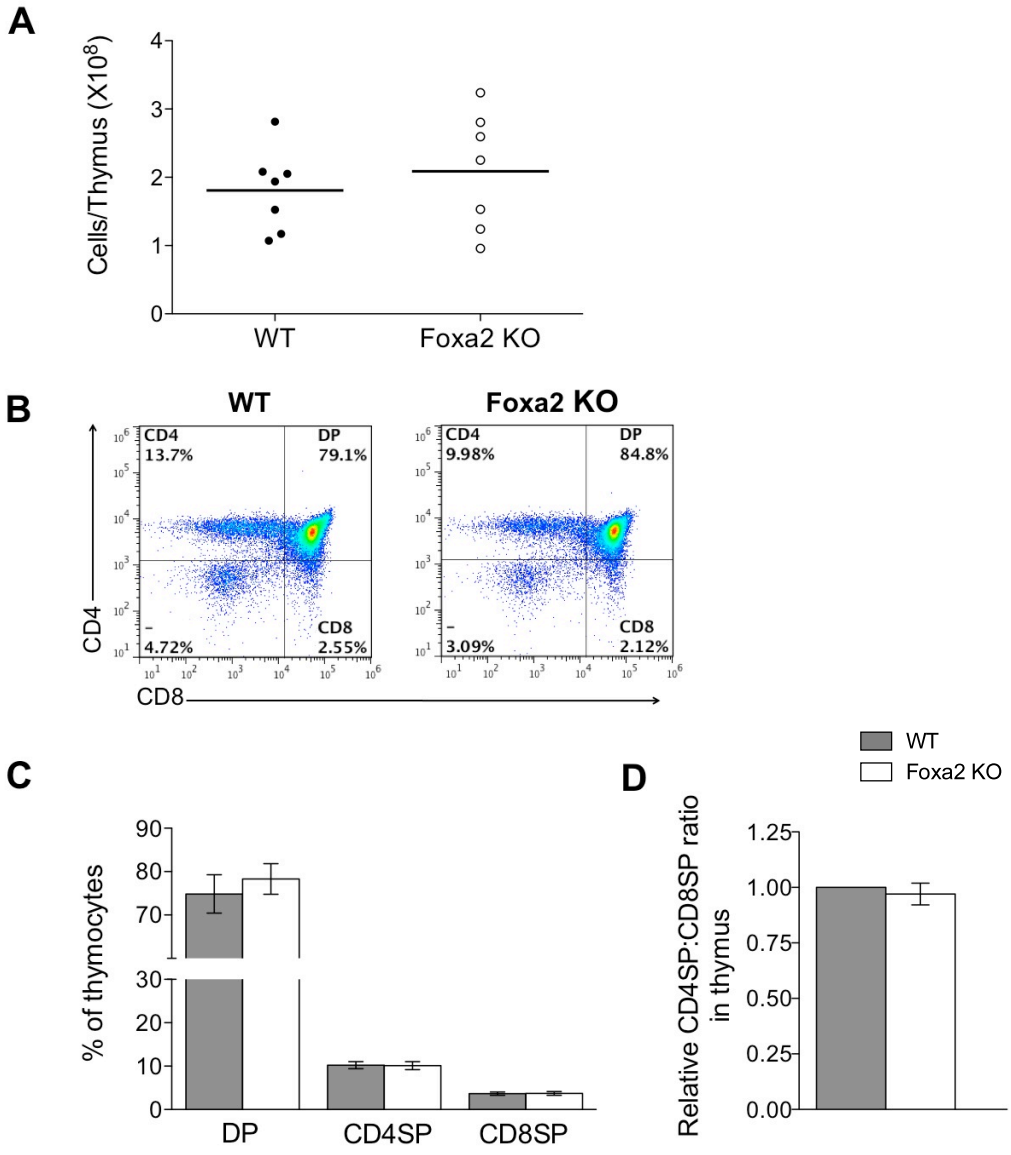

Figure 6.9 Thymocyte development in WT and Foxa2 KO mice

(A) Scatter plot shows thymocyte numbers isolated from WT and Foxa2 KO mice. The mean for each group is indicated with a line. **(B)** The dot plots show representative facs profiles of developing thymocytes isolated from WT and Foxa2 KO thymus stained with anti-CD4 and anti-CD8. Bar charts show **(C)** percentage of DP, CD4SP and CD8SP and **(D)** relative CD4:CD8 ratio in WT and Foxa2 KO thymus. Error bars represent ± SEM. (n=7 for each genotype)

Foxa2 KO - Spleen

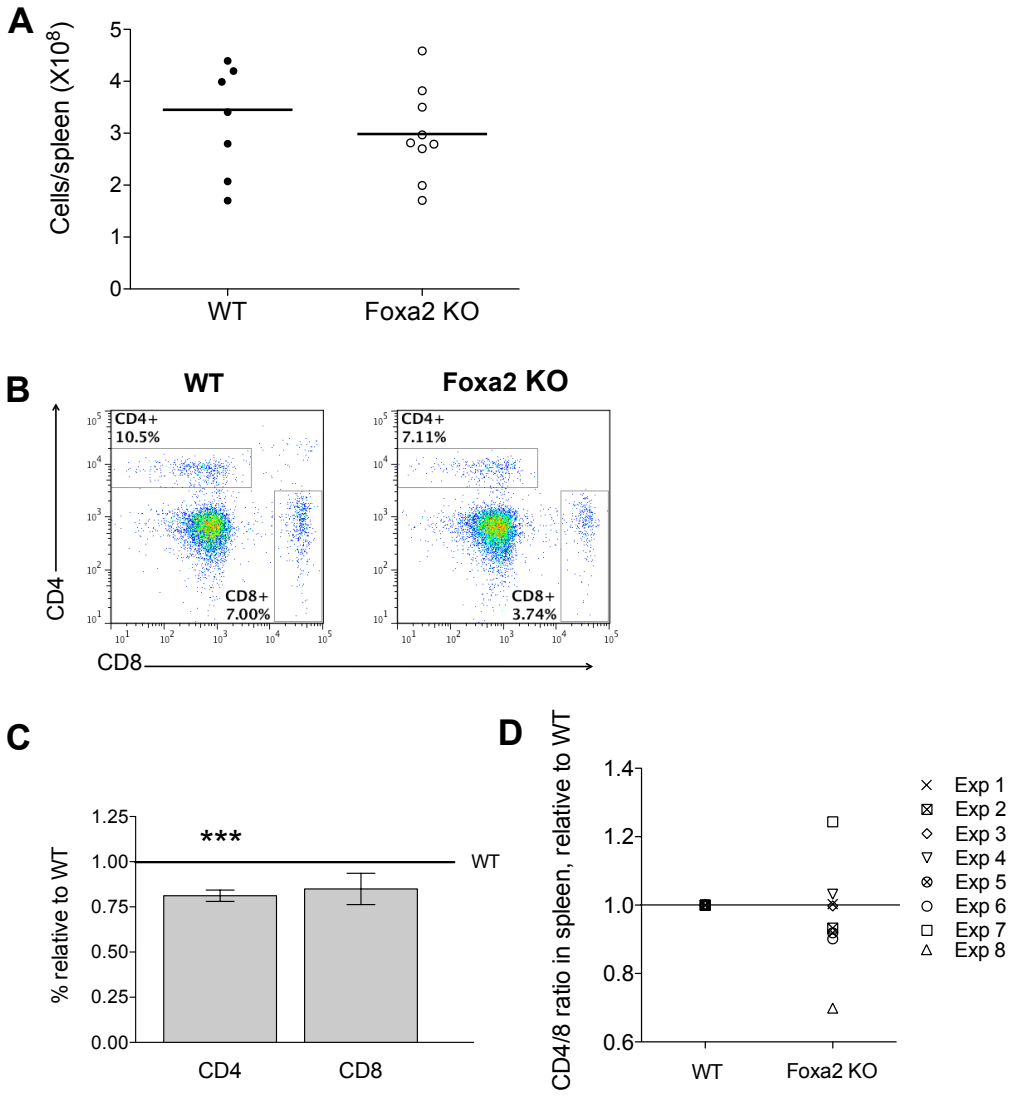

Figure 6.10 T-cell populations in WT and Foxa2 KO spleen

(A) Scatter plot shows spleen cell numbers isolated from WT and Foxa2 KO mice. The mean for each group is indicated with a line. **(B)** The dot plots show representative facs profiles of splenocytes isolated from WT and Foxa2 KO spleen stained with anti-CD4 and anti-CD8. **(C)** Bar chart shows percentage of CD4SP and CD8SP in Foxa2 KO spleen, relative to WT. **(D)** Scatter plot shows relative CD4:CD8 ratio in WT and Foxa2 KO spleen. In each experiment, the average value of the WT is set to 1, so as to allow comparison between litters. Error bars represent ± SEM. (n=7 for each genotype) ***p<0.005; WT versus Foxa2 KO.

Foxa2 KO – LN

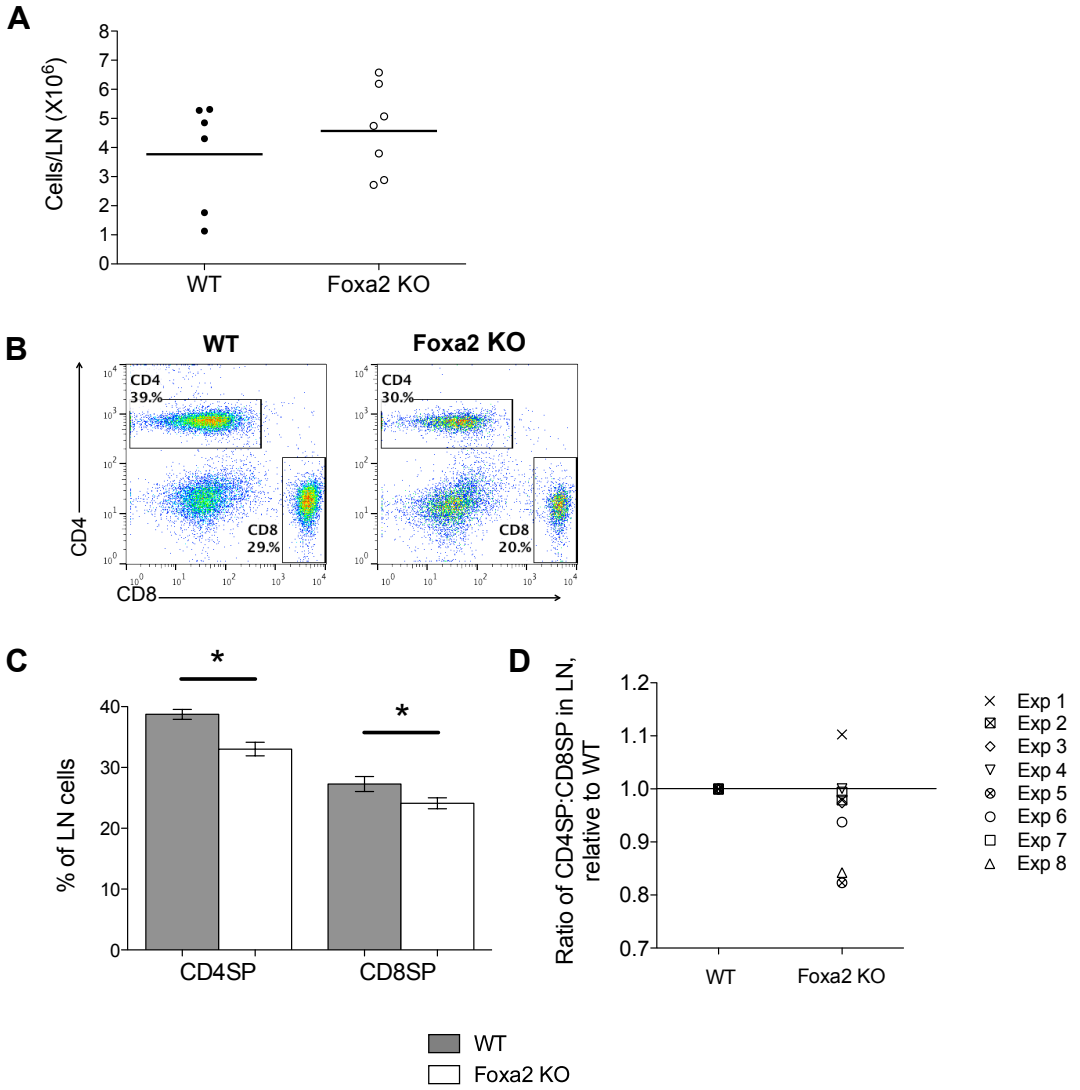

Figure 6.11 T-cell populations in WT and Foxa2 KO LN

(A) Scatter plot shows LN cell numbers isolated from WT and Foxa2 KO mice. The mean for each group is indicated with a line. **(B)** The dot plots show representative facs profiles of LN cells isolated from WT and Foxa2 KO LN stained with anti-CD4 and anti-CD8. **(C)** Bar chart shows percentage of CD4SP and CD8SP in WT and Foxa2 KO LN. **(D)** Scatter plot shows relative CD4:CD8 ratio in WT and Foxa2 KO spleen. In each experiment, the average value of the WT is set to 1, so as to allow comparison between litters. Error bars represent ± SEM. (n=7 for each genotype) *p<0.05; WT versus Foxa2 KO.

Foxa1a2 KO - Thymus

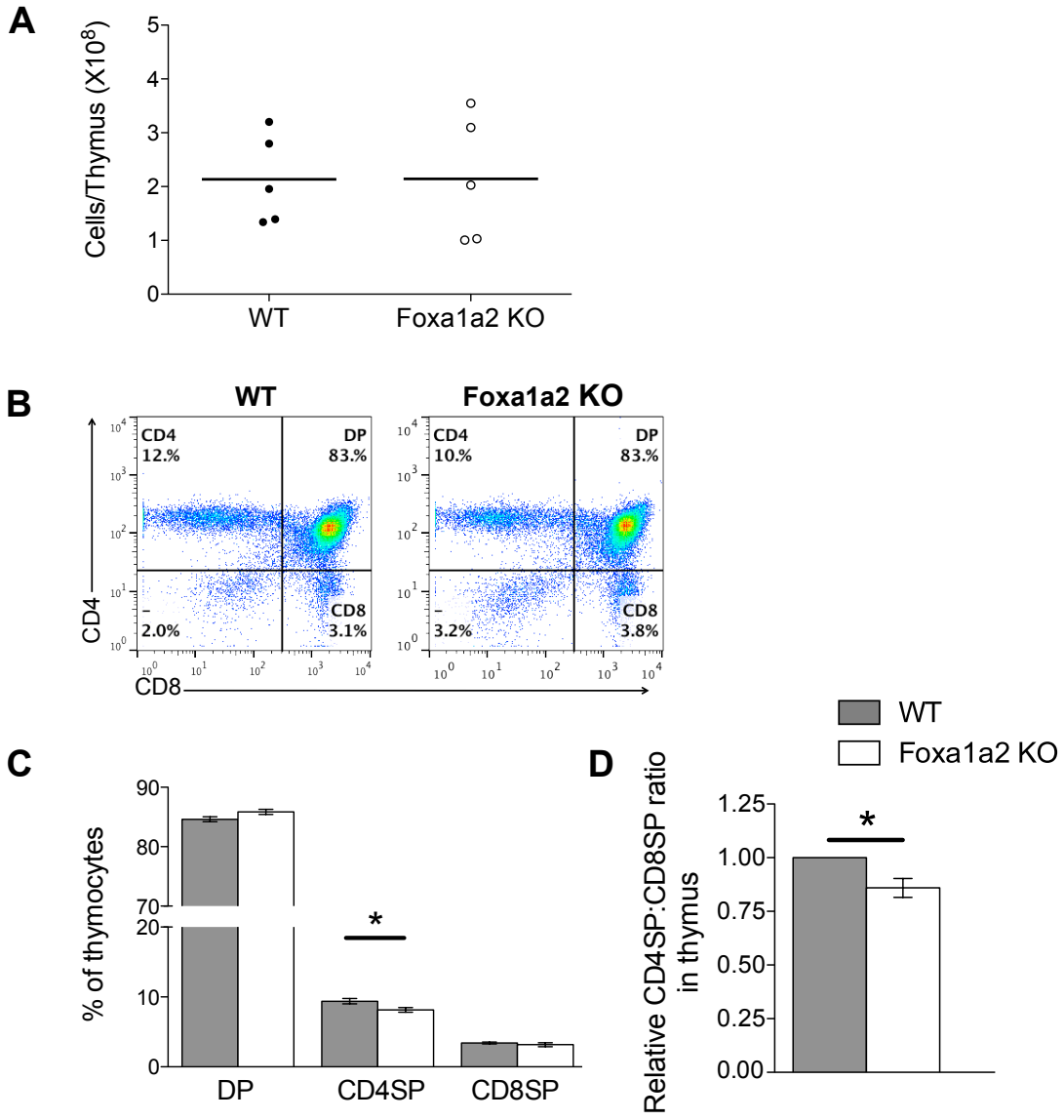

Figure 6.12 Foxa1 and Foxa2 in thymocyte development

(**A**) Scatter plot shows thymocyte numbers isolated from WT and Foxa1a2 KO mice. The mean for each group is indicated with a line. (**B**) The dot plots show representative facs profiles of developing thymocytes isolated from WT and Foxa1a2 KO thymus stained with anti-CD4 and anti-CD8. Bar charts show (**C**) percentage of DP, CD4SP and CD8SP and (**D**) relative CD4:CD8 ratio in WT and Foxa1a2 KO thymus. Error bars represent ± SEM. (n=5 for each genotype) *p<0.05; WT versus Foxa1a2 KO.

Foxa1a2 KO - Spleen

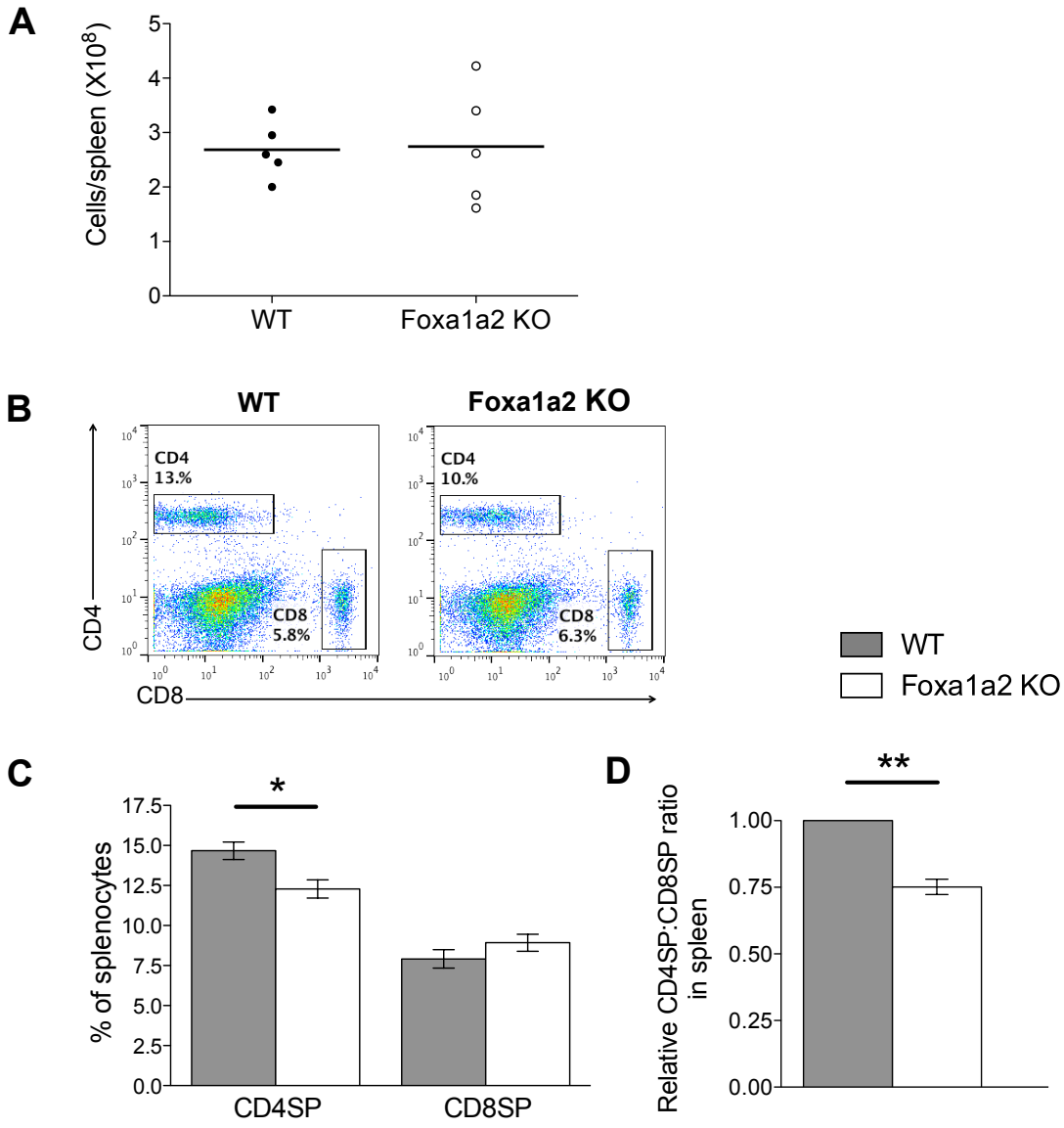

Figure 6.13 T-cell populations in WT and Foxa1a2 KO spleen

(A) Scatter plot shows spleen cell numbers isolated from WT and Foxa1a2 KO mice. The mean for each group is indicated with a line. **(B)** The dot plots show representative facs profiles of splenocytes isolated from WT and Foxa1a2 KO spleen stained with anti-CD4 and anti-CD8. Bar charts show **(C)** percentage of CD4SP and CD8SP and **(D)** relative CD4:CD8 ratio in WT and Foxa1a2 KO spleen. Error bars represent ± SEM. (n=5 for each genotype) *p<0.05; **p<0.01; WT versus Foxa1a2 KO.

Foxa1a2 KO - LN

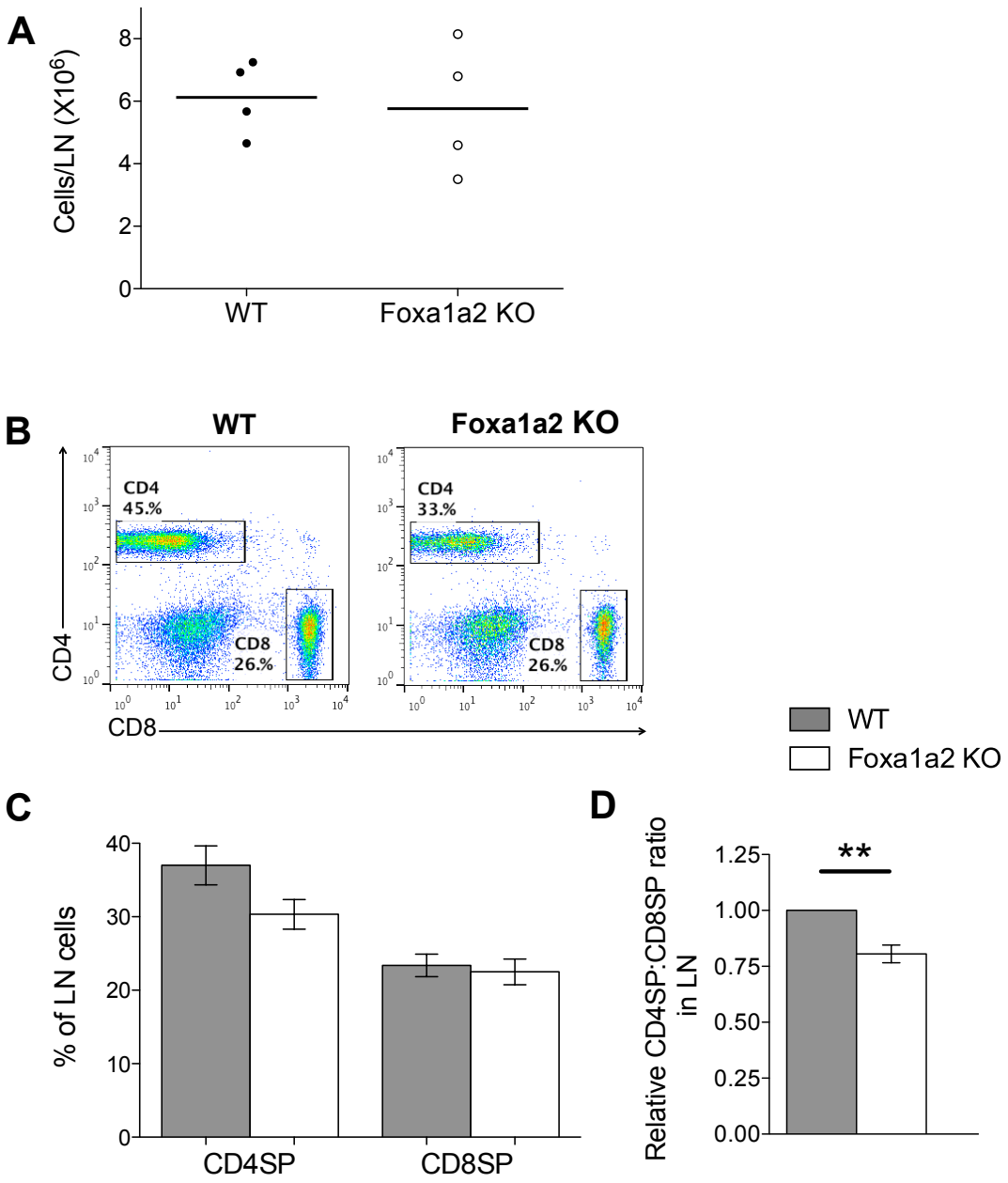

Figure 6.14 T-cell populations in WT and Foxa1a2 KO LN

(A) Scatter plot shows LN cell numbers isolated from WT and Foxa1a2 KO mice. The mean for each group is indicated with a line. **(B)** The dot plots show representative facs profiles of LN cells isolated from WT and Foxa1a2 KO LN stained with anti-CD4 and anti-CD8. Bar charts show **(C)** percentage of CD4SP and CD8SP and **(D)** relative CD4:CD8 ratio in WT and Foxa1a2 KO LN. Error bars represent ± SEM. (n=4 for each genotype) *p<0.01; WT versus Foxa1a2 KO.

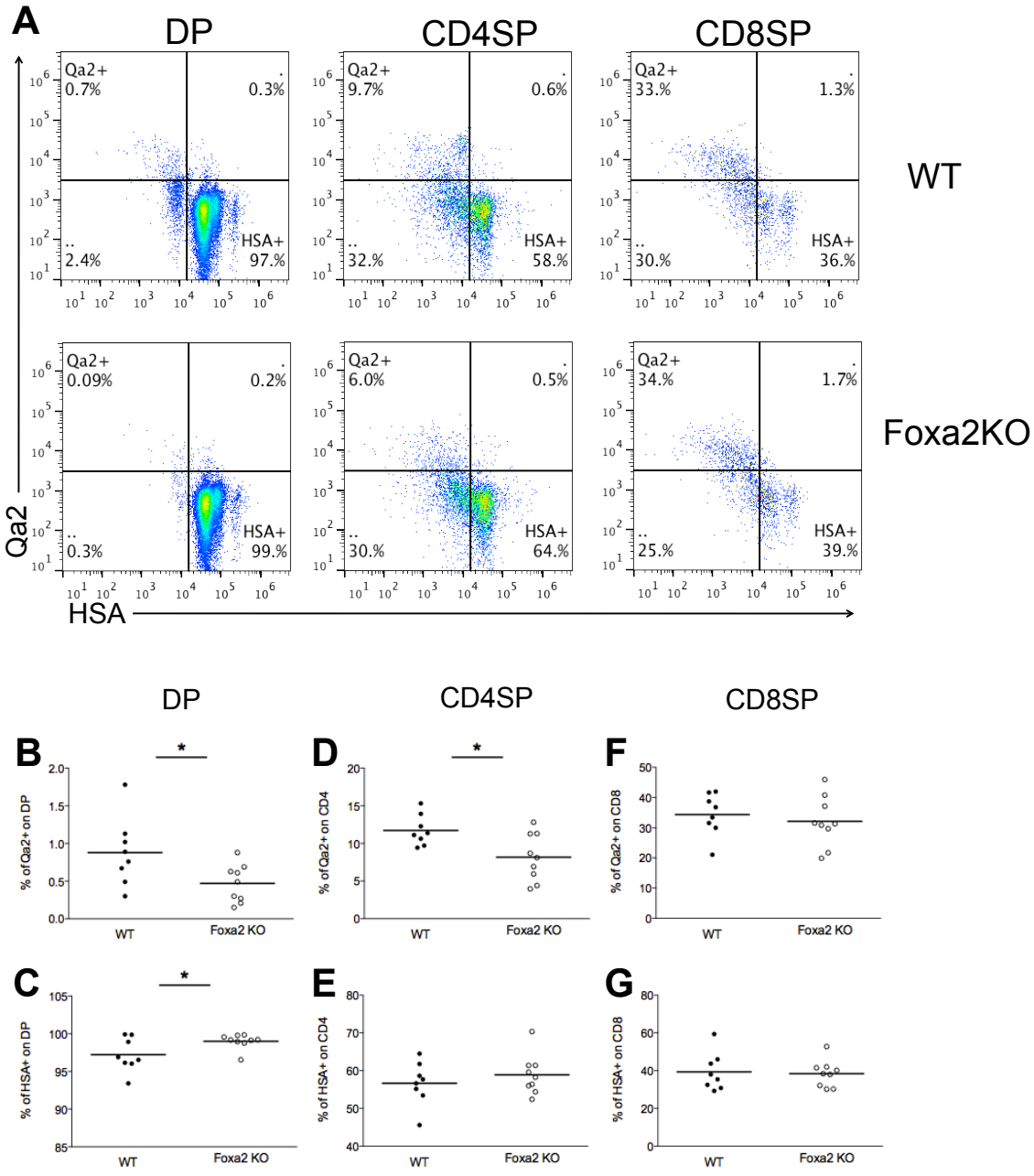

Figure 6.15 Maturity of thymocytes

(**A**)Dot plots show representative facs profiles of Qa2 and HSA expression on DP, CD4SP and CD8SP T-cell in WT and Foxa2 KO thymus. Scatter plots show percentage of Qa2+ and HSA+ cells in DP (**B**,**C**), CD4SP (**D**,**E**) and CD8SP (**F**,**G**) in WT and Foxa2KO thymus. The mean for each group is indicated with a line. (WT, n=8; Foxa2KO, n=9) *p<0.05; WT versus Foxa2 KO.

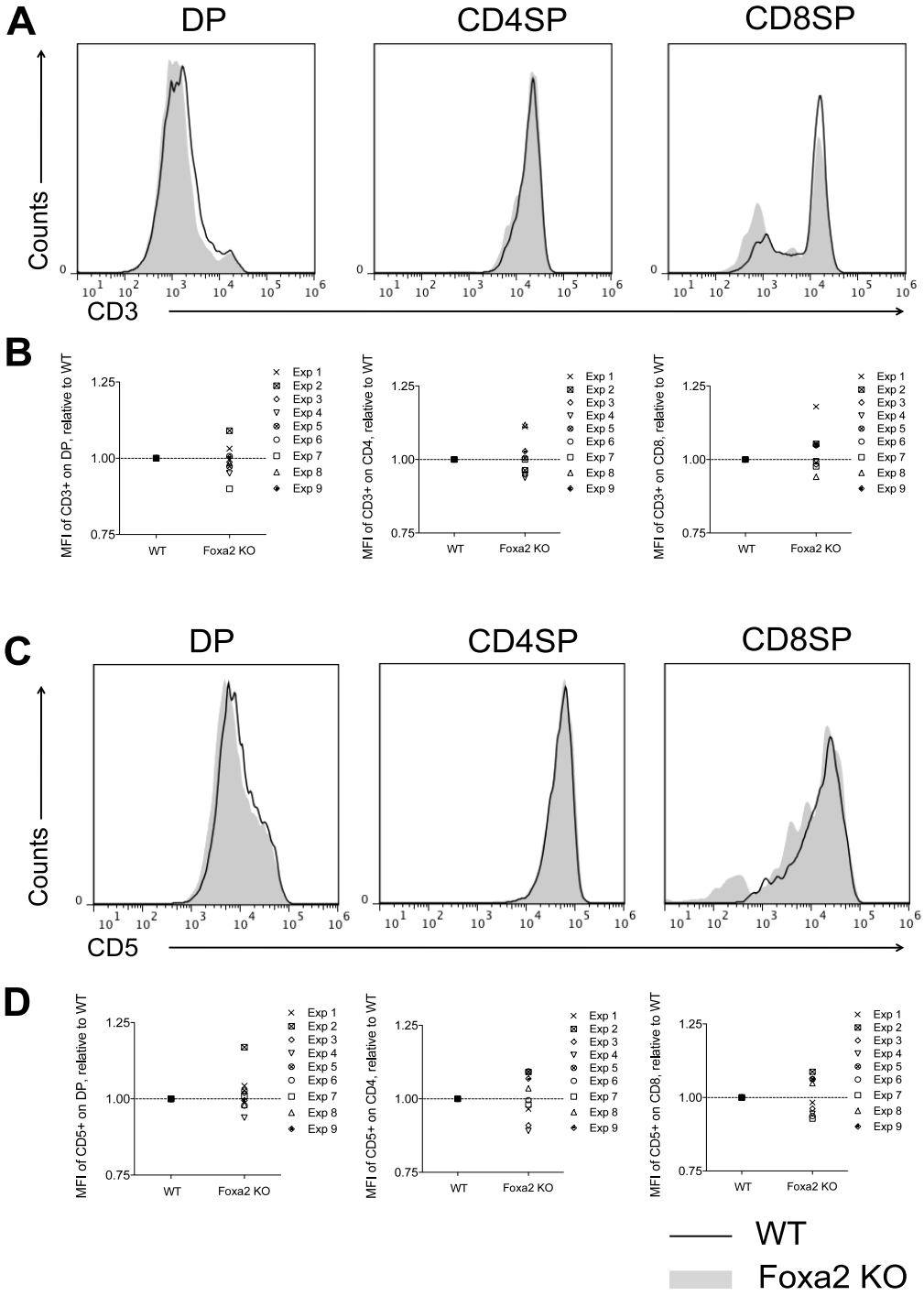

Figure 6.16 The expression of CD3 and CD5 on DP, CD4SP and CD8SP thymocytes

Representative histograms to show intensity of CD3 (**A**) and CD5 (**C**) expression on DP, CD4SP and CD8SP T-cells. Scatter plots show relative mean fluorescent intensity (MFI) of CD3+ (**B**) and CD5+ (**D**) on DP, CD4SP and CD8SP T-cells in WT and Foxa2 KO thymus. In each experiment, the value of WT is set as 1 so as to allow comparison between experiments. (WT, n=8; Foxa2KO, n=9)

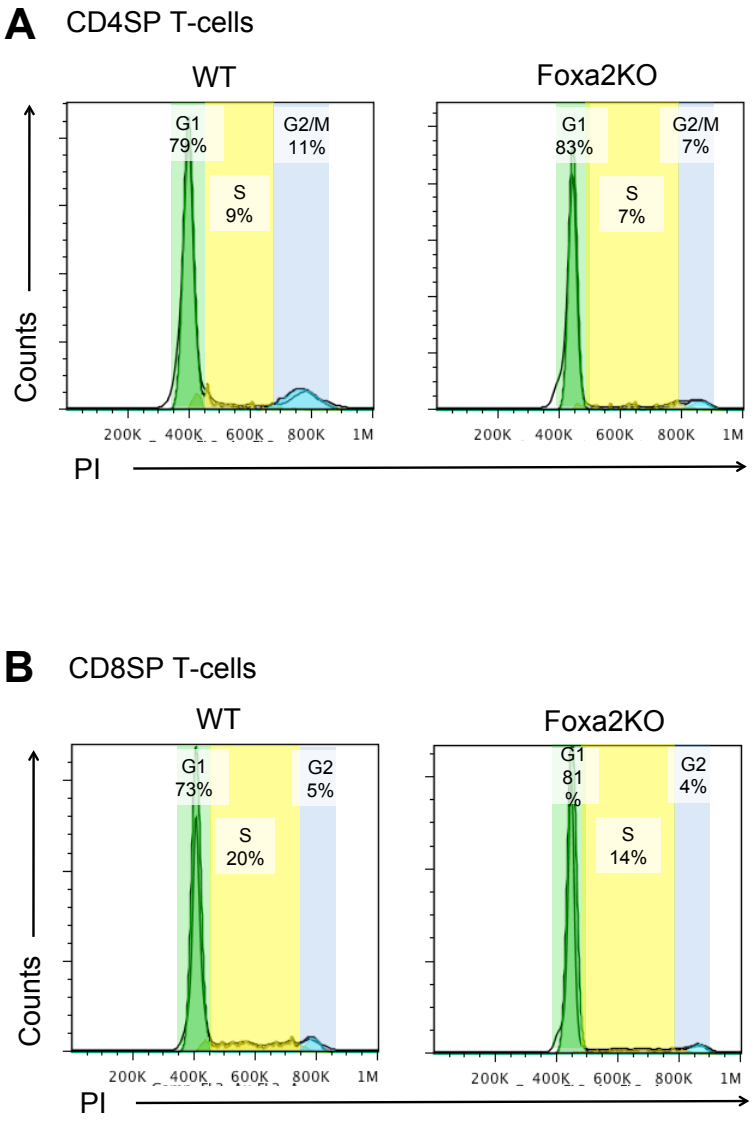

Figure 6.17 Cell cycle analysis of CD4SP and CD8 T-cells by PI

Histograms show PI staining for CD4+(**A**) and CD8+(**B**) T-cell populations from WT and Foxa2 KO thymus. Numbers inside histogram indicate percentages of each phase in the population. Data are representative of at least two independent experiments.

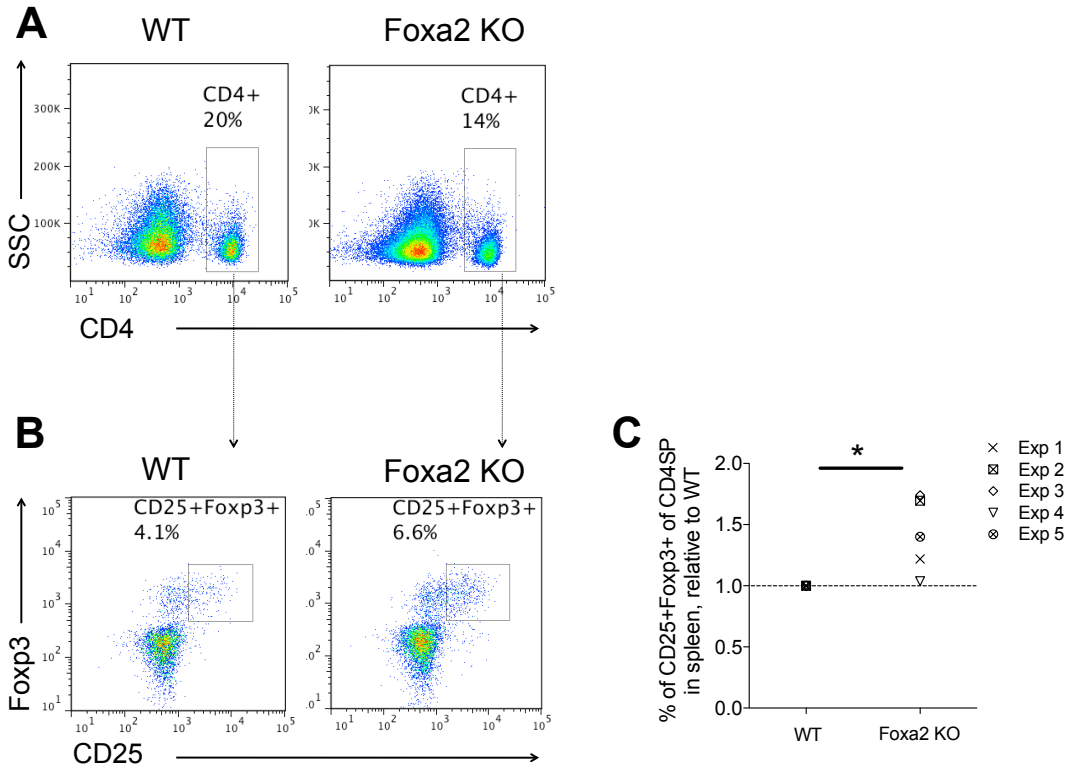

Figure 6.18 Percentage of Treg in WT and Foxa2 KO spleen

The dot plots show representative FACS profiles of staining of CD4+ T-cells (**A**) and population of CD25+Foxp3+ after gating on the CD4+ T-cells (**B**) in the spleen. (**C**) Scatter plot shows relative percentage of CD25+Foxp3+ population in WT and Foxa2 KO spleen. In each experiment, the value of WT is set as 1 so as to allow comparison between experiments. (n=5 for each group) *p<0.05; WT versus Foxa2 KO .

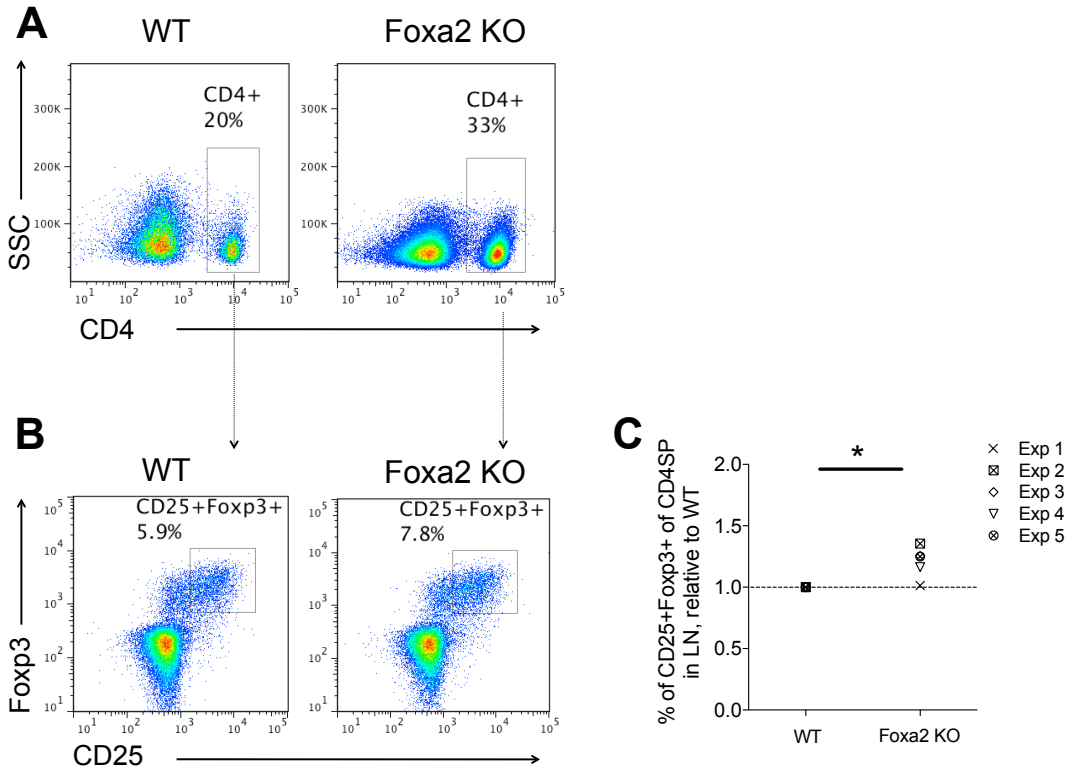

Figure 6.19 Percentage of Treg in WT and Foxa2 KO LN

The dot plots show representative facs profiles of staining of CD4+ T-cells (**A**) and population of CD25+Foxp3+ after gating on the CD4+ T-cells (**B**) in the LN. (**C**) Scatter plot shows relative percentage of CD25+Foxp3+ population in WT and Foxa2 KO LN. In each experiment, the value of WT is set as 1 so as to allow comparison between experiments. (n=5 for each group) *p<0.05; WT versus Foxa2 KO .

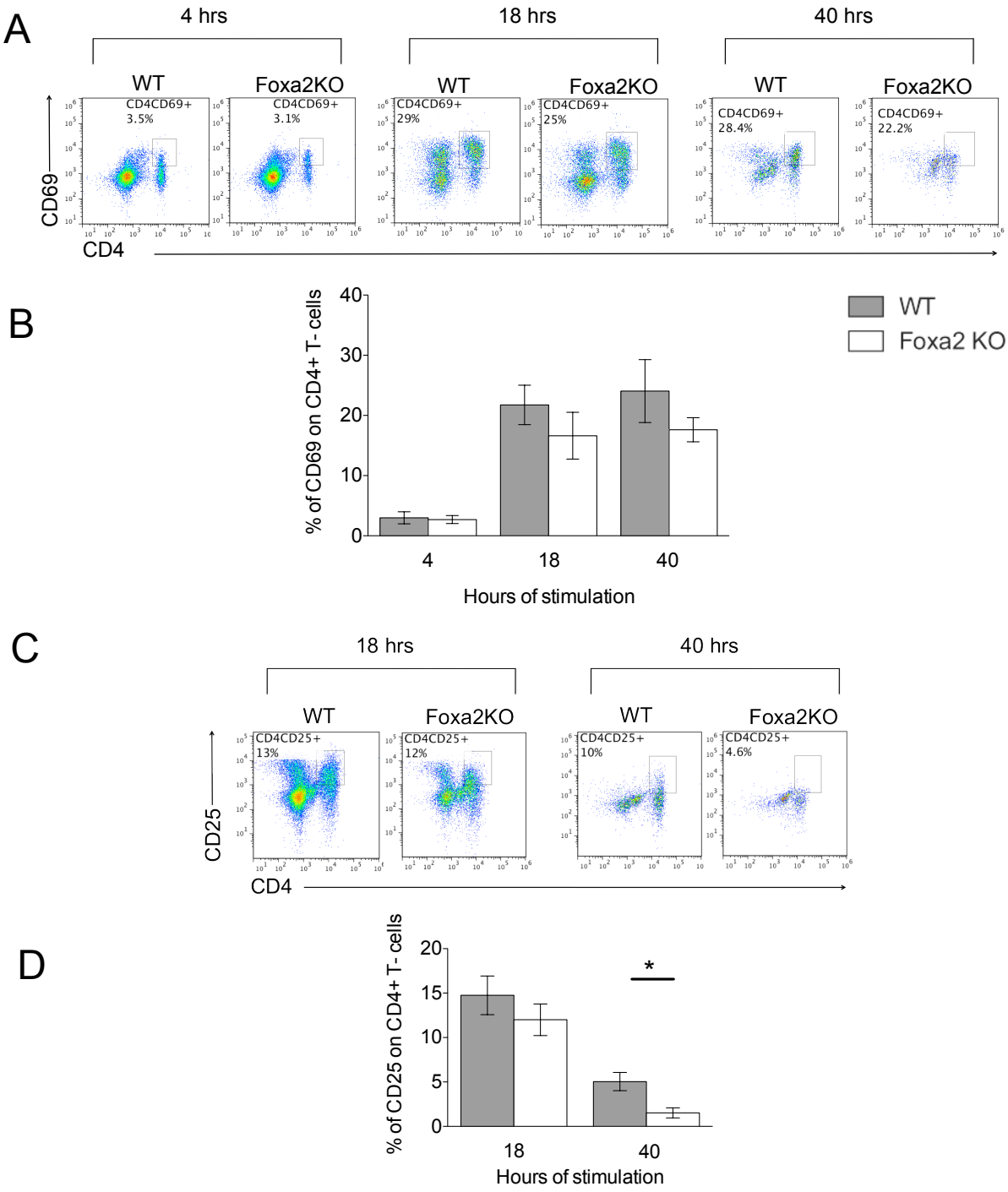

Figure 6.20 Activation of CD4 T-cells by anti-CD3 and anti-CD28 treatment after 4, 18 and 40 hrs culture

Dot plots show representative facs profiles of CD69 staining on CD4+ T-cells after 4, 18 and 40 hours (**A**) and CD25 staining on CD4+ T-cells after 18 and 40 hours (**C**) in culture stimulated with 0.01µg/ml of anti-CD3 and anti-CD28. Bar charts show percentage of CD69+(**B**) and CD25+ (**D**) on WT and Foxa2 KO CD4+ T-cells. Error bars represent ± SEM. (n=4 for each genotype) *p<0.05; WT versus Foxa2 KO.

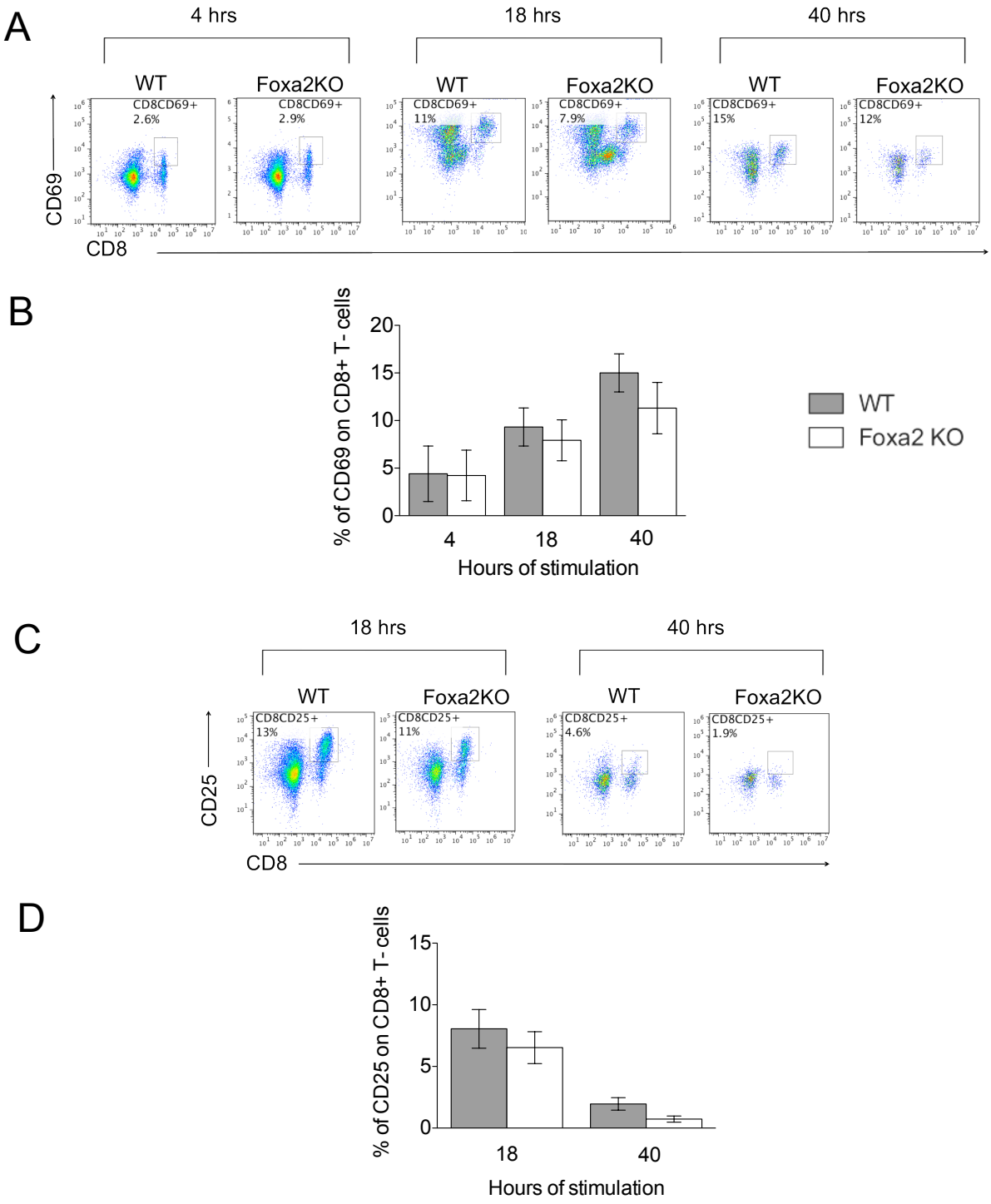

Figure 6.21 Activation of CD8 T-cells by anti-CD3 and anti-CD28 treatment after 4, 18 and 40 hrs culture

Dot plots show representative facs profiles of CD69 staining on CD8+ T-cells after 4, 18 and 40 hours (**A**) and CD25 staining on CD8+ T-cells after 18 and 40 hours (**C**) in culture stimulated with 0.01µg/ml of anti-CD3 and anti-CD28. Bar charts show percentage of CD69+ (**B**) and CD25+ (**D**) on WT and Foxa2 KO CD8+ T-cells. Error bars represent ± SEM. (n=4 for each genotype)

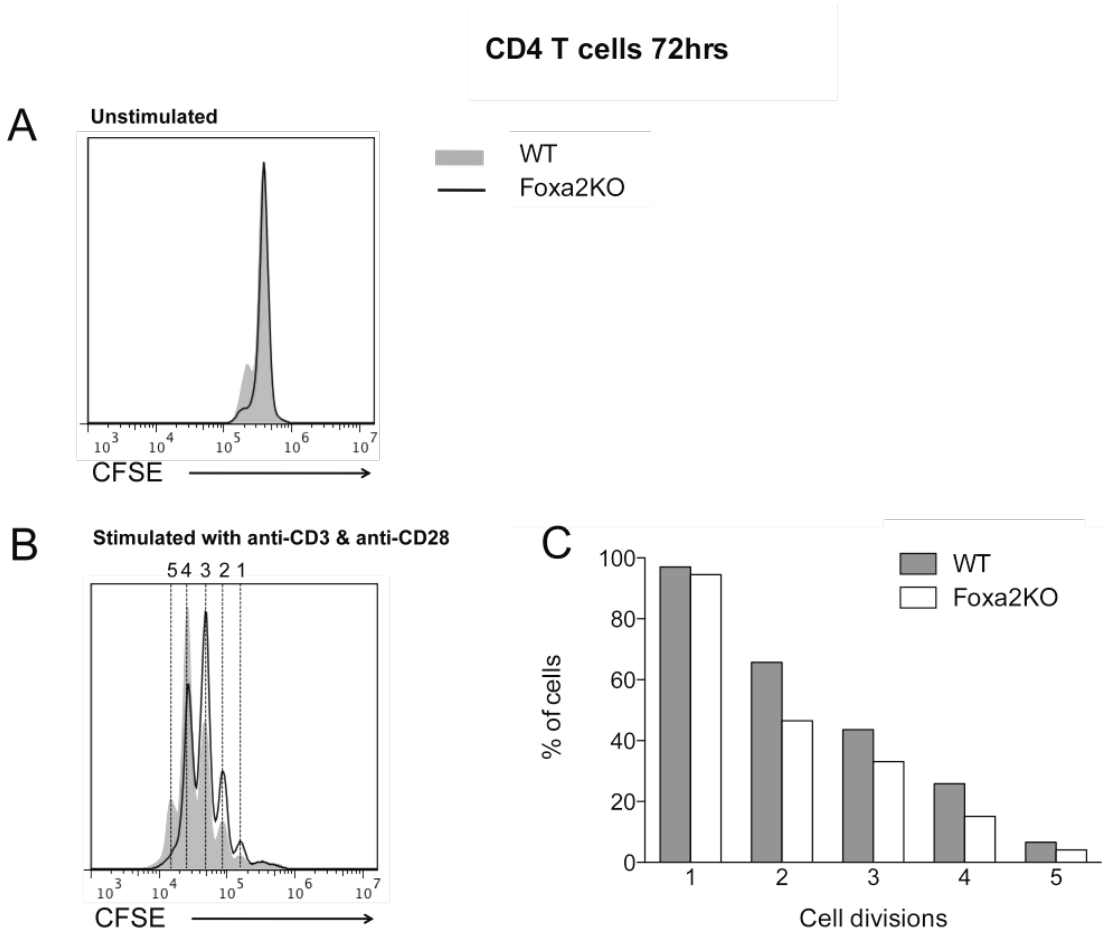

Figure 6.22 Proliferation analysis of CD4+ T-cells by CFSE assay.

Histograms show representative CFSE staining on WT and Foxa2 KO CD4SP T-cells cultured for 72 hours with 0.01µg/ml of anti-CD3 and anti-CD28 (**B**) and unstimulated cells were shown as untreated control (**A**). (**C**) The bar chart shows percentage of cells that have undergone the indicated numbers of cell divisions. Results are representative of two experiments.

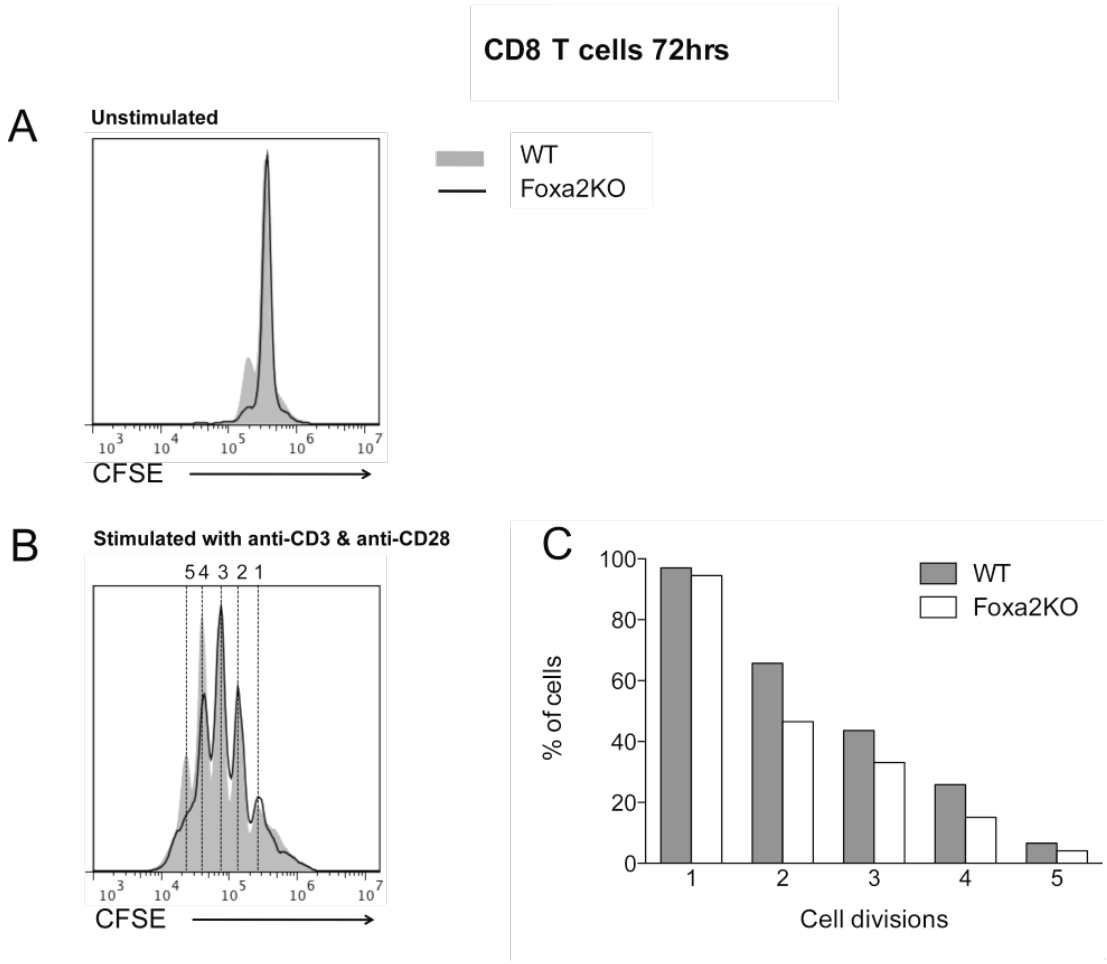

Figure 6.23 Proliferation analysis of CD8+ T-cells by CFSE assay.

Histograms show representative CFSE staining on WT and Foxa2 KO CD8SP T-cells cultured for 72 hours with 0.01µg/ml of anti-CD3 and anti-CD28 (**B**) and unstimulated cells were shown as untreated control (**A**). (**C**) The bar chart shows percentage of cells that have undergone the indicated numbers of cell divisions. Results are representative of two experiments.

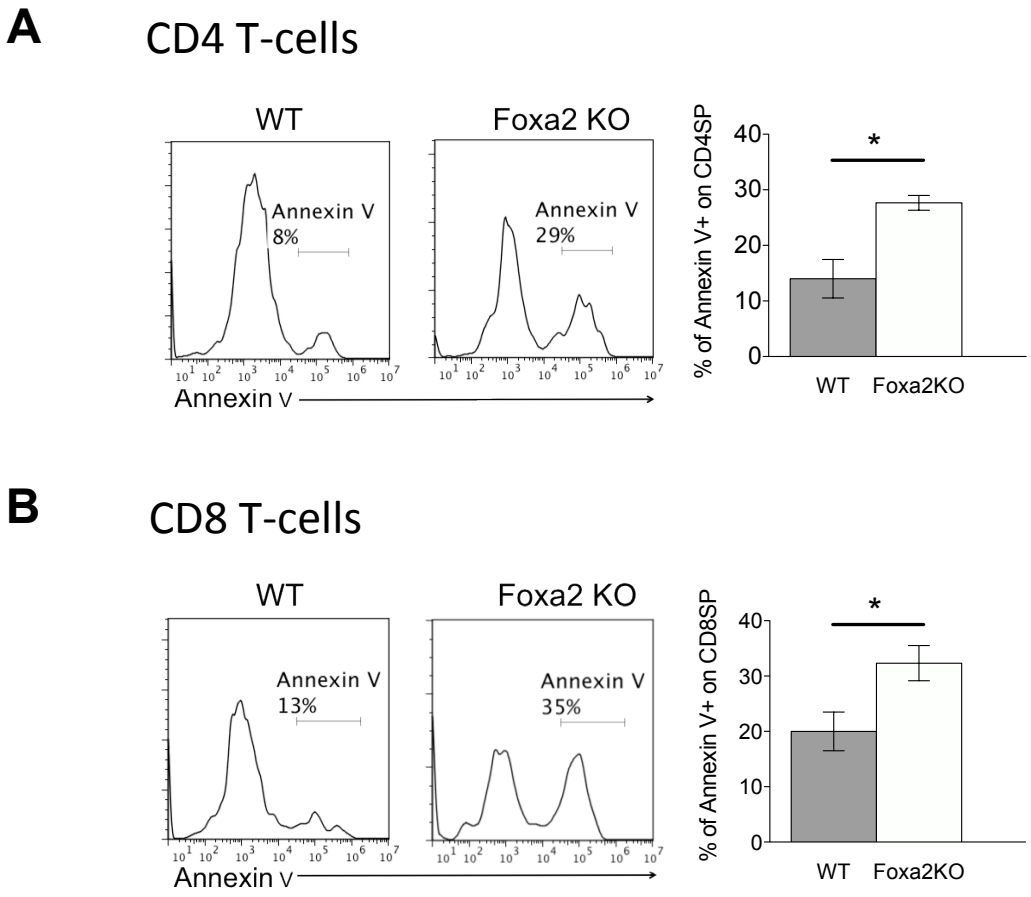

Figure 6.24 Apoptosis in activated T-cells

The graph shows annexin-V staining on CD4 and CD8 T cells after 40 hours in culture stimulated with 0.01μg/ml of anti-CD3 and anti-CD28.
Histrograms show representative facs profiles of annexin-V staining gated on CD4+ (**A**) and CD8+ (**B**) T cells. Bar charts show percentage of annexin-V+ on WT and Foxa2 KO CD4+ (**A**) and CD8+ (**B**) T cells. Error bars represent ± SEM. (n=4 for each genotype) *p<0.05; WT versus Foxa2 KO.

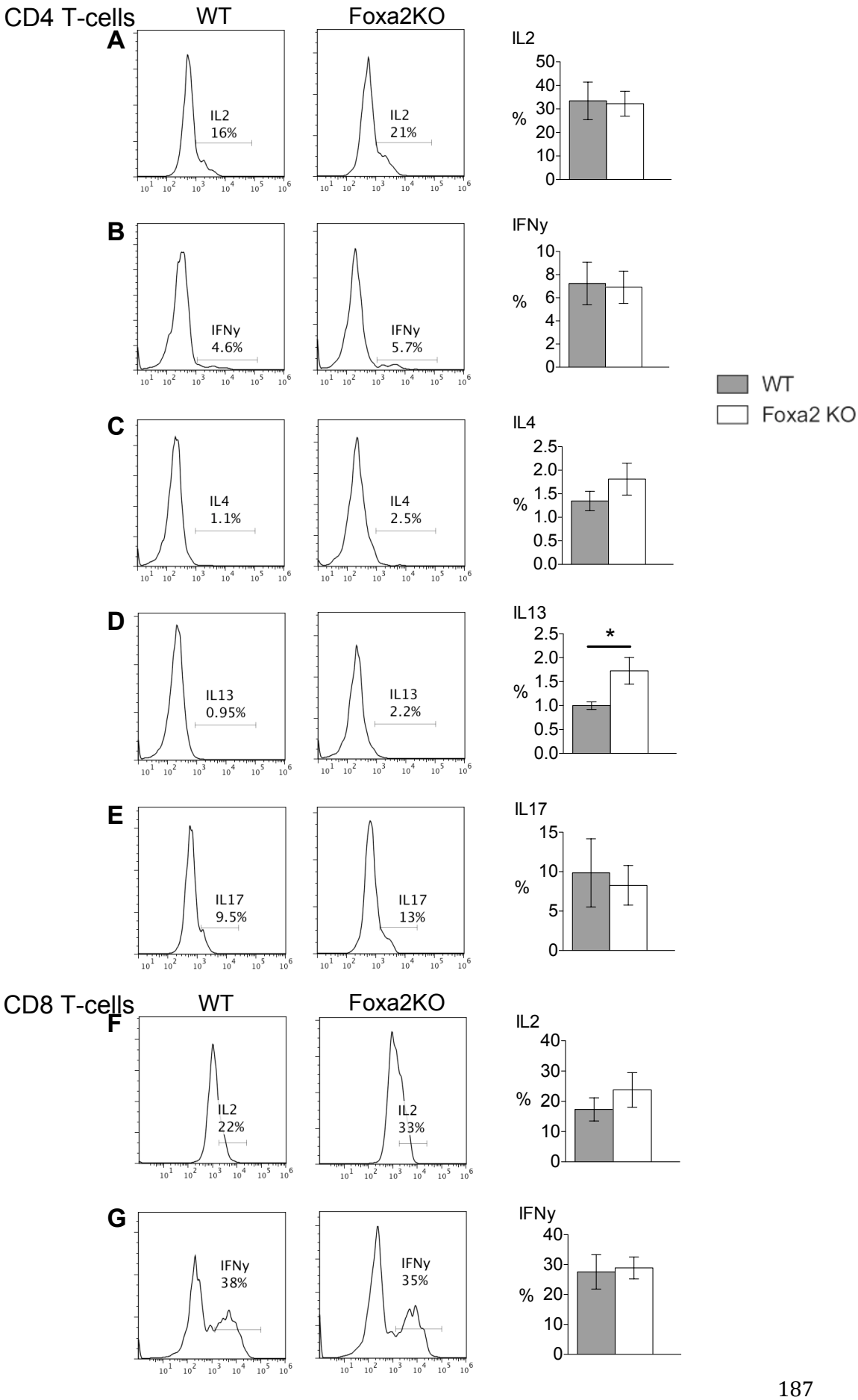
CD4 T-cells
WT
Foxa2KO
A
IL2
16%
IL2
21%
IL2
%
B
IFNy
4.6%
IFNy
5.7%
IFNy
%
C
IL4
1.1%
IL4
2.5%
IL4
%
D
IL13
0.95%
IL13
2.2%
IL13
*
%
E
IL17
9.5%
IL17
13%
IL17
%
WT
Foxa2 KO
CD8 T-cells
WT
Foxa2KO
F
IL2
22%
IL2
33%
IL2
%
G
IFNy
38%
IFNy
35%
IFNy
%

Figure 6.25 Intracellular cytokine staining of CD4 and CD8 T-cells

Histograms and bar charts show intracellular staining of cytokines (IL2, IFNγ, IL4, IL13, and IL17) in CD4 T-cells. Splenocytes from Foxa2 KO and WT mice were cultured with PMA, ionomycin and brefeldin A for 4 hours. Cells were then stained with anti-CD4 and anti-CD8 to identified CD4 and CD8 T-cells, followed by intracellular cytokine staining with anti-IL2, anti-IFNγ, anti-IL4, anti-IL13, and anti-IL17. Numbers in histogram indicate percentages that stained positive with anti-cytokine antibody after gating on CD4+ (**A**-**E**) or CD8+ (**F**-**G)** T-cells. Bar charts show mean of percentage stained positive for a given cytokine in WT and Foxa2 KO CD4 and CD8 T-cells. Error bars represent ± SEM. (n=4 for each genotype) *p<0.05; WT versus Foxa2 KO.

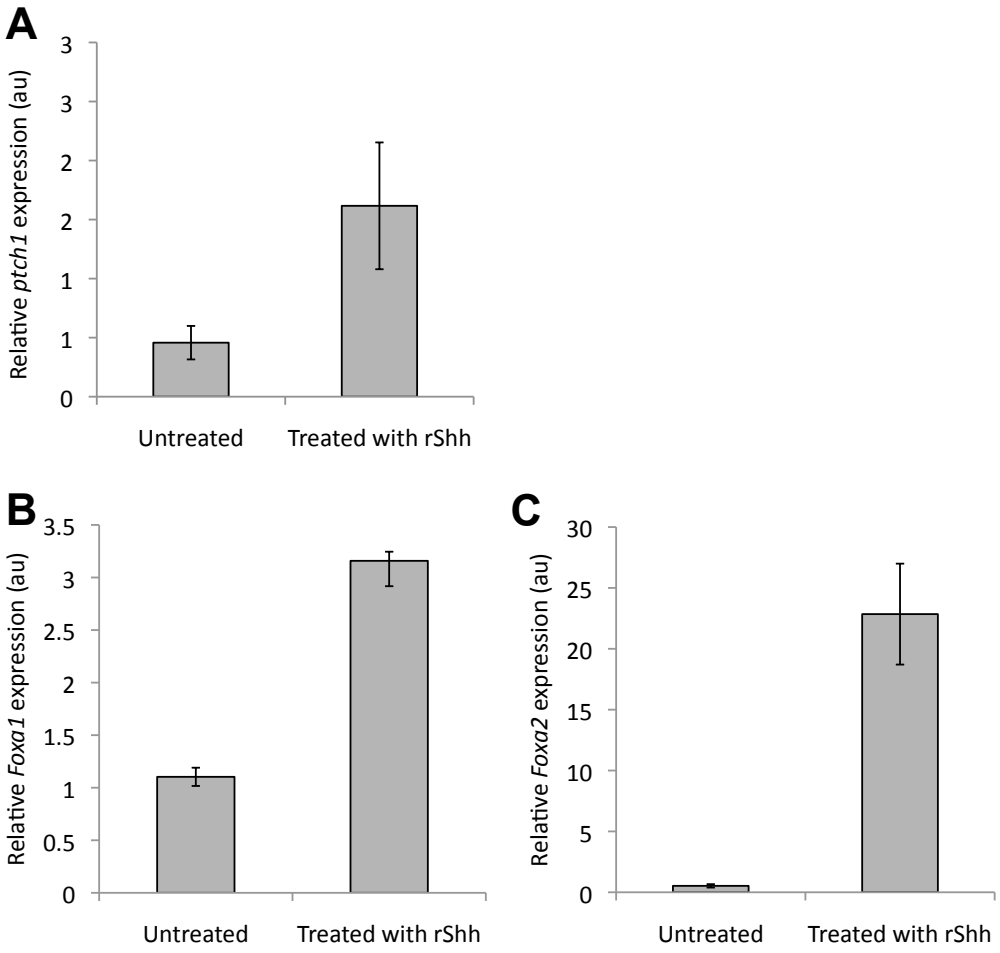

Figure 6.26 Changes in *Foxa1* and *Foxa2* expression in WT E17.5 thymus after treatment with rShh

E17.5 thymi were isolated from WT mice and cultured with rShh for 2 days in FTOC. Bar charts show relative *Ptch1* (**A**)*, Foxa1* (**B**)*,* and *Foxa2* (**C**) expression in the WT treated with rShh, and untreated control. The scale shows expression normalised to the level of the housekeeping gene *HPRT.* Error bars represent ± SEM. Data are representative of three independent experiments.

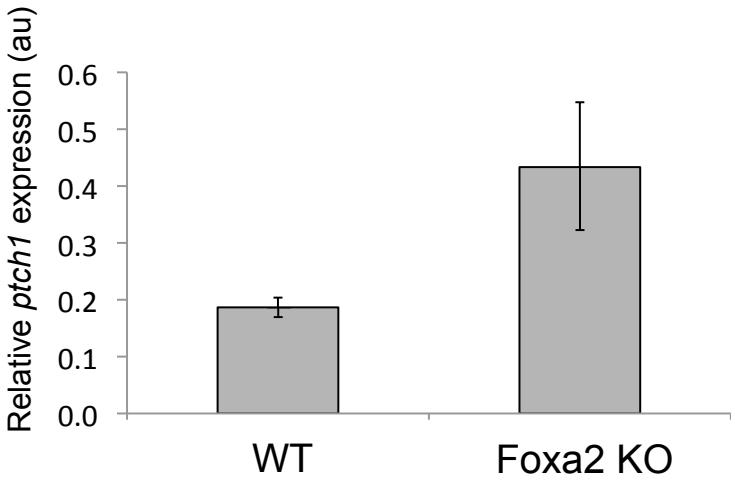

Figure 6.27 Hh signal was elevated in Foxa2 KO thymus

Bar chart to show relative *Ptch1* expression in the WT and Foxa2 KO thymus. The scale shows expression normalised to the level of the housekeeping gene *HPRT*. Error bars represent ± SEM. Data are representative of three independent experiments.

6.3 Discussion

Foxa1 and Foxa2 play complementary roles in late thymocyte development. Here we show that Foxa1 and Foxa2 play complementary roles during the regulation of thymocyte development. Both Foxa1 and Foxa2 are expressed in thymocytes and the lymphoid organs. In the conditional Foxa1/Foxa2 double-mutant mice, CD4/CD8 lineage commitment was altered and there was a decrease in numbers of CD4 T-cells in thymus and periphery. On the other hand, loss of either Foxa1 or Foxa2 alone did not disrupt T-cell development in the thymus to the same extent as the double-mutant. However, since loss of Foxa2 had a higher impact on reduction of CD4 T-cells than loss of Foxa1 in periphery, it is thus possible that Foxa2 is more significant than Foxa1 in regulating T-cells development. These findings indicate that both Foxa1 and Foxa2 are required in late T-cell development and that one Foxa family member may be able to compensate for the loss of another.

In addition, a comparable expression pattern of Foxa1 and Foxa2 was observed in the early stage of developing thymocytes (DN1 - DN3), while a divergent expression was detected at the stage after pre-TCR signalling (DN4 - mature T-cells). These data indicate the possibility that Foxa1 and Foxa2 may be functionally redundant at early stages of T-cell development, whereas different roles are involved during the transition of DN to DP and DP to SP. A similar finding was described previously in the liver: although Foxa1 and Foxa2 share a highly similar binding domain and are functionally redundant during fetal liver development, they perform distinct functions by binding of unique regulatory

regions in adult hepatocytes (Bochkis et al. 2012). Further investigation is required to study the precise function of Foxa1 and Foxa2 and their complementary/redundant actions in T-cell development.

Foxa2 regulates T-cell maturation in the thymus and T-cell homeostasis in the periphery. We observed a lower CD4:CD8 ratio and reduced numbers of CD4 T-cells in Foxa2 KO mice. This suggested that Foxa2 is involved in thymocyte differentiation from DP to SP cells. However, analysis of CD3 and CD5 expression on thymocytes did not show a difference between WT and Foxa2 KO, suggesting that the changes in DP to SP differentiation were not influenced by the TCR signal. During the transition from DP to SP, thymocytes undergo maturation through a series of developmental stages before becoming functionally mature thymocytes that exit the thymus. We analysed the cell surface expression of HSA and Qa2 to measure the maturation status on DP and SP thymocytes in Foxa2 KO mice. We found that Foxa2 KO mice displayed delayed DP to CD4 SP differentiation and partially arrested CD4 SP development. Therefore, these data indicated that Foxa2 regulates CD4 T-cell lineage maturation. This may also account for the reduction in CD4 T-cells in the periphery of Foxa2 KO mice. In addition, the increased Treg production in Foxa2 KO mice may also explain the reduction of T-cells in periphery. More studies will be needed to investigate the precise mechanisms of how Foxa2 regulates T-cell development and the production of Treg.

Foxa2 regulates peripheral T-cell activation and T-helper cell differentiation. We have shown that the activation of both CD4+ and CD8+ T-

cells in Foxa2 KO mice is reduced following stimulation with anti-CD3 and anti-CD28 antibodies. Moreover, the CFSE assay revealed that T-cell proliferation in Foxa2 KO was overall lower than that in WT control. These findings suggested that Foxa2 positively regulates T-cell activation, and proliferation of activated T-cells.

Furthermore, we tested whether Foxa2-deficient T-cells display changes in Th effector cell differentiation. Analysis of intracellular cytokine staining *ex vivo* revealed that Foxa2 KO CD4 T-cells has increased Th2 cytokine production (IL4 and IL13), which suggested that Foxa2 negatively regulates Th2 cells differentiation. Interestingly, our findings were similar to a previous report that Foxa2 is involved in Th2-mediated inflammation. It was found that conditional deletion of Foxa2 in respiratory epithelial cells resulted in an increased recruitment of Th2 cells and enhanced expression of Th2 cytokines in the lung (Chen et al. 2010).

Taken together, Foxa2 may be associated with Th2-mediated disease and it is required in both T-cells and respiratory epithelial cells to maintain the balance of effector cell differentiation.

Foxa1 and Foxa2 are upregulated by Hh signalling and Hh signalling is upregulated in absence of Foxa2. Previous studies have demonstrated that transcription of Foxa2 was downregulated in thymocytes at pre-TCR signal transduction when Hh signalling was inhibited in transgenic mice (Rowbotham et al. 2009). In this study, we showed that both Foxa1 and Foxa2 are also

downstream target genes of Hh signalling after pre-TCR signal transduction. Expression of Foxa1 and Foxa2 were up-regulated when Hh signalling was activated by r-Shh in thymocytes. In addition, we have shown that activation of Hh (induction of expression of *Ptch*) was observed in the Foxa2-deficient thymus.

These findings indicated that Hh regulates Foxa1 and Foxa2 expression in developing thymocytes, however, in the conditional absence of Foxa2, Hh pathway activation was enhanced to maintain the regulatory role of Hh signalling in T-cell development and activation.

The increase in Hh pathway activation and the abnormality in T-cell development observed in Foxa2 KO mice, was comparable to that observed in Gli2ΔN_2 transgenic mice, in which Hh signalling was constitutively activated in thymocytes. As mentioned earlier, analysis of Gli2ΔN_2 transgenic mice indicated that activation of Hh signalling in T-lineage cells reduced numbers of CD4 T-cell populations, inhibited T-cell activation and promoted Th2 differentiation. (Furmanski et al. 2013, Rowbotham et al. 2007). These findings suggested that Hh signalling is required to maintain the expression of Foxa2, and that loss of Foxa2 creates negative feedback to activate Hh signalling, and thus regulates T-cell development via the Hh pathway.

6.4 Conclusion

Analysis of conditional KO of Foxa1 and/or Foxa2 mice suggested that Foxa1 and Foxa2 together are involved in the regulation of T-cell development, specifically in differentiation at the transition from DP to SP, and that they influence the CD4 and CD8 T-cell lineage decision. Although loss of Foxa1 or Foxa2 alone from the DP stage onwards did not alter the CD4 or CD8 T-cell differentiation in the thymus, deletion of Foxa2 significantly reduced the proportion of T-cells in the spleen and LN. A more profound effect was observed in the mice which were double deficient in Foxa1 and Foxa2, which had altered T-cell populations in thymus, spleen and LN. Therefore, both Foxa1 and Foxa2 are required in T-cell differentiation, and there is some functional redundancy in the thymus.

Further investigation of the maturation status of thymocytes showed that Foxa2 KO DP cells had reduced differentiation to SP compared to that of WT. In addition, proliferation was reduced in Foxa2 KO T-cells compared to WT.

Analysis of Foxa2 KO peripheral T-cells showed decreased expression of activation markers on both CD4 and CD8 T-cells after stimulation with anti-CD3 and anti-CD28 antibodies. Given that abnormal T-cell activation in Foxa2 KO mice was observed, intracellular cytokines in T-cells were examined and the analysis revealed that Foxa2 KO CD4 T-cells showed increased production of the Th2 associated cytokines, IL4 and IL13.

In addition, both *Foxa1* and *Foxa2* were upregulated when the E17.5 WT FTOC were treated with rShh to activate Hh signalling, which demonstrated that Foxa1 and Foxa2 are downstream target genes of Hh signalling. An increased *Ptch1* expression was observed on Foxa2 KO thymus compared to WT, which suggested that loss of Foxa2 influences Hh pathway activation.

Chapter Seven : Summaries and future directions

Accurate and efficient haematopoiesis is critical for embryonic development and to maintain steady levels of blood cells in circulation in the adult. Thus, a better understanding of the mechanisms that regulate haematopoietic cell development is essential for the discovery of novel treatments and understand the pathogenesis of erythroid disease and haematological malignancies, such as anaemia and leukaemia.

This thesis has been focused on the role of Hh signalling and its mediator in the development of two main haematopoietic lineages, 1) erythrocytes and 2) thymocytes. Here, we provided evidence that support the importance of the role of Hh signalling in these two areas.

For erythroid development, we showed that Dhh is required for the regulation of erythroid progenitor differentiation and that it acts as a negative regulator of erythropoiesis in both normal and stress conditions. However, study of Dhh+/- and Dhh-/- embryos showed no impact on development of myeloid progenitors and erythroblast populations, which suggested that Dhh is dispensable for embryonic myeloid cell production and erythropoiesis. On the other hand, analysis of Smo conditional KO embryo and Gli3+/- embryo showed changes in the percentages of HSC and myeloid progenitors respectively. These data

indicate that Hh signalling is important in both adult and embryonic haematopoiesis.

For T-cell development, we showed that Foxa1 and Foxa2, transcription factors that are Hh target genes, are involved in T-cell development. Further study of Foxa2 conditional KO mice showed that Foxa2 is important in the regulation of T-cell maturation processes in the thymus and in T-cell activation. Analysis of intracellular cytokine expression revealed that increased Th2 cytokines production in Foxa2-deficient T-cells, which suggested that Foxa2 is important in regulation of effector cells, especially Th2 differentiation.

Future directions:

Although the three Hh family proteins share the same signalling pathway, combining our data and previous studies indicate that they may have different effects on haematopoiesis. In the future, it will be important to clarify the mechanisms and other factors that influence the combined regulatory functions of Hh signalling in haematopoietic cell development. It will also be interesting to know if the Hh proteins regulate one another's functions and the mechanisms behind it.

Here we showed that Foxa1 and Foxa2 are involved in late stages of T-cell development. However, the function of Foxa1 and Foxa2 in early T-cell development and the mechanism underlying the interaction of these two transcription factors are still not yet determined. More investigation will be needed to clarify the compensatory/redundancy mechanism of Foxa1 and

Foxa2 during the regulation of T-cell differentiation in early as well as late stages.

The micro-environment within the thymus is critical for T-cell development and the selection process. Shh is produced by thymic epithelial cells and forms a gradient of different signal strength to activate or repress the Hh target genes to regulate the thymocyte differentiation in different stages. It will be of interest to identify if Foxa1 and/or Foxa2 are also expressed in thymic epithelial cells and if they have interactions with Hh ligands in the thymus microenvironment to control T-cell development and selection.

Moreover, the increased Th2 cytokine production found in Foxa2-deficient T-cells indicated that Foxa2 may be associated with Th2-mediated disease. Th2 cells play a central role in allergic disease, including asthma. More investigation will need to be carried out to study if Foxa2 is important in regulation of Th2-mediated disease immunity *in vivo*.

Reference:

Azzam HS, DeJarnette JB, Huang K, Emmons R, Park CS, Sommers CL, El-Khoury D, Shores EW, Love PE. 2001. Fine tuning of TCR signaling by CD5. J Immunol 166: 5464-5472.

Bajestan SN, Umehara F, Shirahama Y, Itoh K, Sharghi-Namini S, Jessen KR, Mirsky R, Osame M. 2006. Desert hedgehog-patched 2 expression in peripheral nerves during Wallerian degeneration and regeneration. J Neurobiol 66: 243-255.

Bell JJ, Bhandoola A. 2008. The earliest thymic progenitors for T cells possess myeloid lineage potential. Nature 452: 764-767.

Besnard V, Wert SE, Hull WM, Whitsett JA. 2004. Immunohistochemical localization of Foxa1 and Foxa2 in mouse embryos and adult tissues. Gene Expr Patterns 5: 193-208.

Bhardwaj G, Murdoch B, Wu D, Baker DP, Williams KP, Chadwick K, Ling LE, Karanu FN, Bhatia M. 2001. Sonic hedgehog induces the proliferation of primitive human hematopoietic cells via BMP regulation. Nat Immunol 2: 172-180.

Bitgood MJ, McMahon AP. 1995. Hedgehog and Bmp genes are coexpressed at many diverse sites of cell-cell interaction in the mouse embryo. Dev Biol 172: 126-138.

Bitgood MJ, Shen L, McMahon AP. 1996. Sertoli cell signaling by Desert hedgehog regulates the male germline. Curr Biol 6: 298-304.

Bochkis IM, Schug J, Ye DZ, Kurinna S, Stratton SA, Barton MC, Kaestner KH. 2012. Genome-Wide Location Analysis Reveals Distinct Transcriptional Circuitry by Paralogous Regulators Foxa1 and Foxa2. PLoS Genet 8.

Bommhardt U, Basson MA, Krummrei U, Zamoyska R. 1999. Activation of the extracellular signal-related kinase/mitogen-activated protein kinase pathway discriminates CD4 versus CD8 lineage commitment in the thymus. J Immunol 163: 715-722.

Briscoe J, Ericson J. 1999. The specification of neuronal identity by graded Sonic Hedgehog signalling. Semin Cell Dev Biol 10: 353-362.

Briscoe J, Ericson J. 2001. Specification of neuronal fates in the ventral neural tube. Curr Opin Neurobiol 11: 43-49.

Byrd N, Becker S, Maye P, Narasimhaiah R, St-Jacques B, Zhang X, McMahon J, McMahon A, Grabel L. 2002. Hedgehog is required for murine yolk sac angiogenesis. Development 129: 361-372.

Chen G, Wan H, Luo F, Zhang L, Xu Y, Lewkowich I, Wills-Karp M, Whitsett JA. 2010. Foxa2 programs Th2 cell-mediated innate immunity in the developing lung. J Immunol 184: 6133-6141.

Chiang C, Litingtung Y, Lee E, Young KE, Corden JL, Westphal H, Beachy PA. 1996. Cyclopia and defective axial patterning in mice lacking Sonic hedgehog gene function. Nature 383: 407-413.

Clark AM, Garland KK, Russell LD. 2000. Desert hedgehog (Dhh) gene is required in the mouse testis for formation of adult-type Leydig cells and normal

development of peritubular cells and seminiferous tubules. Biol Reprod 63: 1825-1838.

Clark KL, Halay ED, Lai E, Burley SK. 1993. Co-crystal structure of the HNF-3/fork head DNA-recognition motif resembles histone H5. Nature 364: 412-420.

Constant SL, Bottomly K. 1997. Induction of Th1 and Th2 CD4+ T cell responses: the alternative approaches. Annu Rev Immunol 15: 297-322.

Cridland SO, Keys JR, Papathanasiou P, Perkins AC. 2009. Indian hedgehog supports definitive erythropoiesis. Blood Cells Mol Dis 43: 149-155.

Crompton T, Outram SV, Hager-Theodorides AL. 2007. Sonic hedgehog signalling in T-cell development and activation. Nat Rev Immunol 7: 726-735.

Curotto de Lafaille MA, Lafaille JJ. 2009. Natural and adaptive foxp3+ regulatory T cells: more of the same or a division of labor? Immunity 30: 626-635.

de Boer J, Williams A, Skavdis G, Harker N, Coles M, Tolaini M, Norton T, Williams K, Roderick K, Potocnik AJ, Kioussis D. 2003. Transgenic mice with hematopoietic and lymphoid specific expression of Cre. Eur J Immunol 33: 314-325.

Detmer K, Walker AN, Jenkins TM, Steele TA, Dannawi H. 2000. Erythroid differentiation in vitro is blocked by cyclopamine, an inhibitor of hedgehog signaling. Blood Cells Mol Dis 26: 360-372.

Detmer K, Thompson AJ, Garner RE, Walker AN, Gaffield W, Dannawi H. 2005. Hedgehog signaling and cell cycle control in differentiating erythroid progenitors. Blood Cells Mol Dis 34: 60-70.

Dierks C, Beigi R, Guo GR, Zirlik K, Stegert MR, Manley P, Trussell C, Schmitt-Graeff A, Landwerlin K, Veelken H, Warmuth M. 2008. Expansion of Bcr-Abl-positive leukemic stem cells is dependent on Hedgehog pathway activation. Cancer Cell 14: 238-249.

Dyer MA, Farrington SM, Mohn D, Munday JR, Baron MH. 2001. Indian hedgehog activates hematopoiesis and vasculogenesis and can respecify prospective neurectodermal cell fate in the mouse embryo. Development 128: 1717-1730.

Egerton M, Scollay R, Shortman K. 1990. Kinetics of mature T-cell development in the thymus. Proc Natl Acad Sci U S A 87: 2579-2582.

El Andaloussi A, Graves S, Meng F, Mandal M, Mashayekhi M, Aifantis I. 2006. Hedgehog signaling controls thymocyte progenitor homeostasis and differentiation in the thymus. Nat Immunol 7: 418-426.

Ema H, Nakauchi H. 2000. Expansion of hematopoietic stem cells in the developing liver of a mouse embryo. Blood 95: 2284-2288.

Ema H, Douagi I, Cumano A, Kourilsky P. 1998. Development of T cell precursor activity in the murine fetal liver. Eur J Immunol 28: 1563-1569.

Farrington SM, Belaoussoff M, Baron MH. 1997. Winged-helix, Hedgehog and Bmp genes are differentially expressed in distinct cell layers of the murine yolk sac. Mech Dev 62: 197-211.

Fehling HJ, von Boehmer H. 1997. Early alpha beta T cell development in the thymus of normal and genetically altered mice. Curr Opin Immunol 9: 263-275.

Fehling HJ, Krotkova A, Saint-Ruf C, von Boehmer H. 1995. Crucial role of the pre-T-cell receptor alpha gene in development of alpha beta but not gamma delta T cells. Nature 375: 795-798.

Ferri AL, Lin W, Mavromatakis YE, Wang JC, Sasaki H, Whitsett JA, Ang SL. 2007. Foxa1 and Foxa2 regulate multiple phases of midbrain dopaminergic neuron development in a dosage-dependent manner. Development 134: 2761-2769.

Fraser ST, Isern J, Baron MH. 2007. Maturation and enucleation of primitive erythroblasts during mouse embryogenesis is accompanied by changes in cell-surface antigen expression. Blood 109: 343-352.

Friedman JR, Kaestner KH. 2006. The Foxa family of transcription factors in development and metabolism. Cell Mol Life Sci 63: 2317-2328.

Fujiwara Y, Browne CP, Cunniff K, Goff SC, Orkin SH. 1996. Arrested development of embryonic red cell precursors in mouse embryos lacking transcription factor GATA-1. Proc Natl Acad Sci U S A 93: 12355-12358.

Furmanski AL, Saldana JI, Ono M, Sahni H, Paschalidis N, D'Acquisto F, Crompton T. 2013. Tissue-derived hedgehog proteins modulate Th differentiation and disease. J Immunol 190: 2641-2649.

Gao J, Graves S, Koch U, Liu S, Jankovic V, Buonamici S, El Andaloussi A, Nimer SD, Kee BL, Taichman R, Radtke F, Aifantis I. 2009. Hedgehog signaling is dispensable for adult hematopoietic stem cell function. Cell Stem Cell 4: 548-558.

Gao N, LeLay J, Vatamaniuk MZ, Rieck S, Friedman JR, Kaestner KH. 2008. Dynamic regulation of Pdx1 enhancers by Foxa1 and Foxa2 is essential for pancreas development. Genes Dev 22: 3435-3448.

Gao N, Ishii K, Mirosevich J, Kuwajima S, Oppenheimer SR, Roberts RL, Jiang M, Yu X, Shappell SB, Caprioli RM, Stoffel M, Hayward SW, Matusik RJ. 2005. Forkhead box A1 regulates prostate ductal morphogenesis and promotes epithelial cell maturation. Development 132: 3431-3443.

Ghinassi B, Sanchez M, Martelli F, Amabile G, Vannucchi AM, Migliaccio G, Orkin SH, Migliaccio AR. 2007. The hypomorphic Gata1low mutation alters the proliferation/differentiation potential of the common megakaryocytic-erythroid progenitor. Blood 109: 1460-1471.

Godfrey DI, Kennedy J, Suda T, Zlotnik A. 1993. A developmental pathway involving four phenotypically and functionally distinct subsets of CD3-CD4-CD8- triple-negative adult mouse thymocytes defined by CD44 and CD25 expression. J Immunol 150: 4244-4252.

Godfrey DI, Kennedy J, Mombaerts P, Tonegawa S, Zlotnik A. 1994. Onset of TCR-beta gene rearrangement and role of TCR-beta expression during CD3-CD4-CD8- thymocyte differentiation. J Immunol 152: 4783-4792.

Godin I, Garcia-Porrero JA, Dieterlen-Lievre F, Cumano A. 1999. Stem cell emergence and hemopoietic activity are incompatible in mouse intraembryonic sites. J Exp Med 190: 43-52.

Goldman DC, Bailey AS, Pfaffle DL, Al Masri A, Christian JL, Fleming WH. 2009. BMP4 regulates the hematopoietic stem cell niche. Blood 114: 4393-4401.

Goldrath AW, Bevan MJ. 1999. Selecting and maintaining a diverse T-cell repertoire. Nature 402: 255-262.

Gregory CJ, Eaves AC. 1978. Three stages of erythropoietic progenitor cell differentiation distinguished by a number of physical and biologic properties. Blood 51: 527-537.

Guidos C. 2006. Thymus and T-lymphocyte development: what is new in the 21st century? Immunol Rev 209: 5-9.

Gunji Y, Sudo T, Suda J, Yamaguchi Y, Nakauchi H, Nishikawa S, Yanai N, Obinata M, Yanagisawa M, Miura Y, et al. 1991. Support of early B-cell differentiation in mouse fetal liver by stromal cells and interleukin-7. Blood 77: 2612-2617.

Hager-Theodorides AL, Dessens JT, Outram SV, Crompton T. 2005. The transcription factor Gli3 regulates differentiation of fetal CD4- CD8- double-negative thymocytes. Blood 106: 1296-1304.

Hager-Theodorides AL, Furmanski AL, Ross SE, Outram SV, Rowbotham NJ, Crompton T. 2009. The Gli3 transcription factor expressed in the thymus stroma controls thymocyte negative selection via Hedgehog-dependent and -independent mechanisms. J Immunol 183: 3023-3032.

Han W, Yu Y, Liu XY. 2006. Local signals in stem cell-based bone marrow regeneration. Cell Res 16: 189-195.

Hansson A, Zetterblad J, van Duren C, Axelson H, Jonsson JI. 2007. The Lim-only protein LMO2 acts as a positive regulator of erythroid differentiation. Biochem Biophys Res Commun 364: 675-681.

Harfe BD, Scherz PJ, Nissim S, Tian H, McMahon AP, Tabin CJ. 2004. Evidence for an expansion-based temporal Shh gradient in specifying vertebrate digit identities. Cell 118: 517-528.

Hegde GV, Peterson KJ, Emanuel K, Mittal AK, Joshi AD, Dickinson JD, Kollessery GJ, Bociek RG, Bierman P, Vose JM, Weisenburger DD, Joshi SS. 2008. Hedgehog-induced survival of B-cell chronic lymphocytic leukemia cells in a stromal cell microenvironment: a potential new therapeutic target. Mol Cancer Res 6: 1928-1936.

Heussler HS, Suri M. 2003. Sonic hedgehog. Mol Pathol 56: 129-131.

Hofmann I, Stover EH, Cullen DE, Mao J, Morgan KJ, Lee BH, Kharas MG, Miller PG, Cornejo MG, Okabe R, Armstrong SA, Ghilardi N, Gould S, de Sauvage FJ, McMahon AP, Gilliland DG. 2009. Hedgehog signaling is dispensable for adult murine hematopoietic stem cell function and hematopoiesis. Cell Stem Cell 4: 559-567.

Ingham PW, McMahon AP. 2001. Hedgehog signaling in animal development: paradigms and principles. Genes Dev 15: 3059-3087.

Iwasaki H, Mizuno S, Wells RA, Cantor AB, Watanabe S, Akashi K. 2003. GATA-1 converts lymphoid and myelomonocytic progenitors into the megakaryocyte/erythrocyte lineages. Immunity 19: 451-462.

Jackson BC, Carpenter C, Nebert DW, Vasiliou V. 2010. Update of human and mouse forkhead box (FOX) gene families. Hum Genomics 4: 345-352.

Jameson SC, Hogquist KA, Bevan MJ. 1995. Positive selection of thymocytes. Annu Rev Immunol 13: 93-126.

Jeong Y, Epstein DJ. 2003. Distinct regulators of Shh transcription in the floor plate and notochord indicate separate origins for these tissues in the mouse node. Development 130: 3891-3902.

Jiang J, Hui CC. 2008. Hedgehog signaling in development and cancer. Dev Cell 15: 801-812.

June CH, Bluestone JA, Nadler LM, Thompson CB. 1994. The B7 and CD28 receptor families. Immunol Today 15: 321-331.

Kaestner KH, Hiemisch H, Luckow B, Schutz G. 1994. The HNF-3 gene family of transcription factors in mice: gene structure, cDNA sequence, and mRNA distribution. Genomics 20: 377-385.

Kappes DJ, He X. 2005. CD4-CD8 lineage commitment: an inside view. Nat Immunol 6: 761-766.

Keller G, Kennedy M, Papayannopoulou T, Wiles MV. 1993. Hematopoietic commitment during embryonic stem cell differentiation in culture. Mol Cell Biol 13: 473-486.

Killeen N, Irving BA, Pippig S, Zingler K. 1998. Signaling checkpoints during the development of T lymphocytes. Curr Opin Immunol 10: 360-367.

Kingsley PD, Malik J, Fantauzzo KA, Palis J. 2004. Yolk sac-derived primitive erythroblasts enucleate during mammalian embryogenesis. Blood 104: 19-25.

Kingsley PD, Malik J, Emerson RL, Bushnell TP, McGrath KE, Bloedorn LA, Bulger M, Palis J. 2006. "Maturational" globin switching in primary primitive erythroid cells. Blood 107: 1665-1672.

Korn T, Bettelli E, Oukka M, Kuchroo VK. 2009. IL-17 and Th17 Cells. Annu Rev Immunol 27: 485-517.

Koury MJ, Bondurant MC. 1990. Erythropoietin retards DNA breakdown and prevents programmed death in erythroid progenitor cells. Science 248: 378-381.

Kumar S, Balczarek KA, Lai ZC. 1996. Evolution of the hedgehog gene family. Genetics 142: 965-972.

Lai E, Prezioso VR, Tao WF, Chen WS, Darnell JE, Jr. 1991. Hepatocyte nuclear factor 3 alpha belongs to a gene family in mammals that is homologous to the Drosophila homeotic gene fork head. Genes Dev 5: 416-427.

Lai E, Prezioso VR, Smith E, Litvin O, Costa RH, Darnell JE, Jr. 1990. HNF-3A, a hepatocyte-enriched transcription factor of novel structure is regulated transcriptionally. Genes Dev 4: 1427-1436.

Lee CS, Friedman JR, Fulmer JT, Kaestner KH. 2005. The initiation of liver development is dependent on Foxa transcription factors. Nature 435: 944-947.

Mallick CA, Dudley EC, Viney JL, Owen MJ, Hayday AC. 1993. Rearrangement and diversity of T cell receptor beta chain genes in thymocytes: a critical role for the beta chain in development. Cell 73: 513-519.

Marigo V, Johnson RL, Vortkamp A, Tabin CJ. 1996. Sonic hedgehog differentially regulates expression of GLI and GLI3 during limb development. Dev Biol 180: 273-283.

Matise MP, Joyner AL. 1999. Gli genes in development and cancer. Oncogene 18: 7852-7859.

McGrath KE, Frame JM, Fromm GJ, Koniski AD, Kingsley PD, Little J, Bulger M, Palis J. 2011. A transient definitive erythroid lineage with unique regulation of the beta-globin locus in the mammalian embryo. Blood 117: 4600-4608.

McIntyre BA, Ramos-Mejia V, Rampalli S, Mechael R, Lee JH, Alev C, Sheng G, Bhatia M. 2013. Gli3-mediated hedgehog inhibition in human pluripotent stem cells initiates and augments developmental programming of adult hematopoiesis. Blood 121: 1543-1552.

Medvinsky A, Dzierzak E. 1996. Definitive hematopoiesis is autonomously initiated by the AGM region. Cell 86: 897-906.

Merchant A, Joseph G, Wang Q, Brennan S, Matsui W. 2010. Gli1 regulates the proliferation and differentiation of HSCs and myeloid progenitors. Blood 115: 2391-2396.

Monaghan AP, Kaestner KH, Grau E, Schutz G. 1993. Postimplantation expression patterns indicate a role for the mouse forkhead/HNF-3 alpha, beta and gamma genes in determination of the definitive endoderm, chordamesoderm and neuroectoderm. Development 119: 567-578.

Nusslein-Volhard C, Wieschaus E. 1980. Mutations affecting segment number and polarity in Drosophila. Nature 287: 795-801.

Orkin SH, Zon LI. 1997. Genetics of erythropoiesis: induced mutations in mice and zebrafish. Annu Rev Genet 31: 33-60.

Outram SV, Varas A, Pepicelli CV, Crompton T. 2000. Hedgehog signaling regulates differentiation from double-negative to double-positive thymocyte. Immunity 13: 187-197.

Outram SV, Hager-Theodorides AL, Shah DK, Rowbotham NJ, Drakopoulou E, Ross SE, Lanske B, Dessens JT, Crompton T. 2009. Indian hedgehog (Ihh) both promotes and restricts thymocyte differentiation. Blood 113: 2217-2228.

Palis J, Yoder MC. 2001. Yolk-sac hematopoiesis: the first blood cells of mouse and man. Exp Hematol 29: 927-936.

Palis J, Robertson S, Kennedy M, Wall C, Keller G. 1999. Development of erythroid and myeloid progenitors in the yolk sac and embryo proper of the mouse. Development 126: 5073-5084.

Parmantier E, Lynn B, Lawson D, Turmaine M, Namini SS, Chakrabarti L, McMahon AP, Jessen KR, Mirsky R. 1999. Schwann cell-derived Desert hedgehog controls the development of peripheral nerve sheaths. Neuron 23: 713-724.

Perry JM, Harandi OF, Paulson RF. 2007. BMP4, SCF, and hypoxia cooperatively regulate the expansion of murine stress erythroid progenitors. Blood 109: 4494-4502.

Perry JM, Harandi OF, Porayette P, Hegde S, Kannan AK, Paulson RF. 2009. Maintenance of the BMP4-dependent stress erythropoiesis pathway in the murine spleen requires hedgehog signaling. Blood 113: 911.

Razzaque MS, Soegiarto DW, Chang D, Long F, Lanske B. 2005. Conditional deletion of Indian hedgehog from collagen type 2alpha1-expressing cells results in abnormal endochondral bone formation. J Pathol 207: 453-461.

Ren Y, Cowan RG, Migone FF, Quirk SM. 2012. Overactivation of Hedgehog Signaling Alters Development of the Ovarian Vasculature in Mice1. Biol Reprod 86.

Renault MA, Chapouly C, Yao Q, Larrieu-Lahargue F, Vandierdonck S, Reynaud A, Petit M, Jaspard-Vinassa B, Belloc I, Traiffort E, Ruat M, Duplaa C, Couffinhal T, Desgranges C, Gadeau AP. 2013. Desert hedgehog promotes ischemia-induced angiogenesis by ensuring peripheral nerve survival. Circ Res 112: 762-770.

Rieger MA, Schroeder T. 2012. Hematopoiesis. Cold Spring Harb Perspect Biol 4.

Robey E, Fowlkes BJ. 1994. Selective events in T cell development. Annu Rev Immunol 12: 675-705.

Robey E, Fowlkes BJ, Gordon JW, Kioussis D, von Boehmer H, Ramsdell F, Axel R. 1991. Thymic selection in CD8 transgenic mice supports an instructive model for commitment to a CD4 or CD8 lineage. Cell 64: 99-107.

Rowbotham NJ, Hager-Theodorides AL, Furmanski AL, Ross SE, Outram SV, Dessens JT, Crompton T. 2009. Sonic hedgehog negatively regulates pre-TCR-induced differentiation by a Gli2-dependent mechanism. Blood 113: 5144-5156.

Rowbotham NJ, Hager-Theodorides AL, Cebecauer M, Shah DK, Drakopoulou E, Dyson J, Outram SV, Crompton T. 2007. Activation of the Hedgehog signaling pathway in T-lineage cells inhibits TCR repertoire selection in the thymus and peripheral T-cell activation. Blood 109: 3757-3766.

Rowbotham NJ, Furmanski AL, Hager-Theodorides AL, Ross SE, Drakopoulou E, Koufaris C, Outram SV, Crompton T. 2008. Repression of hedgehog signal

transduction in T-lineage cells increases TCR-induced activation and proliferation. Cell Cycle 7: 904-908.

Ruiz i Altaba A. 1998. Combinatorial Gli gene function in floor plate and neuronal inductions by Sonic hedgehog. Development 125: 2203-2212.

Ruiz i Altaba A. 1999. Gli proteins encode context-dependent positive and negative functions: implications for development and disease. Development 126: 3205-3216.

Sacedon R, Varas A, Hernandez-Lopez C, Gutierrez-deFrias C, Crompton T, Zapata AG, Vicente A. 2003. Expression of hedgehog proteins in the human thymus. J Histochem Cytochem 51: 1557-1566.

Sasaki H, Hogan BL. 1993. Differential expression of multiple fork head related genes during gastrulation and axial pattern formation in the mouse embryo. Development 118: 47-59.

Sasaki H, Hui C, Nakafuku M, Kondoh H. 1997. A binding site for Gli proteins is essential for HNF-3beta floor plate enhancer activity in transgenics and can respond to Shh in vitro. Development 124: 1313-1322.

Sasaki H, Nishizaki Y, Hui C, Nakafuku M, Kondoh H. 1999. Regulation of Gli2 and Gli3 activities by an amino-terminal repression domain: implication of Gli2 and Gli3 as primary mediators of Shh signaling. Development 126: 3915-3924.

Schimmang T, Lemaistre M, Vortkamp A, Ruther U. 1992. Expression of the zinc finger gene Gli3 is affected in the morphogenetic mouse mutant extra-toes (Xt). Development 116: 799-804.

Shah DK, Hager-Theodorides AL, Outram SV, Ross SE, Varas A, Crompton T. 2004. Reduced thymocyte development in sonic hedgehog knockout embryos. J Immunol 172: 2296-2306.

Shen W, Scearce LM, Brestelli JE, Sund NJ, Kaestner KH. 2001. Foxa3 (hepatocyte nuclear factor 3gamma) is required for the regulation of hepatic GLUT2 expression and the maintenance of glucose homeostasis during a prolonged fast. J Biol Chem 276: 42812-42817.

Shetlar MD, Hill HA. 1985. Reactions of hemoglobin with phenylhydrazine: a review of selected aspects. Environ Health Perspect 64: 265-281.

Shih DQ, Navas MA, Kuwajima S, Duncan SA, Stoffel M. 1999. Impaired glucose homeostasis and neonatal mortality in hepatocyte nuclear factor 3alpha-deficient mice. Proc Natl Acad Sci U S A 96: 10152-10157.

Shortman K, Wu L. 1996. Early T lymphocyte progenitors. Annu Rev Immunol 14: 29-47.

Shortman K, Egerton M, Spangrude GJ, Scollay R. 1990. The generation and fate of thymocytes. Semin Immunol 2: 3-12.

Socolovsky M, Nam H, Fleming MD, Haase VH, Brugnara C, Lodish HF. 2001. Ineffective erythropoiesis in Stat5a(-/-)5b(-/-) mice due to decreased survival of early erythroblasts. Blood 98: 3261-3273.

Spicer LJ, Sudo S, Aad PY, Wang LS, Chun SY, Ben-Shlomo I, Klein C, Hsueh AJ. 2009. The hedgehog-patched signaling pathway and function in the mammalian ovary: a novel role for hedgehog proteins in stimulating proliferation and steroidogenesis of theca cells. Reproduction 138: 329-339.

St-Jacques B, Hammerschmidt M, McMahon AP. 1999. Indian hedgehog signaling regulates proliferation and differentiation of chondrocytes and is essential for bone formation. Genes Dev 13: 2072-2086.

Stachura DL, Chou ST, Weiss MJ. 2006. Early block to erythromegakaryocytic development conferred by loss of transcription factor GATA-1. Blood 107: 87-97.

Stamataki D, Ulloa F, Tsoni SV, Mynett A, Briscoe J. 2005. A gradient of Gli activity mediates graded Sonic Hedgehog signaling in the neural tube. Genes Dev 19: 626-641.

Szczepny A, Hime GR, Loveland KL. 2006. Expression of hedgehog signalling components in adult mouse testis. Dev Dyn 235: 3063-3070.

Tada T, Widayati DT, Fukuta K. 2006. Morphological study of the transition of haematopoietic sites in the developing mouse during the peri-natal period. Anat Histol Embryol 35: 235-240.

Taipale J, Cooper MK, Maiti T, Beachy PA. 2002. Patched acts catalytically to suppress the activity of Smoothened. Nature 418: 892-897.

te Welscher P, Zuniga A, Kuijper S, Drenth T, Goedemans HJ, Meijlink F, Zeller R. 2002. Progression of vertebrate limb development through SHH-mediated counteraction of GLI3. Science 298: 827-830.

Tober J, Koniski A, McGrath KE, Vemishetti R, Emerson R, de Mesy-Bentley KK, Waugh R, Palis J. 2007. The megakaryocyte lineage originates from hemangioblast precursors and is an integral component both of primitive and of definitive hematopoiesis. Blood 109: 1433-1441.

Trowbridge JJ, Scott MP, Bhatia M. 2006. Hedgehog modulates cell cycle regulators in stem cells to control hematopoietic regeneration. Proc Natl Acad Sci U S A 103: 14134-14139.

Varjosalo M, Taipale J. 2008. Hedgehog: functions and mechanisms. Genes Dev 22: 2454-2472.

Wadman IA, Osada H, Grutz GG, Agulnick AD, Westphal H, Forster A, Rabbitts TH. 1997. The LIM-only protein Lmo2 is a bridging molecule assembling an erythroid, DNA-binding complex which includes the TAL1, E47, GATA-1 and Ldb1/NLI proteins. EMBO J 16: 3145-3157.

Wan H, Dingle S, Xu Y, Besnard V, Kaestner KH, Ang SL, Wert S, Stahlman MT, Whitsett JA. 2005. Compensatory roles of Foxa1 and Foxa2 during lung morphogenesis. J Biol Chem 280: 13809-13816.

Warren AJ, Colledge WH, Carlton MB, Evans MJ, Smith AJ, Rabbitts TH. 1994. The oncogenic cysteine-rich LIM domain protein rbtn2 is essential for erythroid development. Cell 78: 45-57.

Weigel D, Jackle H. 1990. The fork head domain: a novel DNA binding motif of eukaryotic transcription factors? Cell 63: 455-456.

Weigel D, Jurgens G, Kuttner F, Seifert E, Jackle H. 1989. The homeotic gene fork head encodes a nuclear protein and is expressed in the terminal regions of the Drosophila embryo. Cell 57: 645-658.

Weinstein DC, Ruiz i Altaba A, Chen WS, Hoodless P, Prezioso VR, Jessell TM, Darnell JE, Jr. 1994. The winged-helix transcription factor HNF-3 beta is required for notochord development in the mouse embryo. Cell 78: 575-588.

Wijgerde M, Ooms M, Hoogerbrugge JW, Grootegoed JA. 2005. Hedgehog signaling in mouse ovary: Indian hedgehog and desert hedgehog from granulosa cells induce target gene expression in developing theca cells. Endocrinology 146: 3558-3566.

Wong PM, Chung SW, Reicheld SM, Chui DH. 1986. Hemoglobin switching during murine embryonic development: evidence for two populations of embryonic erythropoietic progenitor cells. Blood 67: 716-721.

Xu MJ, Matsuoka S, Yang FC, Ebihara Y, Manabe A, Tanaka R, Eguchi M, Asano S, Nakahata T, Tsuji K. 2001. Evidence for the presence of murine primitive megakaryocytopoiesis in the early yolk sac. Blood 97: 2016-2022.

Zhang J, Socolovsky M, Gross AW, Lodish HF. 2003. Role of Ras signaling in erythroid differentiation of mouse fetal liver cells: functional analysis by a flow cytometry-based novel culture system. Blood 102: 3938-3946.

Zhang XM, Ramalho-Santos M, McMahon AP. 2001. Smoothened mutants reveal redundant roles for Shh and Ihh signaling including regulation of L/R symmetry by the mouse node. Cell 106: 781-792.

Zhao C, Chen A, Jamieson CH, Fereshteh M, Abrahamsson A, Blum J, Kwon HY, Kim J, Chute JP, Rizzieri D, Munchhof M, VanArsdale T, Beachy PA, Reya T. 2009. Hedgehog signalling is essential for maintenance of cancer stem cells in myeloid leukaemia. Nature 458: 776-779.